Physical Review & Research International
3(2): 55-116, 2013

SCIENCEDOMAIN *international*
www.sciencedomain.org

Application of Non-local Quantum Hydrodynamics to the Description of the Charge Density Waves in the Graphene Crystal Lattice

Boris V. Alexeev[1*] and Irina V. Ovchinnikova[1]

[1]Moscow Lomonosov University of Fine Chemical Technologies (MITHT) Prospekt Vernadskogo, 86, Moscow 119570, Russia.

Authors' contributions

This work was carried out in collaboration between all authors. All authors read and approved the final manuscript.

Research Article

Received 13th December 2012
Accepted 11th February 2013
Published 8th March 2013

ABSTRACT

The motion of the charged particles in graphene in the frame of the quantum non-local hydrodynamic description is considered. It is shown as results of the mathematical modeling that the mentioned motion is realizing in the soliton forms. The dependence of the size and structure of solitons on the different physical parameters is investigated.

Keywords: The theory of solitons; generalized hydrodynamic equations; quantum non-local hydrodynamics; theory of transport processes in graphene.

1. INTRODUCTION

We deliver here some main ideas and deductions of the generalized Boltzmann physical kinetics and non-local physics developed by B. Alexeev [1–10]. For simplicity, the fundamental methodic aspects are considered from the qualitative standpoint of view avoiding excessively cumbersome formulas. A rigorous description can be found, for example, in the monograph [6].

[*]Corresponding author: Email: boris.vlad.alexeev@gmail.com;

In 1872 L Boltzmann [11,12] published his kinetic equation for the one-particle distribution function (DF) $f(\mathbf{r},\mathbf{v},t)$. He expressed the equation in the form

$$Df/Dt = J^B(f), \tag{1.1}$$

where J^B is the local collision integral, and $\frac{D}{Dt} = \frac{\partial}{\partial t} + \mathbf{v}\cdot\frac{\partial}{\partial \mathbf{r}} + \mathbf{F}\cdot\frac{\partial}{\partial \mathbf{v}}$ is the substantial (particle) derivative, $\mathbf{v}$ and $\mathbf{r}$ being the velocity and radius vector of the particle, respectively. Boltzmann equation (1.1) governs the transport processes in a one-component gas, which is sufficiently rarefied that only binary collisions between particles are of importance and valid only for two character scales, connected with the hydrodynamic time-scale and the time-scale between particle collisions. While we are not concerned here with the explicit form of the collision integral, note that it should satisfy conservation laws of point-like particles in binary collisions. Integrals of the distribution function (i.e. its moments) determine the macroscopic hydrodynamic characteristics of the system, in particular the number density of particles n and the temperature T. The Boltzmann equation (BE) is not of course as simple as its symbolic form above might suggest, and it is in only a few special cases that it is amenable to a solution. One example is that of a maxwellian distribution in a locally, thermodynamically equilibrium gas in the event when no external forces are present. In this case the equality $J^B = 0$ and $f = f_0$ is met, giving the maxwellian distribution function f_0. A weak point of the classical Boltzmann kinetic theory is the way it treats the dynamic properties of interacting particles. On the one hand, as the so-called "physical" derivation of the BE suggests, Boltzmann particles are treated as material points; on the other hand, the collision integral in the BE brings into existence the cross sections for collisions between particles. A rigorous approach to the derivation of the kinetic equation for f (noted in following as KE_f) is based on the hierarchy of the Bogolyubov-Born-Green-Kirkwood-Yvon (BBGKY) [1,6,13,14] equations.

A KE_f obtained by the multi-scale method turns into the BE if one ignores the change of the distribution function (DF) over a time of the order of the collision time (or, equivalently, over a length of the order of the particle interaction radius). It is important to note [1 - 6] that accounting for the third of the scales mentioned above leads (*prior* to introducing any approximation destined to break the Bogolyubov chain) to additional terms, generally of the same order of magnitude, appear in the BE. If the correlation functions are used to derive KE_f from the BBGKY equations, then the passage to the BE means the neglect of non-local effects.

Given the above difficulties of the Boltzmann kinetic theory, the following clearly inter related questions arise. First, what is a physically infinitesimal volume and how does its introduction (and, as the consequence, the unavoidable smoothing out of the DF) affect the kinetic equation? This question can be formulated in (from the first glance) the paradox form – what is the size of the point in the physical system? Second, how does a systematic account for the proper diameter of the particle in the derivation of the KE_f affect the Boltzmann equation? In the theory developed by B. Alexeev, we refer to the corresponding KE_f as

Generalized Boltzmann Equation (GBE). The derivation of the GBE and the applications of GBE are presented, in particular, in monograph [6]. Accordingly, our purpose is first to explain the essence of the physical generalization of the BE.

Let a particle of finite radius be characterized, as before, by the position vector $\mathbf{r}$ and velocity $\mathbf{v}$ of its center of mass at some instant of time t. Let us introduce physically small volume (**PhSV**) as element of measurement of macroscopic characteristics of physical system for a point containing in this **PhSV**. We should hope that **PhSV** contains sufficient particles N_{ph} for statistical description of the system. In other words, a net of physically small volumes covers the whole investigated physical system.

Every **PhSV** contains entire quantity of point-like Boltzmann particles, and *the same DF* f *is prescribed for whole **PhSV** in Boltzmann physical kinetics.* Therefore, Boltzmann particles are fully "packed" in the reference volume. Let us consider two adjoining physically small volumes $\mathbf{PhSV}_1$ and $\mathbf{PhSV}_2$. We have in principle another situation for the particles of finite size moving in physical small volumes, which are *open* thermodynamic systems.

Then, the situation is possible where, at some instant of time *t*, the particle is located on the interface between two volumes. In so doing, the lead effect is possible (say, for $\mathbf{PhSV}_2$), when the center of mass of particle moving to the neighboring volume $\mathbf{PhSV}_2$ is still in $\mathbf{PhSV}_1$. However, the delay effect takes place as well, when the center of mass of particle moving to the neighboring volume (say, $\mathbf{PhSV}_2$) is already located in $\mathbf{PhSV}_2$ but a part of the particle still belongs to $\mathbf{PhSV}_1$.

Moreover, even the point-like particles (starting after the last collision near the boundary between two mentioned volumes) can change the distribution functions in the neighboring volume. The adjusting of the particles dynamic characteristics for translational degrees of freedom takes several collisions. As result, we have in the definite sense "the Knudsen layer" between these volumes. This fact unavoidably leads to fluctuations in mass and hence in other hydrodynamic quantities. Existence of such "Knudsen layers" is not connected with the choice of space nets and fully defined by the reduced description for ensemble of particles of finite diameters in the conceptual frame of open physically small volumes, therefore – with the chosen method of measurement.

This entire complex of effects defines non-local effects in space and time. The corresponding situation is typical for the theoretical physics – we could remind about the role of probe charge in electrostatics or probe circuit in the physics of magnetic effects.

Suppose that DF f corresponds to $\mathbf{PhSV}_1$ and DF $f - \Delta f$ is connected with $\mathbf{PhSV}_2$ for Boltzmann particles. In the boundary area in the first approximation, fluctuations will be proportional to the mean free path (or, equivalently, to the mean time between the collisions). Then for **PhSV** the correction for DF should be introduced as

$$f^a = f - \tau\, Df / Dt \tag{1.2}$$

in the left hand side of classical BE describing the translation of DF in phase space. As the result

$$Df^{a}/Dt = J^{B}, \tag{1.3}$$

where J^{B} is the Boltzmann local collision integral.

Important to notice that it is only qualitative explanation of GBE derivation obtained earlier (see for example [6]) by different strict methods from the BBGKY – chain of kinetic equations. The structure of the KE_f is generally as follows

$$\frac{Df}{Dt} = J^{B} + J^{nonlocal}, \tag{1.4}$$

where $J^{nonlocal}$ is the non-local integral term incorporating the non-local time and space effects. The generalized Boltzmann physical kinetics, in essence, involves a local approximation

$$J^{nonlocal} = \frac{D}{Dt}\left(\tau \frac{Df}{Dt}\right) \tag{1.5}$$

for the second collision integral, here τ being the mean time *between* the particle collisions. We can draw here an analogy with the Bhatnagar - Gross - Krook (BGK) approximation for J^{B},

$$J^{B} = \frac{f_0 - f}{\tau}, \tag{1.6}$$

which popularity as a means to represent the Boltzmann collision integral is due to the huge simplifications it offers. In other words – the local Boltzmann collision integral admits approximation via the BGK algebraic expression, but more complicated non-local integral can be expressed as differential form (1.5). The ratio of the second to the first term on the right-hand side of Eq. (1.4) is given to an order of magnitude as $J^{nonlocal}/J^{B} \approx O(\mathrm{Kn}^{2})$ and at large Knudsen numbers (Kn defining as ratio of mean free path of particles to the character hydrodynamic length) these terms become of the same order of magnitude. It would seem that at small Knudsen numbers answering to hydrodynamic description the contribution from the second term on the right-hand side of Eq. (1.4) is negligible.

This is not the case, however. When one goes over to the hydrodynamic approximation (by multiplying the kinetic equation by collision invariants and then integrating over velocities), the Boltzmann integral part vanishes, and the second term on the right-hand side of Eq. (1.4) gives a single-order contribution in the generalized Navier-Stokes description. Mathematically, we cannot neglect a term with a small parameter in front of the higher derivative. Physically, the appearing additional terms are due to viscosity and they correspond to the small-scale Kolmogorov turbulence [6]. The integral term $J^{nonlocal}$ turns out to be important both at small and large Knudsen numbers in the theory of transport processes. Thus, $\tau Df/Dt$ is the distribution function fluctuation, and writing Eq. (1.3) without taking into account Eq. (1.2) makes the BE non-closed. From viewpoint of the fluctuation theory, Boltzmann employed the simplest possible closure procedure $f^{a} = f$.

Then, the additional GBE terms (as compared to the BE) are significant for any Kn, and the order of magnitude of the difference between the BE and GBE solutions is impossible to tell beforehand. For GBE the generalized H-theorem is proven [3,6].

It means that the local Boltzmann equation does not belong even to the class of minimal physical models and corresponds so to speak to “the likelihood models”. This remark refers also to all consequences of the Boltzmann kinetic theory including “classical” hydrodynamics.

Obviously the generalized hydrodynamic equations (GHE) will explicitly involve fluctuations proportional to τ. In the hydrodynamic approximation, the mean time τ between the collisions is related to the dynamic viscosity μ by

$$\tau \; p = \Pi \mu \,, \tag{1.7}$$

[13,14]. For example, the continuity equation changes its form and will contain terms proportional to viscosity. On the other hand, if the reference volume extends over the whole cavity with the hard walls, then the classical conservation laws should be obeyed, and this is exactly what the monograph [6] proves. Now several remarks of principal significance:

1. All fluctuations are found from the strict kinetic considerations and tabulated [6]. The appearing additional terms in GHE are due to viscosity and they correspond to the small-scale Kolmogorov turbulence. The neglect of formally small terms is equivalent, in particular, to dropping the (small-scale) Kolmogorov turbulence from consideration and is the origin of all principal difficulties in usual turbulent theory. Fluctuations on the wall are equal to zero, from the physical point of view this fact corresponds to the laminar sub-layer. Mathematically it leads to additional boundary conditions for GHE. Major difficulties arose when the question of existence and uniqueness of solutions of the Navier - Stokes equations was addressed. O.A. Ladyzhenskaya has shown for three-dimensional flows that under smooth initial conditions a unique solution is only possible over a finite time interval. Ladyzhenskaya even introduced a “correction” into the Navier - Stokes equations in order that its unique solvability could be proved; GHE do not lead to these difficulties.

2. It would appear that in continuum mechanics the idea of discreteness can be abandoned altogether and the medium under study be considered as a continuum in the literal sense of the word. Such an approach is of course possible and indeed leads to the Euler equations in hydrodynamics. However, when the viscosity and thermal conductivity effects are to be included, a totally different situation arises. As is well known, the dynamical viscosity is proportional to the mean time τ between the particle collisions, and a continuum medium in the Euler model with $\tau = 0$ implies that neither viscosity nor thermal conductivity is possible.

3. The non-local kinetic effects listed above will always be relevant to a kinetic theory using one particle description – including, in particular, applications to liquids or plasmas, where self-consistent forces with appropriately cut-off radius of their action are introduced to expand the capability of GBE [5, 6]. Fluctuation effects occur in any open thermodynamic system bounded by a control surface

transparent to particles. GBE (1.3) leads to generalized hydrodynamic equations [6] as the local approximation of non local effects, for example, to the continuity equation

$$\frac{\partial \rho^a}{\partial t} + \frac{\partial}{\partial \mathbf{r}} \cdot \left(\rho \mathbf{v}_0\right)^a = 0, \tag{1.8}$$

where ρ^a, $\mathbf{v}_0{}^a$, $\left(\rho \mathbf{v}_0\right)^a$ are calculated in view of non-locality effect in terms of gas density ρ, hydrodynamic velocity of flow $\mathbf{v}_0$, and density of momentum flux $\rho \mathbf{v}_0$; for locally Maxwellian distribution, ρ^a, $\left(\rho \mathbf{v}_0\right)^a$ are defined by the relations

$$\left(\rho - \rho^a\right)/\tau = \frac{\partial \rho}{\partial t} + \frac{\partial}{\partial \mathbf{r}} \cdot \left(\rho \mathbf{v}_0\right), \ \left(\rho \mathbf{v}_0 - \left(\rho \mathbf{v}_0\right)^a\right)/\tau = \frac{\partial}{\partial t}\left(\rho \mathbf{v}_0\right) + \frac{\partial}{\partial \mathbf{r}} \cdot \rho \mathbf{v}_0 \mathbf{v}_0 + \vec{\mathrm{I}} \cdot \frac{\partial p}{\partial \mathbf{r}} - \rho \mathbf{a}, \tag{1.9}$$

where $\vec{\mathrm{I}}$ is a unit tensor, and $\mathbf{a}$ is the acceleration due to the effect of mass forces.

In the general case, the parameter τ? is the non-locality parameter; in quantum hydrodynamics, the "time-energy" uncertainty relation defines its magnitude. Obviously the mentioned non-local effects can be discussed from viewpoint of breaking of the Bell's inequalities [15] because in the non-local theory the measurement (realized in $\mathbf{PhSV_1}$) has influence on the measurement realized in the adjoining space-time point in $\mathbf{PhSV_2}$ and verse versa.

The violation of Bell's inequalities [15] is found for local statistical theories, and the transition to non-local description is inevitable.

Notice that the application of the above principles also leads to the modification of the system of Maxwell equations. While the traditional formulation of this system does not involve the continuity equation, its derivation explicitly employs the equation

$$\frac{\partial \rho^a}{\partial t} + \frac{\partial}{\partial \mathbf{r}} \cdot \mathbf{j}^a = 0, \tag{1.10}$$

where ρ^a is the charge per unit volume, and $\mathbf{j}^a$ is the current density, both calculated without accounting for the fluctuations. As a result, the system of Maxwell equations written in the standard notation, namely

$$\frac{\partial}{\partial \mathbf{r}} \cdot \mathbf{B} = 0, \ \frac{\partial}{\partial \mathbf{r}} \cdot \mathbf{D} = \rho^a, \ \frac{\partial}{\partial \mathbf{r}} \times \mathbf{E} = -\frac{\partial \mathbf{B}}{\partial t}, \ \frac{\partial}{\partial \mathbf{r}} \times \mathbf{H} = \mathbf{j}^a + \frac{\partial \mathbf{D}}{\partial t} \tag{1.11}$$

contains

$$\rho^a = \rho - \rho^{fl}, \ \mathbf{j}^a = \mathbf{j} - \mathbf{j}^{fl}. \tag{1.12}$$

The ρ^{fl}, $\mathbf{j}^{fl}$ fluctuations calculated using the generalized Boltzmann equation are given, for example, in Ref. [2,4,6].

Now we can turn our attention to the quantum hydrodynamic description of individual particles. The abstract of the classical Madelung's paper [16] contains only one phrase: "It is shown that the Schrödinger equation for one-electron problems can be transformed into the form of hydrodynamic equations".

The following conclusion of principal significance can be done from the generalized quantum consideration [7,8]:

1. Madelung's quantum hydrodynamics is equivalent to the Schrödinger equation (SE) and leads to description of the quantum particle evolution in the form of Euler equation and continuity equation.
2. SE is consequence of the Liouville equation as result of the local approximation of non-local equations.
3. Generalized Boltzmann physical kinetics defines the strict approximation of non-local effects in space and time and after transmission to the local approximation leads to parameter τ, which on the quantum level corresponds to the uncertainty principle "time-energy".
4. GHE lead to SE as a deep particular case of the generalized Boltzmann physical kinetics and therefore of non-local hydrodynamics.

In principal GHE needn't in using of the "time-energy" uncertainty relation for estimation of the value of the non-locality parameter τ. Moreover, the "time-energy" uncertainty relation does not lead to the exact relations and from position of non-local physics is only the simplest estimation of the non-local effects.

Really, let us consider two neighboring physically infinitely small volumes $\mathbf{PhSV_1}$ and $\mathbf{PhSV_2}$ in a non-equilibrium system. Obviously the time τ should tend to diminish with increasing of the velocities u of particles invading in the nearest neighboring physically infinitely small volume ($\mathbf{PhSV_1}$ or $\mathbf{PhSV_2}$):

$$\tau = H/u^n \,. \tag{1.13}$$

However, the value τ cannot depend on the velocity direction and naturally to tie τ with the particle kinetic energy, then

$$\tau = H/mu^2 \,, \tag{1.14}$$

where H is a coefficient of proportionality, which reflects the state of physical system. In the simplest case H is equal to Plank constant $\hbar$ and relation (1.14) becomes compatible with the Heisenberg relation.

It is known that Ehrenfest adiabatic theorem is one of the most important and widely studied theorems in Schrödinger quantum mechanics. It states that if we have a slowly changing Hamiltonian that depends on time, and the system is prepared in one of the instantaneous

eigenstates of the Hamiltonian then the state of the system at any time is given by an the instantaneous eigenfunction of the Hamiltonian up to multiplicative phase factors [17-21]. Since the establishment of this theorem many fundamental results have been obtained, such as Landau–Zener transition [17,18], the Gell-Mann-Low theorem [19], Berry phase [20] and holonomy [21].

The adiabatic theory can be naturally incorporated in generalized quantum hydrodynamics based on local approximations of non-local terms. In the simplest case if ΔQ is the elementary heat quantity delivered for a system executing the transfer from one state (the corresponding time moment is t_{in}) to the next one (the time moment t_e) then

$$\Delta Q = \frac{1}{\tau} 2\delta\left(\overline{T}\tau\right), \tag{1.15}$$

where $\tau = t_e - t_{in}$ and $\overline{T}$ is the average kinetic energy. For adiabatic case Ehrenfest supposes that

$$2\overline{T}\tau = \Omega_1, \Omega_2, ... \tag{1.16}$$

where $\Omega_1, \Omega_2, ...$ are adiabatic invariants. Obviously for Plank's oscillator (compare with (1.14))

$$2\overline{T}\tau = nh\,. \tag{1.17}$$

Conclusion: adiabatic theorem and consequences of this theory deliver the general quantization conditions for non-local quantum hydrodynamics.

Non-local physics demonstrates its high efficiency in many fields – from the atom structure problems to cosmology [9,10].

The possibility of the non local physics application in the theory of superconductivity is investigated in [22-24]. It is shown that by the superconducting conditions the relay ("estafette") motion of the soliton' system ("lattice ion – electron") is realizing without creation of the additional chemical bonds. From the position of the quantum hydrodynamics the problem of creation of the high temperature superconductors leads to finding of materials which lattices could realize the soliton' motion without the soliton destruction. These materials should be created using the technology of quantum dots.

This paper is directed on investigation of possible applications of the non-local quantum hydrodynamics in the theory of transport processes in graphene including the effects of the charge density waves (CDW). Is known that graphene, a single-atom-thick sheet of graphite, is a new material which combines aspects of semiconductors and metals. For example the mobility, a measure of how well a material conducts electricity, is higher than for other known materials at room temperature. In graphene, a resistivity is of about 1.0 microOhm-cm (resistivity defined as a specific measure of resistance; the resistance of a piece material is its resistivity times its length and divided by its cross-sectional area). This is about 35 percent less than the resistivity of copper, the lowest resistivity material known at room temperature.

Measurements lead to conclusion that the influence of thermal vibrations on the conduction of electrons in graphene is extraordinarily small. From the other side the typical reasoning exists:

“In any material, the energy associated with the temperature of the material causes the atoms of the material to vibrate in place. As electrons travel through the material, they can bounce off these vibrating atoms, giving rise to electrical resistance. This electrical resistance is "intrinsic" to the material: it cannot be eliminated unless the material is cooled to absolute zero temperature, and hence sets the upper limit to how well a material can conduct electricity.”

Obviously this point of view leads to the principal elimination of effects of the high temperature superconductivity. From the mentioned point of view the restrictions in mobilities of known semiconductors can be explained as the influence of the thermal vibration of the atoms. The limit to mobility of electrons in graphene is about 200,000 $cm^2/(V \cdot s))$ at room temperature, compared to about 1,400 $cm^2/(V \cdot s))$ in silicon, and 77,000 $cm^2/(V \cdot s))$ in indium antimonide, the highest mobility conventional semiconductor known. The opinion of a part of investigators can be formulated as follows: "Other extrinsic sources in today's fairly dirty graphene samples add some extra resistivity to graphene," [25] "so the overall resistivity isn't quite as low as copper's at room temperature yet. However, graphene has far fewer electrons than copper, so in graphene the electrical current is carried by only a few electrons moving much faster than the electrons in copper." Mobility determines the speed at which an electronic device (for instance, a field-effect transistor, which forms the basis of modern computer chips) can turn on and off. The very high mobility makes graphene promising for applications in which transistors much switch extremely fast, such as in processing extremely high frequency signals. The low resistivity and extremely thin nature of graphene also promises applications in thin, mechanically tough, electrically conducting, transparent films. Such films are sorely needed in a variety of electronics applications from touch screens to photovoltaic cells.

In the last years the direct observation of the atomic structures of superconducting materials (as usual superconducting materials in the cuprate family like $YBa_2Cu_3O_{6.67}$ (T_c = 67 K)) was realized with the scanning tunneling microscope (STM) and other instruments, STMs scan a surface in steps smaller than an atom.

Superconductivity, in which an electric current flows with zero resistance, was first discovered in metals cooled very close to absolute zero. New materials called cuprates - copper oxides "doped" with other atoms -- superconduct as "high" as minus 123 Celsius. Some conclusions from direct observations [26,27]:

1. Observations of high-temperature superconductors show an "energy gap" where electronic states are missing. Sometimes this energy gap appears but the material still does not superconduct - a so-called "pseudogap" phase. The pseudogap appears at higher temperatures than any superconductivity, offering the promise of someday developing materials that would superconduct at or near room temperature.

2. STM image of a partially doped cuprate superconductor shows regions with an electronic "pseudogap". As doping increases, pseudogap regions spread and connect, making the whole sample a superconductor.

3. High temperature superconductivity in layered cuprates can develop from an electronically ordered state called a charge density wave (CDW). The results of observation can be interpreted as the creation of the "checkerboard pattern" due to the modulation of the atomic positions in the CuO_2 layers of $YBa_2Cu_3O_{6+x}$ caused by the charge density wave.

4. Application of the method of high-energy X-ray diffraction shows that a CDW develop at zero field in the normal state of superconducting $YBa_2Cu_3O_{6.67}$ ($T_c = 67$ K). Below T_c the application of a magnetic field suppresses superconductivity and enhances the CDW. It means that the high-T_c superconductivity forms from a pre-existing CDW environment.

Important conclusion: high temperature superconductors demonstrate new type of electronic order and modulation of atomic positions. As it was shown in [22,24] the mentioned above graphene properties can be explained only in the frame of the self-consistent non-local quantum theory [7,8] which leads to appearance of the soliton waves moving in graphene.

2. GENERALIZED QUANTUM HYDRODYNAMIC EQUATIONS

Strict consideration leads to the following system of the generalized quantum hydrodynamic equations (GHE) [6] written in the dimensional generalized Euler form:
Continuity equation for species α :

$$\frac{\partial}{\partial t}\left\{\rho_\alpha - \tau_\alpha\left[\frac{\partial \rho_\alpha}{\partial t} + \frac{\partial}{\partial \mathbf{r}}\cdot\left(\rho_\alpha \mathbf{v}_0\right)\right]\right\} + \frac{\partial}{\partial \mathbf{r}}\cdot\left\{\rho_\alpha \mathbf{v}_0 - \tau_\alpha\left[\frac{\partial}{\partial t}\left(\rho_\alpha \mathbf{v}_0\right) + \frac{\partial}{\partial \mathbf{r}}\cdot\left(\rho_\alpha \mathbf{v}_0 \mathbf{v}_0\right) + \right.\right. \tag{2.1}$$
$$\left.\left.\vec{\mathrm{I}}\cdot\frac{\partial p_\alpha}{\partial \mathbf{r}} - \rho_\alpha \mathbf{F}_\alpha^{(1)} - \frac{q_\alpha}{m_\alpha}\rho_\alpha \mathbf{v}_0 \times \mathbf{B}\right]\right\} = R_\alpha,$$

and continuity equation for mixture

$$\frac{\partial}{\partial t}\left\{\rho - \sum_\alpha \tau_\alpha\left[\frac{\partial \rho_\alpha}{\partial t} + \frac{\partial}{\partial \mathbf{r}}\cdot\left(\rho_\alpha \mathbf{v}_0\right)\right]\right\} + \frac{\partial}{\partial \mathbf{r}}\cdot\left\{\rho \mathbf{v}_0 - \sum_\alpha \tau_\alpha\left[\frac{\partial}{\partial t}\left(\rho_\alpha \mathbf{v}_0\right) + \right.\right. \tag{2.2}$$
$$\left.\left.\frac{\partial}{\partial \mathbf{r}}\cdot\left(\rho_\alpha \mathbf{v}_0 \mathbf{v}_0\right) + \vec{\mathrm{I}}\cdot\frac{\partial p_\alpha}{\partial \mathbf{r}} - \rho_\alpha \mathbf{F}_\alpha^{(1)} - \frac{q_\alpha}{m_\alpha}\rho_\alpha \mathbf{v}_0 \times \mathbf{B}\right]\right\} = 0.$$

Momentum equation for species

$$\frac{\partial}{\partial t}\left\{\rho_\alpha \mathbf{v}_0 - \tau_\alpha\left[\frac{\partial}{\partial t}\left(\rho_\alpha \mathbf{v}_0\right)+\frac{\partial}{\partial \mathbf{r}}\cdot\rho_\alpha \mathbf{v}_0\mathbf{v}_0+\frac{\partial p_\alpha}{\partial \mathbf{r}}-\rho_\alpha \mathbf{F}_\alpha^{(1)}-\right.\right.$$
$$\left.\left.\frac{q_\alpha}{m_\alpha}\rho_\alpha \mathbf{v}_0\times\mathbf{B}\right]\right\}-\mathbf{F}_\alpha^{(1)}\left[\rho_\alpha-\tau_\alpha\left(\frac{\partial \rho_\alpha}{\partial t}+\frac{\partial}{\partial \mathbf{r}}\left(\rho_\alpha \mathbf{v}_0\right)\right)\right]-$$
$$\frac{q_\alpha}{m_\alpha}\left\{\rho_\alpha \mathbf{v}_0 - \tau_\alpha\left[\frac{\partial}{\partial t}\left(\rho_\alpha \mathbf{v}_0\right)+\frac{\partial}{\partial \mathbf{r}}\cdot\rho_\alpha \mathbf{v}_0\mathbf{v}_0+\frac{\partial p_\alpha}{\partial \mathbf{r}}-\rho_\alpha \mathbf{F}_\alpha^{(1)}-\right.\right.$$
$$\left.\left.\frac{q_\alpha}{m_\alpha}\rho_\alpha \mathbf{v}_0\times\mathbf{B}\right]\right\}\times\mathbf{B}+\frac{\partial}{\partial \mathbf{r}}\cdot\left\{\rho_\alpha \mathbf{v}_0\mathbf{v}_0+p_\alpha\vec{\mathrm{I}}-\tau_\alpha\left[\frac{\partial}{\partial t}\left(\rho_\alpha \mathbf{v}_0\mathbf{v}_0+\right.\right.\right. \quad (2.3)$$
$$\left.\left.\left.p_\alpha\vec{\mathrm{I}}\right)+\frac{\partial}{\partial \mathbf{r}}\cdot\rho_\alpha\left(\mathbf{v}_0\mathbf{v}_0\right)\mathbf{v}_0+2\vec{\mathrm{I}}\left(\frac{\partial}{\partial \mathbf{r}}\cdot\left(p_\alpha \mathbf{v}_0\right)\right)+\frac{\partial}{\partial \mathbf{r}}\cdot\left(\vec{\mathrm{I}}p_\alpha \mathbf{v}_0\right)-\right.\right.$$
$$\left.\left.\mathbf{F}_\alpha^{(1)}\rho_\alpha \mathbf{v}_0-\rho_\alpha \mathbf{v}_0\mathbf{F}_\alpha^{(1)}-\frac{q_\alpha}{m_\alpha}\rho_\alpha\left[\mathbf{v}_0\times\mathbf{B}\right]\mathbf{v}_0-\frac{q_\alpha}{m_\alpha}\rho_\alpha \mathbf{v}_0\left[\mathbf{v}_0\times\mathbf{B}\right]\right]\right\}=$$
$$\int m_\alpha \mathbf{v}_\alpha J_\alpha^{st,el}d\mathbf{v}_\alpha+\int m_\alpha \mathbf{v}_\alpha J_\alpha^{st,inel}d\mathbf{v}_\alpha.$$

Generalized moment equation for mixture

$$\frac{\partial}{\partial t}\left\{\rho \mathbf{v}_0-\sum_\alpha\tau_\alpha\left[\frac{\partial}{\partial t}\left(\rho_\alpha \mathbf{v}_0\right)+\frac{\partial}{\partial \mathbf{r}}\cdot\rho_\alpha \mathbf{v}_0\mathbf{v}_0+\frac{\partial p_\alpha}{\partial \mathbf{r}}-\rho_\alpha \mathbf{F}_\alpha^{(1)}-\right.\right.$$
$$\left.\left.\frac{q_\alpha}{m_\alpha}\rho_\alpha \mathbf{v}_0\times\mathbf{B}\right]\right\}-\sum_\alpha\mathbf{F}_\alpha^{(1)}\left[\rho_\alpha-\tau_\alpha\left(\frac{\partial \rho_\alpha}{\partial t}+\frac{\partial}{\partial \mathbf{r}}\left(\rho_\alpha \mathbf{v}_0\right)\right)\right]-$$
$$\sum_\alpha\frac{q_\alpha}{m_\alpha}\left\{\rho_\alpha \mathbf{v}_0-\tau_\alpha^{(0)}\left[\frac{\partial}{\partial t}\left(\rho_\alpha \mathbf{v}_0\right)+\frac{\partial}{\partial \mathbf{r}}\cdot\rho_\alpha \mathbf{v}_0\mathbf{v}_0+\frac{\partial p_\alpha}{\partial \mathbf{r}}-\rho_\alpha \mathbf{F}_\alpha^{(1)}-\right.\right.$$
$$\left.\left.\frac{q_\alpha}{m_\alpha}\rho_\alpha \mathbf{v}_0\times\mathbf{B}\right]\right\}\times\mathbf{B}+\frac{\partial}{\partial \mathbf{r}}\cdot\left\{\rho \mathbf{v}_0\mathbf{v}_0+p\vec{\mathrm{I}}-\sum_\alpha\tau_\alpha\left[\frac{\partial}{\partial t}\left(\rho_\alpha \mathbf{v}_0\mathbf{v}_0+\right.\right.\right. \quad (2.4)$$
$$\left.\left.\left.p_\alpha\vec{\mathrm{I}}\right)+\frac{\partial}{\partial \mathbf{r}}\cdot\rho_\alpha\left(\mathbf{v}_0\mathbf{v}_0\right)\mathbf{v}_0+2\vec{\mathrm{I}}\left(\frac{\partial}{\partial \mathbf{r}}\cdot\left(p_\alpha \mathbf{v}_0\right)\right)+\frac{\partial}{\partial \mathbf{r}}\cdot\left(\vec{\mathrm{I}}p_\alpha \mathbf{v}_0\right)-\right.\right.$$
$$\left.\left.\mathbf{F}_\alpha^{(1)}\rho_\alpha \mathbf{v}_0-\rho_\alpha \mathbf{v}_0\mathbf{F}_\alpha^{(1)}-\frac{q_\alpha}{m_\alpha}\rho_\alpha\left[\mathbf{v}_0\times\mathbf{B}\right]\mathbf{v}_0-\frac{q_\alpha}{m_\alpha}\rho_\alpha \mathbf{v}_0\left[\mathbf{v}_0\times\mathbf{B}\right]\right]\right\}=0$$

Energy equation for component

$$\frac{\partial}{\partial t}\left\{\frac{\rho_\alpha v_0^2}{2}+\frac{3}{2}p_\alpha+\varepsilon_\alpha n_\alpha-\tau_\alpha\left[\frac{\partial}{\partial t}\left(\frac{\rho_\alpha v_0^2}{2}+\frac{3}{2}p_\alpha+\varepsilon_\alpha n_\alpha\right)+\right.\right.$$
$$\left.\left.\frac{\partial}{\partial \mathbf{r}}\cdot\left(\frac{1}{2}\rho_\alpha v_0^2\mathbf{v}_0+\frac{5}{2}p_\alpha\mathbf{v}_0+\varepsilon_\alpha n_\alpha\mathbf{v}_0\right)-\mathbf{F}_\alpha^{(1)}\cdot\rho_\alpha\mathbf{v}_0\right]\right\}+$$
$$\frac{\partial}{\partial \mathbf{r}}\cdot\left\{\frac{1}{2}\rho_\alpha v_0^2\mathbf{v}_0+\frac{5}{2}p_\alpha\mathbf{v}_0+\varepsilon_\alpha n_\alpha\mathbf{v}_0-\tau_\alpha\left[\frac{\partial}{\partial t}\left(\frac{1}{2}\rho_\alpha v_0^2\mathbf{v}_0+\right.\right.\right.$$
$$\left.\left.\frac{5}{2}p_\alpha\mathbf{v}_0+\varepsilon_\alpha n_\alpha\mathbf{v}_0\right)+\frac{\partial}{\partial \mathbf{r}}\cdot\left(\frac{1}{2}\rho_\alpha v_0^2\mathbf{v}_0\mathbf{v}_0+\frac{7}{2}p_\alpha\mathbf{v}_0\mathbf{v}_0+\frac{1}{2}p_\alpha v_0^2\vec{\mathrm{I}}+\right.$$
$$\left.\left.\frac{5}{2}\frac{p_\alpha^2}{\rho_\alpha}\vec{\mathrm{I}}+\varepsilon_\alpha n_\alpha\mathbf{v}_0\mathbf{v}_0+\varepsilon_\alpha\frac{p_\alpha}{m_\alpha}\vec{\mathrm{I}}\right)-\rho_\alpha\mathbf{F}_\alpha^{(1)}\cdot\mathbf{v}_0\mathbf{v}_0-p_\alpha\mathbf{F}_\alpha^{(1)}\cdot\vec{\mathrm{I}}-\right.$$
$$\frac{1}{2}\rho_\alpha v_0^2\mathbf{F}_\alpha^{(1)}-\frac{3}{2}\mathbf{F}_\alpha^{(1)}p_\alpha-\frac{\rho_\alpha v_0^2}{2}\frac{q_\alpha}{m_\alpha}[\mathbf{v}_0\times\mathbf{B}]-\frac{5}{2}p_\alpha\frac{q_\alpha}{m_\alpha}[\mathbf{v}_0\times\mathbf{B}]-$$
$$\left.\varepsilon_\alpha n_\alpha\frac{q_\alpha}{m_\alpha}[\mathbf{v}_0\times\mathbf{B}]-\varepsilon_\alpha n_\alpha\mathbf{F}_\alpha^{(1)}\right]\Big\}-\Big\{\ \rho_\alpha\mathbf{F}_\alpha^{(1)}\cdot\mathbf{v}_0-\tau_\alpha\Big[\ \mathbf{F}_\alpha^{(1)}\cdot$$
$$\left.\left.\left(\frac{\partial}{\partial t}(\rho_\alpha\mathbf{v}_0)+\frac{\partial}{\partial \mathbf{r}}\cdot\rho_\alpha\mathbf{v}_0\mathbf{v}_0+\frac{\partial}{\partial \mathbf{r}}\cdot p_\alpha\vec{\mathrm{I}}-\rho_\alpha\mathbf{F}_\alpha^{(1)}-q_\alpha n_\alpha[\mathbf{v}_0\times\mathbf{B}]\right)\right]\right\}=\qquad(2.5)$$
$$\int\left(\frac{m_\alpha v_\alpha^2}{2}+\varepsilon_\alpha\right)J_\alpha^{st,el}d\mathbf{v}_\alpha+\int\left(\frac{m_\alpha v_\alpha^2}{2}+\varepsilon_\alpha\right)J_\alpha^{st,inel}d\mathbf{v}_\alpha.$$

and after summation the generalized energy equation for mixture

$$\frac{\partial}{\partial t}\left\{\frac{\rho v_0^2}{2}+\frac{3}{2}p+\sum_\alpha\varepsilon_\alpha n_\alpha-\sum_\alpha\tau_\alpha\left[\frac{\partial}{\partial t}\left(\frac{\rho_\alpha v_0^2}{2}+\frac{3}{2}p_\alpha+\varepsilon_\alpha n_\alpha\right)+\right.\right.$$
$$\left.\left.\frac{\partial}{\partial \mathbf{r}}\cdot\left(\frac{1}{2}\rho_\alpha v_0^2\mathbf{v}_0+\frac{5}{2}p_\alpha\mathbf{v}_0+\varepsilon_\alpha n_\alpha\mathbf{v}_0\right)-\mathbf{F}_\alpha^{(1)}\cdot\rho_\alpha\mathbf{v}_0\right]\right\}+$$
$$\frac{\partial}{\partial \mathbf{r}}\cdot\left\{\frac{1}{2}\rho v_0^2\mathbf{v}_0+\frac{5}{2}p\mathbf{v}_0+\mathbf{v}_0\sum_\alpha\varepsilon_\alpha n_\alpha-\sum_\alpha\tau_\alpha\left[\frac{\partial}{\partial t}\left(\frac{1}{2}\rho_\alpha v_0^2\mathbf{v}_0+\right.\right.\right.$$
$$\left.\left.\frac{5}{2}p_\alpha\mathbf{v}_0+\varepsilon_\alpha n_\alpha\mathbf{v}_0\right)+\frac{\partial}{\partial \mathbf{r}}\cdot\left(\frac{1}{2}\rho_\alpha v_0^2\mathbf{v}_0\mathbf{v}_0+\frac{7}{2}p_\alpha\mathbf{v}_0\mathbf{v}_0+\frac{1}{2}p_\alpha v_0^2\vec{\mathrm{I}}+\right.$$
$$\left.\left.\frac{5}{2}\frac{p_\alpha^2}{\rho_\alpha}\vec{\mathrm{I}}+\varepsilon_\alpha n_\alpha\mathbf{v}_0\mathbf{v}_0+\varepsilon_\alpha\frac{p_\alpha}{m_\alpha}\vec{\mathrm{I}}\right)-\rho_\alpha\mathbf{F}_\alpha^{(1)}\cdot\mathbf{v}_0\mathbf{v}_0-p_\alpha\mathbf{F}_\alpha^{(1)}\cdot\vec{\mathrm{I}}-\right.$$
$$\frac{1}{2}\rho_\alpha v_0^2\mathbf{F}_\alpha^{(1)}-\frac{3}{2}\mathbf{F}_\alpha^{(1)}p_\alpha-\frac{\rho_\alpha v_0^2}{2}\frac{q_\alpha}{m_\alpha}[\mathbf{v}_0\times\mathbf{B}]-\frac{5}{2}p_\alpha\frac{q_\alpha}{m_\alpha}[\mathbf{v}_0\times\mathbf{B}]-$$
$$\left.\varepsilon_\alpha n_\alpha\frac{q_\alpha}{m_\alpha}[\mathbf{v}_0\times\mathbf{B}]-\varepsilon_\alpha n_\alpha\mathbf{F}_\alpha^{(1)}\right]\Big\}-\mathbf{v}_0\cdot\sum_\alpha\rho_\alpha\mathbf{F}_\alpha^{(1)}+$$
$$\sum_\alpha\tau_\alpha\mathbf{F}_\alpha^{(1)}\cdot\left[\frac{\partial}{\partial t}(\rho_\alpha\mathbf{v}_0)+\frac{\partial}{\partial \mathbf{r}}\cdot\rho_\alpha\mathbf{v}_0\mathbf{v}_0+\frac{\partial}{\partial \mathbf{r}}\cdot p_\alpha\vec{\mathrm{I}}-\rho_\alpha\mathbf{F}_\alpha^{(1)}-q_\alpha n_\alpha[\mathbf{v}_0\times\mathbf{B}]\right]=0.$$

(2.6)

Here $\mathbf{F}_{\alpha}^{(1)}$ are the forces of the non-magnetic origin, $\mathbf{B}$ - magnetic induction, $\vec{\vec{\mathrm{I}}}$ - unit tensor, q_{α} - charge of the α-component particle, p_{α} - static pressure for α-component, ε_{α} - internal energy for the particles of α- component, $\mathbf{v}_0$ - hydrodynamic velocity for mixture. For calculations in the self-consistent electro-magnetic field the system of non-local Maxwell equations should be added (see (1.11), (1.12)).

It is well known that basic Schrödinger equation (SE) of quantum mechanics firstly was introduced as a quantum mechanical postulate. The obvious next step should be done and was realized by E. Madelung in 1927 – the derivation of special hydrodynamic form of SE after introduction wave function Ψ as

$$\Psi(x,y,z,t) = \alpha(x,y,z,t)\ e^{i\beta(x,y,z,t)}. \tag{2.7}$$

Using (2.7) and separating the real and imagine parts of SE one obtains

$$\frac{\partial \alpha^2}{\partial t} + \frac{\partial}{\partial \mathbf{r}} \cdot \left(\frac{\alpha^2 \hbar}{m} \frac{\partial \beta}{\partial \mathbf{r}} \right) = 0, \tag{2.8}$$

and Eq. (2.8) immediately transforms in continuity equation if the identifications in the Madelung's notations for density ρ and velocity $\mathbf{v}$

$$\rho = \alpha^2 = \Psi\Psi*, \tag{2.9}$$

$$\mathbf{v} = \frac{\partial}{\partial \mathbf{r}}(\beta\hbar / m) \tag{2.10}$$

introduce in Eq. (2.8). Identification for velocity (2.10) is obvious because for 1D flow

$$v = \frac{\partial}{\partial x}(\beta\hbar / m) = \frac{\hbar}{m}\frac{\partial}{\partial x}\left[-\frac{1}{\hbar}\left(E_k t - px\right)\right] = \frac{1}{m}\frac{\partial}{\partial x}\left(px\right) = v_{\phi}, \tag{2.11}$$

where v_{ϕ} is phase velocity. The existence of the condition (2.10) means that the corresponding flow has potential

$$\Phi = \beta\hbar / m. \tag{2.12}$$

As result two effective hydrodynamic equations take place:

$$\frac{\partial \rho}{\partial t} + \frac{\partial}{\partial \mathbf{r}} \cdot \left(\rho \mathbf{v}\right) = 0, \tag{2.13}$$

$$\frac{\partial \mathbf{v}}{\partial t} + \frac{1}{2}\frac{\partial}{\partial \mathbf{r}} v^2 = -\frac{1}{m}\frac{\partial}{\partial \mathbf{r}}\left(U - \frac{\hbar^2}{2m}\frac{\Delta\alpha}{\alpha}\right). \tag{2.14}$$

But

$$\frac{\Delta\alpha}{\alpha}=\frac{\Delta\alpha^2}{2\alpha^2}-\frac{1}{\alpha^2}\left(\frac{\partial\alpha}{\partial\mathbf{r}}\right)^2, \tag{2.15}$$

and the relation (2.15) transforms (2.14) in particular case of the Euler motion equation

$$\frac{\partial\mathbf{v}}{\partial t}+(\mathbf{v}\cdot\frac{\partial}{\partial\mathbf{r}})\mathbf{v}=-\frac{1}{m}\frac{\partial}{\partial\mathbf{r}}U^*, \tag{2.16}$$

where introduced the efficient potential

$$U^*=U-\frac{\hbar^2}{4m\rho}\left[\Delta\rho-\frac{1}{2\rho}\left(\frac{\partial\rho}{\partial\mathbf{r}}\right)^2\right]. \tag{2.17}$$

Additive quantum part of potential can be written in the so called Bohm form

$$\frac{\hbar^2}{2m\sqrt{\rho}}\Delta\sqrt{\rho}=\frac{\hbar^2}{4m\rho}\left[\Delta\rho-\frac{1}{2\rho}\left(\frac{\partial\rho}{\partial\mathbf{r}}\right)^2\right]. \tag{2.18}$$

Then

$$U^*=U+U_{qu}=U-\frac{\hbar^2}{2m\sqrt{\rho}}\Delta\sqrt{\rho}=U-\frac{\hbar^2}{4m\rho}\left[\Delta\rho-\frac{1}{2\rho}\left(\frac{\partial\rho}{\partial\mathbf{r}}\right)^2\right]. \tag{2.19}$$

Some remarks:

a) SE transforms in hydrodynamic form without additional assumptions. But numerical methods of hydrodynamics are very good developed. As result at the end of seventieth of the last century we realized the systematic calculations of quantum problems using quantum hydrodynamics (see for example [1,28].
b) SE reduces to the system of continuity equation and particular case of the Euler equation with the additional potential proportional to $\hbar^2$. The physical sense and the origin of the Bohm potential are established later in [7, 8, 29].
c) SE (obtained in the frame of the theory of classical complex variables) cannot contain the energy equation in principle. As result in many cases the palliative approach is used when for solution of dissipative quantum problems the classical hydrodynamics is used with insertion of additional Bohm potential in the system of hydrodynamic equations.
d) The system of the generalized quantum hydrodynamic equations contains energy equation written for unknown dependent value which can be specified as quantum pressure p_α of non-local origin.

The transport properties in graphene can be described at low energies by a massless Dirac-fermion model with chiral quasiparticles [30,31]. The Boltzmann and Schrödinger approaches are used also [32,33]. Applications of these approaches are directed on the calculation of kinetic coefficients. The non-local kinetic equations also are used by the authors of this article for calculation of graphene electrical conductivity [34]. Here we intend to investigate the possibilities of non-local quantum hydrodynamics for modeling of the charge density waves in grafene. In non-local quantum hydrodynamics the many particles correlations manifest itself in equations in the terms proportional to non-locality parameter τ

The influence of spin and magnetic moment of particles can be taken into account by the natural elegant way via the internal energy of particles. Really for example electron has the internal energy ε

$$\varepsilon = \varepsilon_{el,sp} + \varepsilon_{el,m}, \tag{2.20}$$

containing the spin and magnetic parts, namely

$$\varepsilon_{el,sp} = \hbar\omega/2, \ \varepsilon_{el,m} = -\mathbf{p_m}\cdot\mathbf{B}; \tag{2.21}$$

$\mathbf{p_m}$ - electron magnetic moment, $\mathbf{B}$ - magnetic induction. But $p_m = -\frac{e}{m_e}\frac{\hbar}{2c}$, then $\varepsilon_{el} = \frac{\hbar}{2}\omega_{eff}$. Relation (2.20) can be written as

$$\varepsilon = \frac{\hbar}{2}\left[\omega \pm \frac{e}{m_e c}B\right], \tag{2.22}$$

if $\mathbf{B}$ is directed along the spin direction. On this stage of investigations we omit the influence of the internal energy of particles, therefore spin waves will be investigated separately.

3. GENERALIZED QUANTUM HYDRODYNAMIC EQUATIONS DESCRIBING THE SOLITON MOVEMENT IN THE CRYSTAL LATTICE

Let us consider the charge density waves which are periodic modulation of conduction electron density. From direct observations of charge density waves follow that CDW develop at zero external fields. For our aims is sufficient in the following to suppose that the effective charge movement was created in graphene lattice as result of an initial fluctuation.

The movement of the soliton waves at the presence of the external electrical potential difference will be considered also in this article.

The effective charge is created due to interference of the induced electron waves and correlating potentials as result of the polarized modulation of atomic positions. Therefore in this approach the conduction in graphene convoys the transfer of the positive ($+e, m_p$) and negative ($-e, m_e$) charges. Let us formulate the problem in detail. The non-stationary 1D motion of the combined soliton is considered under influence of the self-consistent electric forces of the potential and non-potential origin. It was shown [22-24] that mentioned soliton can exist without a chemical bond formation. First of all for better understanding of the situation let us investigate the situation for the case when the external forces are absent. Introduce the coordinate system ($\xi = x - Ct$) moving along the positive direction of the x axis with the velocity $C = u_0$, which is equal to the phase velocity of this quantum object.

Let us find the soliton type solutions for the system of the generalized quantum equations for two species mixture. The graphene crystal lattice is 2D flat structure which is considered in the moving coordinate system ($\xi = x - u_0 t, y$). In the following we intend (without taking into account the component's internal energy) to apply generalized non-local quantum

hydrodynamic equations (2.1) – (2.6) to the investigation of the charge density waves (CDW) in the frame of two species model which lied to the following dimensional equations [6, 8]: Poisson equation for the self-consistent electric field:

$$\frac{\partial^2\varphi}{\partial\xi^2}+\frac{\partial^2\varphi}{\partial y^2}=-4\pi e\left\{\left[n_p-\tau_p\frac{\partial}{\partial\xi}\left(n_p\left(u-u_0\right)\right)\right]-\left[n_e-\tau_e\frac{\partial}{\partial\xi}\left(n_e\left(u-u_0\right)\right)\right]\right\} \tag{3.1}$$

Continuity equation for the positive particles:

$$\begin{aligned}&\frac{\partial}{\partial\xi}\left[\rho_p\left(u_0-u\right)\right]+\frac{\partial}{\partial\xi}\left\{\tau_p\frac{\partial}{\partial\xi}\left[\rho_p\left(u-u_0\right)^2\right]\right\}+\\&\frac{\partial}{\partial\xi}\left\{\tau_p\left[\frac{\partial}{\partial\xi}p_p-\rho_pF_{p\xi}\right]\right\}+\frac{\partial}{\partial y}\left\{\tau_p\left[\frac{\partial}{\partial y}p_p-\rho_pF_{py}\right]\right\}=0\end{aligned} \tag{3.2}$$

Continuity equation for electrons:

$$\begin{aligned}&\frac{\partial}{\partial\xi}\left[\rho_e\left(u_0-u\right)\right]+\frac{\partial}{\partial\xi}\left\{\tau_e\frac{\partial}{\partial\xi}\left[\rho_e\left(u-u_0\right)^2\right]\right\}+\\&\frac{\partial}{\partial\xi}\left\{\tau_e\left[\frac{\partial}{\partial\xi}p_e-\rho_eF_{e\xi}\right]\right\}+\frac{\partial}{\partial y}\left\{\tau_e\left[\frac{\partial}{\partial y}p_e-\rho_eF_{ey}\right]\right\}=0\end{aligned} \tag{3.3}$$

Momentum equation for the *x* direction:

$$\begin{aligned}&\frac{\partial}{\partial\xi}\left\{\rho u\left(u-u_0\right)+p\right\}-\rho_pF_{p\xi}-\rho_eF_{e\xi}+\\&\frac{\partial}{\partial\xi}\left\{\tau_p\left[\frac{\partial}{\partial\xi}\left(2p_p\left(u_0-u\right)-\rho_pu\left(u_0-u\right)^2\right)-\rho_pF_{p\xi}\left(u_0-u\right)\right]\right\}+\\&\frac{\partial}{\partial\xi}\left\{\tau_e\left[\frac{\partial}{\partial\xi}\left(2p_e\left(u_0-u\right)-\rho_eu\left(u_0-u\right)^2\right)-\rho_eF_{e\xi}\left(u_0-u\right)\right]\right\}+\\&\tau_pF_{p\xi}\left(\frac{\partial}{\partial\xi}\left(\rho_p\left(u-u_0\right)\right)\right)+\tau_eF_{e\xi}\left(\frac{\partial}{\partial\xi}\left(\rho_e\left(u-u_0\right)\right)\right)-\\&\frac{\partial}{\partial\xi}\left\{\tau_p\frac{\partial}{\partial\xi}\left(p_pu\right)\right\}-\frac{\partial}{\partial\xi}\left\{\tau_e\frac{\partial}{\partial\xi}\left(p_eu\right)\right\}-\frac{\partial}{\partial y}\left\{\tau_p\frac{\partial}{\partial y}\left(p_pu\right)\right\}-\frac{\partial}{\partial y}\left\{\tau_e\frac{\partial}{\partial y}\left(p_eu\right)\right\}+\\&\frac{\partial}{\partial\xi}\left\{\tau_p\left[F_{p\xi}\rho_pu\right]\right\}+\frac{\partial}{\partial\xi}\left\{\tau_e\left[F_{e\xi}\rho_eu\right]\right\}+\frac{\partial}{\partial y}\left\{\tau_p\left[F_{py}\rho_pu\right]\right\}+\frac{\partial}{\partial y}\left\{\tau_e\left[F_{ey}\rho_eu\right]\right\}=0\end{aligned} \tag{3.4}$$

Energy equation for the positive particles:

$$\begin{aligned}
&\frac{\partial}{\partial\xi}\left[\rho_p u^2(u-u_0)+5p_p u-3p_p u_0\right]-2\rho_p F_{p\xi}u+\\
&\frac{\partial}{\partial\xi}\left\{\tau_p\left[\begin{array}{l}\dfrac{\partial}{\partial\xi}\left(-\rho_p u^2(u_0-u)^2+7p_p u(u_0-u)+3p_p u_0(u-u_0)-p_p u^2-5\dfrac{p_p^2}{\rho_p}\right)-\\ -2F_{p\xi}\rho_p u(u_0-u)+\rho_p u^2F_{p\xi}+5p_pF_{p\xi}\end{array}\right]\right\}-\\
&\frac{\partial}{\partial y}\left\{\tau_p\left[\frac{\partial}{\partial y}\left(p_p u^2+5\frac{p_p^2}{\rho_p}\right)-\rho_p F_{py}u^2-5p_pF_{py}\right]\right\}-\\
&2\tau_p F_{p\xi}\left[\frac{\partial}{\partial\xi}\left(\rho_p u(u_0-u)\right)\right]-2\tau_p\rho_p\left[(F_{p\xi})^2+(F_{py})^2\right]+\\
&2\tau_p F_{p\xi}\left[\frac{\partial}{\partial\xi}p_p\right]+2\tau_p F_{py}\left[\frac{\partial}{\partial y}p_p\right]=-\frac{p_p-p_e}{\tau_{ep}}
\end{aligned}\tag{3.5}$$

Energy equation for electrons:

$$\begin{aligned}
&\frac{\partial}{\partial\xi}\left[\rho_e u^2(u-u_0)+5p_e u-3p_e u_0\right]-2\rho_e F_{e\xi}u+\\
&\frac{\partial}{\partial\xi}\left\{\tau_e\left[\begin{array}{l}\dfrac{\partial}{\partial\xi}\left(-\rho_e u^2(u_0-u)^2+7p_e u(u_0-u)+3p_e u_0(u-u_0)-p_e u^2-5\dfrac{p_e^2}{\rho_e}\right)-\\ -2F_{e\xi}\rho_e u(u_0-u)+\rho_e u^2F_{e\xi}+5p_eF_{e\xi}\end{array}\right]\right\}-\\
&\frac{\partial}{\partial y}\left\{\tau_e\left[\frac{\partial}{\partial y}\left(p_e u^2+5\frac{p_e^2}{\rho_e}\right)-\rho_e F_{ey}u^2-5p_eF_{ey}\right]\right\}-\\
&2\tau_e F_{e\xi}\left[\frac{\partial}{\partial\xi}\left(\rho_e u(u_0-u)\right)\right]-2\tau_e\rho_e\left[(F_{e\xi})^2+(F_{ey})^2\right]+\\
&2\tau_e F_{e\xi}\left[\frac{\partial}{\partial\xi}p_e\right]+2\tau_e F_{ey}\left[\frac{\partial}{\partial y}p_e\right]=-\frac{p_e-p_p}{\tau_{ep}}
\end{aligned}\tag{3.6}$$

Here u - hydrodynamic velocity; φ - self-consistent electric potential; ρ_e , ρ_p - densities for the electron and positive species; p_e, p_p - quantum electron pressure and the pressure of positive species; F_e, F_p - the forces acting on the mass unit of electrons and the positive particles.

The right hand sides of the energy equations are written in the relaxation forms following from BGK kinetic approximation

Non-local parameters can be written in the form (see (1.14))

$$\tau_p = \frac{N_R \hbar}{m_p u^2},\ \tau_e = \frac{N_R \hbar}{m_e u^2},\ \ \frac{1}{\tau_{ep}} = \frac{1}{\tau_e} + \frac{1}{\tau_p} \tag{3.7}$$

where N_R - integer.

Acting forces are the sum of three terms: the self-consistent potential force (scalar potential φ), connected with the displacement of positive and negative charges, potential forces originated by the graphene crystal lattice (potential U) and the external electrical field creating the intensity **E**. As result the following relations are valid

$$F_{p\xi} = \frac{e}{m_p}\left(-\frac{\partial\varphi}{\partial\xi} - \frac{\partial U}{\partial\xi} + E_{0\xi}\right),\quad F_{e\xi} = \frac{e}{m_e}\left(\frac{\partial\varphi}{\partial\xi} + \frac{\partial U}{\partial\xi} - E_{0\xi}\right),$$

$$F_{py} = \frac{e}{m_p}\left(-\frac{\partial\varphi}{\partial y} - \frac{\partial U}{\partial y} + E_{0y}\right),\quad F_{ey} = \frac{e}{m_e}\left(\frac{\partial\varphi}{\partial y} + \frac{\partial U}{\partial y} - E_{0y}\right). \tag{3.8}$$

Let write down these equations in the dimensionless form, where dimensionless symbols are marked by tildes; introduce the scales:

$$u = u_0\tilde{u},\quad \xi = x_0\tilde{\xi},\ y = x_0\tilde{y},\quad \varphi = \varphi_0\tilde{\varphi},\qquad \rho_e = \rho_0\tilde{\rho}_e,\ \rho_p = \rho_0\tilde{\rho}_p,$$

where u_0, x_0, φ_0, ρ_0 - scales for velocity, distance, potential and density. Let there be also $p_p = \rho_0 V_{0p}^2 \tilde{p}_p$, $p_e = \rho_0 V_{0e}^2 \tilde{p}_e$, where V_{0p} и V_{0e} - the scales for thermal velocities for the electron and positive species; $F_p = \tilde{\mathrm{F}}_\mathrm{p}\frac{e\varphi_0}{m_p x_0}$, $F_e = \tilde{\mathrm{F}}_\mathrm{e}\frac{e\varphi_0}{m_e x_0}$; $\tau_p = \frac{m_e x_0 H}{m_p u_0 \tilde{u}^2}$, $\tau_e = \frac{x_0 H}{u_0 \tilde{u}^2}$, where dimensionless parameter $H = \frac{N_R\hbar}{m_e x_0 u_0}$ is introduced. Then $\frac{1}{\tau_{ep}} = \frac{u_0}{x_0}\frac{\tilde{u}^2}{H}\left(1 + \frac{m_p}{m_e}\right)$.

Let us introduce also the following dimensionless parameters

$$R = \frac{e\rho_0 x_0^2}{m_e\varphi_0},\ E = \frac{\mathrm{e}\varphi_0}{m_e u_0^2}. \tag{3.9}$$

Taking into account the introduced values the following system of dimensionless non-local hydrodynamic equations for the 2D soliton description can be written:
Poisson equation for the self-consistent electric field:

$$\frac{\partial^2\widetilde{\varphi}}{\partial\widetilde{\xi}^{\,2}}+\frac{\partial^2\widetilde{\varphi}}{\partial\widetilde{y}^{\,2}}=-4\pi R\left\{\frac{m_e}{m_p}\left[\widetilde{\rho}_p-\frac{m_e H}{m_p\widetilde{u}^{\,2}}\frac{\partial}{\partial\widetilde{\xi}}\left(\widetilde{\rho}_p\left(\widetilde{u}-1\right)\right)\right]-\left[\widetilde{\rho}_e-\frac{H}{\widetilde{u}^{\,2}}\frac{\partial}{\partial\widetilde{\xi}}\left(\widetilde{\rho}_e\left(\widetilde{u}-1\right)\right)\right]\right\}. \quad (3.10)$$

Continuity equation for the positive particles:

$$\begin{aligned}&\frac{\partial}{\partial\widetilde{\xi}}\left[\widetilde{\rho}_p\left(1-\widetilde{u}\right)\right]+\frac{m_e}{m_p}\frac{\partial}{\partial\widetilde{\xi}}\left\{\frac{H}{\widetilde{u}^{\,2}}\frac{\partial}{\partial\widetilde{\xi}}\left[\widetilde{\rho}_p\left(\widetilde{u}-1\right)^2\right]\right\}+\\&\frac{m_e}{m_p}\frac{\partial}{\partial\widetilde{\xi}}\left\{\frac{H}{\widetilde{u}^{\,2}}\left[\frac{V_{0p}^2}{u_0^2}\frac{\partial}{\partial\widetilde{\xi}}\widetilde{p}_p-\frac{m_e}{m_p}E\widetilde{\rho}_p\widetilde{\mathrm{F}}_{\mathrm{p}\xi}\right]\right\}+\\&\frac{m_e}{m_p}\frac{\partial}{\partial\widetilde{y}}\left\{\frac{H}{\widetilde{u}^{\,2}}\left[\frac{V_{0p}^2}{u_0^2}\frac{\partial}{\partial\widetilde{y}}\widetilde{p}_p-\frac{m_e}{m_p}E\widetilde{\rho}_p\widetilde{\mathrm{F}}_{\mathrm{py}}\right]\right\}=0\end{aligned} \quad (3.11)$$

Continuity equation for electrons:

$$\begin{aligned}&\frac{\partial}{\partial\widetilde{\xi}}\left[\widetilde{\rho}_e\left(1-\widetilde{u}\right)\right]+\frac{\partial}{\partial\widetilde{\xi}}\left\{\frac{H}{\widetilde{u}^{\,2}}\frac{\partial}{\partial\widetilde{\xi}}\left[\widetilde{\rho}_e\left(\widetilde{u}-1\right)^2\right]\right\}+\\&\frac{\partial}{\partial\widetilde{\xi}}\left\{\frac{H}{\widetilde{u}^{\,2}}\left[\frac{V_{0e}^2}{u_0^2}\frac{\partial}{\partial\widetilde{\xi}}\widetilde{p}_e-\widetilde{\rho}_e E\widetilde{\mathrm{F}}_{\mathrm{e}\xi}\right]\right\}+\frac{\partial}{\partial\widetilde{y}}\left\{\frac{H}{\widetilde{u}^{\,2}}\left[\frac{V_{0e}^2}{u_0^2}\frac{\partial}{\partial\widetilde{y}}\widetilde{p}_e-\widetilde{\rho}_e E\widetilde{\mathrm{F}}_{\mathrm{ey}}\right]\right\}=0\end{aligned} \quad (3.12)$$

Momentum equation for the *x* direction:

$$\begin{aligned}&\frac{\partial}{\partial\widetilde{\xi}}\left\{\left(\widetilde{\rho}_p+\widetilde{\rho}_e\right)\widetilde{u}\left(\widetilde{u}-1\right)+\frac{V_{0p}^2}{u_0^2}\widetilde{p}_p+\frac{V_{0e}^2}{u_0^2}\widetilde{p}_e\right\}-\frac{m_e}{m_p}\widetilde{\rho}_p E\widetilde{\mathrm{F}}_{\mathrm{p}\xi}-\widetilde{\rho}_e E\widetilde{\mathrm{F}}_{\mathrm{e}\xi}+\\&\frac{m_e}{m_p}\frac{\partial}{\partial\widetilde{\xi}}\left\{\frac{H}{\widetilde{u}^{\,2}}\left[\frac{\partial}{\partial\widetilde{\xi}}\left(2\frac{V_{0p}^2}{u_0^2}\widetilde{p}_p\left(1-\widetilde{u}\right)-\widetilde{\rho}_p\widetilde{u}\left(1-\widetilde{u}\right)^2\right)-\frac{m_e}{m_p}\widetilde{\rho}_p E\widetilde{\mathrm{F}}_{\mathrm{p}\xi}\left(1-\widetilde{u}\right)\right]\right\}+\\&\frac{\partial}{\partial\widetilde{\xi}}\left\{\frac{H}{\widetilde{u}^{\,2}}\left[\frac{\partial}{\partial\widetilde{\xi}}\left(2\frac{V_{0e}^2}{u_0^2}\widetilde{p}_e\left(1-\widetilde{u}\right)-\widetilde{\rho}_e\widetilde{u}\left(1-\widetilde{u}\right)^2\right)-\widetilde{\rho}_e E\widetilde{\mathrm{F}}_{\mathrm{e}\xi}\left(1-\widetilde{u}\right)\right]\right\}+\\&\frac{H}{\widetilde{u}^{\,2}}E\left(\frac{m_e}{m_p}\right)^2\widetilde{\mathrm{F}}_{\mathrm{p}\xi}\left(\frac{\partial}{\partial\widetilde{\xi}}\left(\widetilde{\rho}_p\left(\widetilde{u}-1\right)\right)\right)+\frac{H}{\widetilde{u}^{\,2}}E\widetilde{\mathrm{F}}_{\mathrm{e}\xi}\left(\frac{\partial}{\partial\widetilde{\xi}}\left(\widetilde{\rho}_e\left(\widetilde{u}-1\right)\right)\right)-\\&\frac{m_e}{m_p}\frac{\partial}{\partial\widetilde{\xi}}\left\{\frac{H}{\widetilde{u}^{\,2}}\frac{V_{0p}^2}{u_0^2}\frac{\partial}{\partial\widetilde{\xi}}\left(\widetilde{p}_p\widetilde{u}\right)\right\}-\frac{\partial}{\partial\widetilde{\xi}}\left\{\frac{H}{\widetilde{u}^{\,2}}\frac{V_{0e}^2}{u_0^2}\frac{\partial}{\partial\widetilde{\xi}}\left(\widetilde{p}_e\widetilde{u}\right)\right\}-\end{aligned}$$

$$\frac{m_e}{m_p}\frac{\partial}{\partial\tilde{y}}\left\{\frac{H}{\tilde{u}^2}\frac{V_{0p}^2}{u_0^2}\frac{\partial}{\partial\tilde{y}}\left(\tilde{p}_p\tilde{u}\right)\right\}-\frac{\partial}{\partial\tilde{y}}\left\{\frac{H}{\tilde{u}^2}\frac{V_{0e}^2}{u_0^2}\frac{\partial}{\partial\tilde{y}}\left(\tilde{p}_e\tilde{u}\right)\right\}+$$
$$\left(\frac{m_e}{m_p}\right)^2\frac{\partial}{\partial\tilde{\xi}}\left\{\frac{H}{\tilde{u}^2}E\left[\tilde{\mathrm{F}}_{\mathrm{p}\xi}\tilde{\rho}_p\tilde{u}\right]\right\}+\frac{\partial}{\partial\tilde{\xi}}\left\{\frac{H}{\tilde{u}^2}E\left[\tilde{\mathrm{F}}_{\mathrm{e}\xi}\tilde{\rho}_e\tilde{u}\right]\right\}+$$
$$\left(\frac{m_e}{m_p}\right)^2\frac{\partial}{\partial\tilde{y}}\left\{\frac{H}{\tilde{u}^2}E\left[\tilde{\mathrm{F}}_{\mathrm{py}}\tilde{\rho}_p\tilde{u}\right]\right\}+\frac{\partial}{\partial\tilde{y}}\left\{\frac{H}{\tilde{u}^2}E\left[\tilde{\mathrm{F}}_{\mathrm{ey}}\tilde{\rho}_e\tilde{u}\right]\right\}=0 \qquad (3.13)$$

Energy equation for the positive particles:

$$\frac{\partial}{\partial\tilde{\xi}}\left[\tilde{\rho}_p\tilde{u}^2\left(\tilde{u}-1\right)+5\frac{V_{0p}^2}{u_0^2}\tilde{p}_p\tilde{u}-3\frac{V_{0p}^2}{u_0^2}\tilde{p}_p\right]-2\frac{m_e}{m_p}\tilde{\rho}_pE\tilde{\mathrm{F}}_{\mathrm{p}\xi}\tilde{u}+$$
$$\frac{\partial}{\partial\tilde{\xi}}\left\{\frac{H}{\tilde{u}^2}\frac{m_e}{m_p}\left[\begin{array}{l}\frac{\partial}{\partial\tilde{\xi}}\left(-\tilde{\rho}_p\tilde{u}^2\left(1-\tilde{u}\right)^2+7\frac{V_{0p}^2}{u_0^2}\tilde{p}_p\tilde{u}\left(1-\tilde{u}\right)+3\frac{V_{0p}^2}{u_0^2}\tilde{p}_p\left(\tilde{u}-1\right)-\frac{V_{0p}^2}{u_0^2}\tilde{p}_p\tilde{u}^2-\right.\\ \left.5\frac{V_{0p}^4}{u_0^4}\frac{\tilde{p}_p^2}{\tilde{\rho}_p}\right)-2\frac{m_e}{m_p}E\tilde{\mathrm{F}}_{\mathrm{p}\xi}\tilde{\rho}_p\tilde{u}\left(1-\tilde{u}\right)+\frac{m_e}{m_p}\tilde{\rho}_p\tilde{u}^2E\tilde{\mathrm{F}}_{\mathrm{p}\xi}+5\frac{m_e}{m_p}\frac{V_{0p}^2}{u_0^2}\tilde{p}_pE\tilde{\mathrm{F}}_{\mathrm{p}\xi}\end{array}\right]\right\}-$$
$$\frac{\partial}{\partial\tilde{y}}\left\{\frac{H}{\tilde{u}^2}\frac{m_e}{m_p}\left[\frac{\partial}{\partial\tilde{y}}\left(\frac{V_{0p}^2}{u_0^2}\tilde{p}_p\tilde{u}^2+5\frac{V_{0p}^4}{u_0^4}\frac{\tilde{p}_p^2}{\tilde{\rho}_p}\right)-\frac{m_e}{m_p}\tilde{\rho}_pE\tilde{\mathrm{F}}_{\mathrm{py}}\tilde{u}^2-5\frac{m_e}{m_p}\frac{V_{0p}^2}{u_0^2}\tilde{p}_pE\tilde{\mathrm{F}}_{\mathrm{py}}\right]\right\}-$$
$$2\frac{H}{\tilde{u}^2}\left(\frac{m_e}{m_p}\right)^2E\tilde{\mathrm{F}}_{\mathrm{p}\xi}\left[\frac{\partial}{\partial\tilde{\xi}}\left(\tilde{\rho}_p\tilde{u}\left(1-\tilde{u}\right)\right)\right]-2\frac{H}{\tilde{u}^2}\left(\frac{m_e}{m_p}\right)^3\tilde{\rho}_pE^2\left[\left(\tilde{\mathrm{F}}_{\mathrm{p}\xi}\right)^2+\left(\tilde{\mathrm{F}}_{\mathrm{py}}\right)^2\right]+$$
$$2\frac{H}{\tilde{u}^2}\left(\frac{m_e}{m_p}\right)^2E\tilde{\mathrm{F}}_{\mathrm{p}\xi}\left[\frac{V_{0p}^2}{u_0^2}\frac{\partial}{\partial\tilde{\xi}}\tilde{p}_p\right]+2\frac{H}{\tilde{u}^2}\left(\frac{m_e}{m_p}\right)^2E\tilde{\mathrm{F}}_{\mathrm{py}}\left[\frac{V_{0p}^2}{u_0^2}\frac{\partial}{\partial\tilde{y}}\tilde{p}_p\right]=$$
$$-\frac{\tilde{u}^2}{Hu_0^2}\left(V_{0p}^2\tilde{p}_p-\tilde{p}_eV_{0e}^2\right)\left(1+\frac{m_p}{m_e}\right) \qquad (3.14)$$

Energy equation for electrons:

$$\frac{\partial}{\partial\tilde{\xi}}\left[\tilde{\rho}_e\tilde{u}^2\left(\tilde{u}-1\right)+5\frac{V_{0e}^2}{u_0^2}\tilde{p}_e\tilde{u}-3\frac{V_{0e}^2}{u_0^2}\tilde{p}_e\right]-2\tilde{\rho}_eE\tilde{\mathrm{F}}_{\mathrm{e}\xi}\tilde{u}+$$
$$\frac{\partial}{\partial\tilde{\xi}}\left\{\frac{H}{\tilde{u}^2}\left[\begin{array}{l}\frac{\partial}{\partial\tilde{\xi}}\left(-\tilde{\rho}_e\tilde{u}^2\left(1-\tilde{u}\right)^2+7\frac{V_{0e}^2}{u_0^2}\tilde{p}_e\tilde{u}\left(1-\tilde{u}\right)+3\frac{V_{0e}^2}{u_0^2}\tilde{p}_e\left(\tilde{u}-1\right)-\frac{V_{0e}^2}{u_0^2}\tilde{p}_e\tilde{u}^2-\right.\\ \left.5\frac{V_{0e}^4}{u_0^4}\frac{\tilde{p}_e^2}{\tilde{\rho}_e}\right)-2E\tilde{\mathrm{F}}_{\mathrm{e}\xi}\tilde{\rho}_e\tilde{u}\left(1-\tilde{u}\right)+\tilde{\rho}_e\tilde{u}^2E\tilde{\mathrm{F}}_{\mathrm{e}\xi}+5\frac{V_{0e}^2}{u_0^2}\tilde{p}_eE\tilde{\mathrm{F}}_{\mathrm{e}\xi}\end{array}\right]\right\}-$$
$$\frac{\partial}{\partial\tilde{y}}\left\{\frac{H}{\tilde{u}^2}\left[\frac{\partial}{\partial\tilde{y}}\left(\frac{V_{0e}^2}{u_0^2}\tilde{p}_e\tilde{u}^2+5\frac{V_{0e}^4}{u_0^4}\frac{\tilde{p}_e^2}{\tilde{\rho}_e}\right)-\tilde{\rho}_eE\tilde{\mathrm{F}}_{\mathrm{ey}}\tilde{u}^2-5\frac{V_{0e}^2}{u_0^2}\tilde{p}_eE\tilde{\mathrm{F}}_{\mathrm{ey}}\right]\right\}-$$
$$2\frac{H}{\tilde{u}^2}E\tilde{\mathrm{F}}_{\mathrm{e}\xi}\left[\frac{\partial}{\partial\tilde{\xi}}\left(\tilde{\rho}_e\tilde{u}\left(1-\tilde{u}\right)\right)\right]-2\frac{H}{\tilde{u}^2}\tilde{\rho}_eE^2\left[\left(\tilde{\mathrm{F}}_{\mathrm{e}\xi}\right)^2+\left(\tilde{\mathrm{F}}_{\mathrm{ey}}\right)^2\right]+$$
$$2\frac{H}{\tilde{u}^2}E\tilde{F}_{e\xi}\left[\frac{V_{0e}^2}{u_0^2}\frac{\partial}{\partial\tilde{\xi}}\tilde{p}_e\right]+2\frac{H}{\tilde{u}^2}E\tilde{\mathrm{F}}_{\mathrm{ey}}\left[\frac{V_{0e}^2}{u_0^2}\frac{\partial}{\partial\tilde{y}}\tilde{p}_e\right]=$$
$$-\frac{\tilde{u}^2}{Hu_0^2}\left(V_{0e}^2\tilde{p}_e-V_{0p}^2\tilde{p}_p\right)\left(1+\frac{m_p}{m_e}\right) \qquad (3.15)$$

We have the following dimensionless relations for forces:

$$\widetilde{\mathrm{F}}_{\mathrm{p}\xi} = -\frac{\partial\widetilde{\varphi}}{\partial\widetilde{\xi}} - \frac{\partial\widetilde{U}}{\partial\widetilde{\xi}} + \widetilde{E}_{\xi}, \quad \widetilde{\mathrm{F}}_{\mathrm{e}\xi} = \frac{\partial\widetilde{\varphi}}{\partial\widetilde{\xi}} + \frac{\partial\widetilde{U}}{\partial\widetilde{\xi}} - \widetilde{E}_{\xi},$$

$$\widetilde{\mathrm{F}}_{\mathrm{py}} = -\frac{\partial\widetilde{\varphi}}{\partial\widetilde{y}} - \frac{\partial\widetilde{U}}{\partial\widetilde{y}} + \widetilde{E}_{y}, \quad \widetilde{\mathrm{F}}_{\mathrm{ey}} = \frac{\partial\widetilde{\varphi}}{\partial\widetilde{y}} + \frac{\partial\widetilde{U}}{\partial\widetilde{y}} - \widetilde{E}_{y}. \tag{3.16}$$

Graphene is a single layer of carbon atoms densely packed in a honeycomb lattice. Figure 1 reflects the structure of graphene as the 2D hexagonal carbon crystal, the distance a between the nearest atoms is equal to $a = 0.142 \quad nm$.

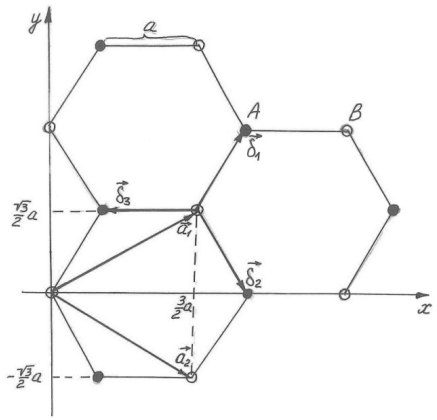

Figure. 1. Crystal graphene lattice

Elementary cell contains two atoms (for example A and B, Figure 1) and the primitive lattice vectors are given by

$$\mathbf{a}_1 = \frac{a}{2}\left(3;\sqrt{3}\right), \ \mathbf{a}_2 = \frac{a}{2}\left(3;-\sqrt{3}\right).$$

Coordinates of the nearest atoms to the given atom define by vectors

$$\boldsymbol{\delta}_1 = \frac{a}{2}\left(1;\sqrt{3}\right), \ \boldsymbol{\delta}_2 = \frac{a}{2}\left(1;-\sqrt{3}\right), \ \boldsymbol{\delta}_3 = -a\left(1;0\right).$$

Six neighboring atoms of the second order are placed in knots defined by vectors

$$\boldsymbol{\delta}'_1 = \pm\mathbf{a}_1, \ \boldsymbol{\delta}'_2 = \pm\mathbf{a}_2, \ \boldsymbol{\delta}'_3 = \pm\left(\mathbf{a}_2 - \mathbf{a}_1\right).$$

Let us take the first atom of the elementary cell in the origin of the coordinate system (Figure. 1) and compose the radii-vector of the second atom with respect to the basis $\mathbf{a}_1$ и $\mathbf{a}_2$:

$$\mathbf{r}_1 = u\mathbf{a}_1 + v\mathbf{a}_2 = u\left(3\frac{a}{2}\mathbf{e}_x + \sqrt{3}\frac{a}{2}\mathbf{e}_y\right) + v\left(3\frac{a}{2}\mathbf{e}_x - \sqrt{3}\frac{a}{2}\mathbf{e}_y\right). \tag{3.17}$$

Let us find *u* и *v*, taking into account that

$$\mathbf{r}_1 = \boldsymbol{\delta}_1 = \frac{a}{2}\left(1;\sqrt{3}\right) = \frac{a}{2}\mathbf{e}_x + \frac{a}{2}\sqrt{3}\mathbf{e}_y . \tag{3.18}$$

Equalizing (3.17) и (3.18), we have $u = \frac{2}{3}$, $v = -\frac{1}{3}$, then

$$\mathbf{r}_1 = \frac{2}{3}\mathbf{a}_1 - \frac{1}{3}\mathbf{a}_2 . \tag{3.19}$$

Assume that $V_1(\mathbf{r})$ is the periodical potential created by one sublattice. Then potential of crystal is

$$V(\mathbf{r}) = V_1(\mathbf{r}) + V_1(\mathbf{r} - \mathbf{r}_1) = \sum_{n=0}^{1} V_1(\mathbf{r} - \mathbf{r}_n) . \tag{3.20}$$

Atoms in crystal form the periodic structure and as the consequence the corresponding potential is periodic function

$$V_1(\mathbf{r}) = V_1(\mathbf{r} + \mathbf{a}_m),$$

where for 2D structure

$$\mathbf{a}_m = m_1\mathbf{a}_1 + m_2\mathbf{a}_2,$$

and m_1 и m_2 are arbitrary entire numbers. Expanding $V_1(\mathbf{r})$ in the Fourier series one obtains

$$V_1(\mathbf{r} - \mathbf{r}_n) = \sum_{\mathbf{b}} V_{\mathbf{b}} e^{i\mathbf{b}\cdot(\mathbf{r}-\mathbf{r}_n)} . \tag{3.21}$$

In our case the both basis atoms (*n*=0,1) are the same. Here

$$\mathbf{b} = g_1\mathbf{b}_1 + g_2\mathbf{b}_2 ,$$

$\mathbf{b}_1$ и $\mathbf{b}_2$ are the translational vectors of the reciprocal lattice. For graphene

$$\mathbf{b}_1 = \frac{2\pi}{3a}\left(1;\sqrt{3}\right), \quad \mathbf{b}_2 = \frac{2\pi}{3a}\left(1;-\sqrt{3}\right). \tag{3.22}$$

Then

$$V(\mathbf{r}) = \sum_{\mathbf{b}} \sum_{n=0}^{1} V_{1\mathbf{b}} e^{i\mathbf{b}\cdot(\mathbf{r}-\mathbf{r}_n)} = \sum_{\mathbf{b}} V_{\mathbf{b}} e^{i\mathbf{b}\cdot\mathbf{r}} , \tag{3.23}$$

where $V_{\mathbf{b}} = V_{1\mathbf{b}} \cdot \sum_n e^{-i\mathbf{b}\cdot\mathbf{r}_n} = V_{1\mathbf{b}} \cdot S_{\mathbf{b}}$. The structure factor $S_{\mathbf{b}}$ for graphene:

$$S_{\mathbf{b}} = e^{-i\mathbf{b}\cdot 0} + e^{-i\mathbf{b}\cdot\left(\frac{2}{3}\mathbf{a}_1 - \frac{1}{3}\mathbf{a}_2\right)} = 1 + e^{i\frac{2\pi}{3}(g_2 - 2g_1)} . \tag{3.24}$$

$$V(\mathbf{r}) = \sum_{g_1,g_2} V_{1g_1,g_2} e^{i(g_1\mathbf{b}_1+g_2\mathbf{b}_2)\cdot\mathbf{r}} \left(1 + e^{i\frac{2\pi}{3}(g_2-2g_1)}\right). \tag{3.25}$$

For the approximate calculation we use the terms of the series with $|g_1| \le 2$, $|g_2| \le 2$. Therefore

$$\begin{aligned}
V(\mathbf{r}) &= 2V_{1,(00)} + 4V_{1,(10)}\left(\cos\left(\frac{1}{2}(\mathbf{b}_1+\mathbf{b}_2)\cdot\mathbf{r}\right)\cos\left(\frac{1}{2}(\mathbf{b}_1-\mathbf{b}_2)\cdot\mathbf{r}\right)+\right.\\
&\left.\cos\left(\frac{1}{2}(\mathbf{b}_1+\mathbf{b}_2)\cdot\mathbf{r}+\frac{2\pi}{3}\right)\cos\left(\frac{1}{2}(\mathbf{b}_1-\mathbf{b}_2)\cdot\mathbf{r}\right)\right)+\\
&2V_{1,(11)}\left(\cos\left((\mathbf{b}_1+\mathbf{b}_2)\cdot\mathbf{r}\right)+\cos\left((\mathbf{b}_1+\mathbf{b}_2)\cdot\mathbf{r}-\frac{2\pi}{3}\right)+2\cos\left((\mathbf{b}_1-\mathbf{b}_2)\cdot\mathbf{r}\right)\right)-\\
&4V_{1,(20)}\cos\left((\mathbf{b}_2-\mathbf{b}_1)\cdot\mathbf{r}\right)\cos\left((\mathbf{b}_2+\mathbf{b}_1)\cdot\mathbf{r}+\frac{2\pi}{3}\right)+\\
&2V_{1,(12)}\left(2\cos\left((\mathbf{b}_1+2\mathbf{b}_2)\cdot\mathbf{r}\right)+2\cos\left((2\mathbf{b}_1+\mathbf{b}_2)\cdot\mathbf{r}\right)+\right.\\
&\left.\cos\left((\mathbf{b}_1-2\mathbf{b}_2)\cdot\mathbf{r}-\frac{\pi}{3}\right)-\cos\left((2\mathbf{b}_1-\mathbf{b}_2)\cdot\mathbf{r}-\frac{2\pi}{3}\right)\right)+\\
&2V_{1,(22)}\left(2\cos\left(2(\mathbf{b}_1-\mathbf{b}_2)\cdot\mathbf{r}\right)-\cos\left(2(\mathbf{b}_1+\mathbf{b}_2)\cdot\mathbf{r}-\frac{2\pi}{3}\right)\right).
\end{aligned} \tag{3.26}$$

Using the vectors $\mathbf{b}_1$ and $\mathbf{b}_2$ of the reciprocal lattice from (3.22) and coordinates *x* and *y* one obtains from (3.26):

$$\begin{aligned}
V(x,y) &= 2V_{1,(00)} + 4V_{1,(10)}\cos\left(\frac{2\pi}{3a}x+\frac{\pi}{3}\right)\cos\left(\frac{2\pi}{3a}\sqrt{3}y\right)+\\
&2V_{1,(11)}\left(\cos\left(\frac{4\pi}{3a}x-\frac{\pi}{3}\right)+2\cos\left(\frac{4\pi}{3a}\sqrt{3}y\right)\right)-4V_{1,(20)}\cos\left(\frac{4\pi}{3a}\sqrt{3}y\right)\cos\left(\frac{4\pi}{3a}x+\frac{2\pi}{3}\right)+\\
&4V_{1,(12)}\left(2\cos\left(\frac{2\pi}{a}x\right)\cos\left(\frac{2\pi}{3a}\sqrt{3}y\right)-\sin\left(\frac{2\pi}{3a}x-\frac{\pi}{6}\right)\cos\left(\frac{2\pi}{a}\sqrt{3}y\right)\right)+\\
&2V_{1,(22)}\left(2\cos\left(\frac{8\pi}{3a}\sqrt{3}y\right)-\cos\left(\frac{8\pi}{3a}x-\frac{2\pi}{3}\right)\right).
\end{aligned} \tag{3.27}$$

We need the derivatives for the forces components in dimensionless form

$$-\frac{\partial\widetilde{U}}{\partial\widetilde{\xi}}=\widetilde{U}'_{10}\sin\left(\frac{2\pi}{3\widetilde{a}}\widetilde{x}+\frac{\pi}{3}\right)\cos\left(\frac{2\pi}{3\widetilde{a}}\sqrt{3}\widetilde{y}\right)+\widetilde{U}'_{11}\sin\left(\frac{4\pi}{3\widetilde{a}}\widetilde{x}-\frac{\pi}{3}\right)-$$
$$\widetilde{U}'_{20}\cos\left(\frac{4\pi}{3\widetilde{a}}\sqrt{3}y\right)\sin\left(\frac{4\pi}{3\widetilde{a}}x+\frac{2\pi}{3}\right)+\widetilde{U}'_{12}\left(6\sin\left(\frac{2\pi}{\widetilde{a}}\widetilde{x}\right)\cos\left(\frac{2\pi}{3\widetilde{a}}\sqrt{3}\widetilde{y}\right)+\right.$$
$$\left.\cos\left(\frac{2\pi}{3\widetilde{a}}\widetilde{x}-\frac{\pi}{6}\right)\cos\left(\frac{2\pi}{\widetilde{a}}\sqrt{3}\widetilde{y}\right)\right)-\widetilde{U}'_{22}\sin\left(\frac{8\pi}{3\widetilde{a}}\widetilde{x}-\frac{2\pi}{3}\right), \tag{3.28}$$

$$-\frac{\partial\widetilde{U}}{\partial\widetilde{y}}=\widetilde{U}'_{10}\sqrt{3}\cos\left(\frac{2\pi}{3\widetilde{a}}\widetilde{x}+\frac{\pi}{3}\right)\sin\left(\frac{2\pi}{3\widetilde{a}}\sqrt{3}\widetilde{y}\right)+\widetilde{U}'_{11}2\sqrt{3}\sin\left(\frac{4\pi}{3\widetilde{a}}\sqrt{3}\widetilde{y}\right)-$$
$$\sqrt{3}\widetilde{U}'_{20}\sin\left(\frac{4\pi}{3\widetilde{a}}\sqrt{3}\widetilde{y}\right)\cos\left(\frac{4\pi}{3\widetilde{a}}\widetilde{x}+\frac{2\pi}{3}\right)+\widetilde{U}'_{12}\left(2\sqrt{3}\cos\left(\frac{2\pi}{\widetilde{a}}\widetilde{x}\right)\sin\left(\frac{2\pi}{3\widetilde{a}}\sqrt{3}\widetilde{y}\right)-\right.$$
$$\left.3\sqrt{3}\sin\left(\frac{2\pi}{3\widetilde{a}}\widetilde{x}-\frac{\pi}{6}\right)\sin\left(\frac{2\pi}{\widetilde{a}}\sqrt{3}\widetilde{y}\right)\right)+2\sqrt{3}\widetilde{U}'_{22}\sin\left(\frac{8\pi}{3\widetilde{a}}\sqrt{3}\widetilde{y}\right), \tag{3.29}$$

where the notations are introduced:

$$\widetilde{U}'_{10}=\frac{8\pi}{3\widetilde{a}}\widetilde{V}_{1,(10)},\ \widetilde{U}'_{11}=\frac{8\pi}{3\widetilde{a}}\widetilde{V}_{1,(11)},\ \widetilde{U}'_{20}=\frac{16\pi}{3\widetilde{a}}\widetilde{V}_{1,(20)},\ \widetilde{U}'_{12}=\frac{8\pi}{3\widetilde{a}}\widetilde{V}_{1,(12)},\ \widetilde{U}'_{22}=\frac{16\pi}{3\widetilde{a}}\widetilde{V}_{1,(22)}. \tag{3.30}$$

Consider as the approximation the acting forces by $\widetilde{t}=0$, when $\widetilde{\xi}=\widetilde{x}$. After substitution of (3.28) and (3.29) in (3.16), one obtains the expressions for the dimensionless forces acting on the unit of mass of particles:

$$\widetilde{\mathrm{F}}_{\mathrm{p}\xi}=-\frac{\partial\widetilde{\varphi}}{\partial\widetilde{\xi}}+\widetilde{U}'_{10}\sin\left(\frac{2\pi}{3\widetilde{a}}\widetilde{\xi}+\frac{\pi}{3}\right)\cos\left(\frac{2\pi}{3\widetilde{a}}\sqrt{3}\widetilde{y}\right)+\widetilde{U}'_{11}\sin\left(\frac{4\pi}{3\widetilde{a}}\widetilde{\xi}-\frac{\pi}{3}\right)-$$
$$\widetilde{U}'_{20}\cos\left(\frac{4\pi}{3\widetilde{a}}\sqrt{3}\widetilde{y}\right)\sin\left(\frac{4\pi}{3\widetilde{a}}\widetilde{\xi}+\frac{2\pi}{3}\right)+\widetilde{U}'_{12}\left(6\sin\left(\frac{2\pi}{\widetilde{a}}\widetilde{\xi}\right)\cos\left(\frac{2\pi}{3\widetilde{a}}\sqrt{3}\widetilde{y}\right)+\right. \tag{3.31}$$
$$\left.\cos\left(\frac{2\pi}{3\widetilde{a}}\widetilde{\xi}-\frac{\pi}{6}\right)\cos\left(\frac{2\pi}{\widetilde{a}}\sqrt{3}\widetilde{y}\right)\right)-\widetilde{U}'_{22}\sin\left(\frac{8\pi}{3\widetilde{a}}\widetilde{\xi}-\frac{2\pi}{3}\right)+\widetilde{E}_{\xi},$$

$$\widetilde{\mathrm{F}}_{\mathrm{py}}=-\frac{\partial\widetilde{\varphi}}{\partial\widetilde{y}}+\widetilde{U}'_{10}\sqrt{3}\cos\left(\frac{2\pi}{3\widetilde{a}}\widetilde{\xi}+\frac{\pi}{3}\right)\sin\left(\frac{2\pi}{3\widetilde{a}}\sqrt{3}\widetilde{y}\right)+\widetilde{U}'_{11}2\sqrt{3}\sin\left(\frac{4\pi}{3\widetilde{a}}\sqrt{3}\widetilde{y}\right)-$$
$$\sqrt{3}\widetilde{U}'_{20}\sin\left(\frac{4\pi}{3\widetilde{a}}\sqrt{3}\widetilde{y}\right)\cos\left(\frac{4\pi}{3\widetilde{a}}\widetilde{\xi}+\frac{2\pi}{3}\right)+\widetilde{U}'_{12}\left(2\sqrt{3}\cos\left(\frac{2\pi}{\widetilde{a}}\widetilde{\xi}\right)\sin\left(\frac{2\pi}{3\widetilde{a}}\sqrt{3}\widetilde{y}\right)-\right. \tag{3.32}$$
$$\left.3\sqrt{3}\sin\left(\frac{2\pi}{3\widetilde{a}}\widetilde{\xi}-\frac{\pi}{6}\right)\sin\left(\frac{2\pi}{\widetilde{a}}\sqrt{3}\widetilde{y}\right)\right)+2\sqrt{3}\widetilde{U}'_{22}\sin\left(\frac{8\pi}{3\widetilde{a}}\sqrt{3}\widetilde{y}\right)+\widetilde{E}_{y}.$$

Analogically

$$\widetilde{\mathrm{F}}_{\mathrm{e}\xi} = -\widetilde{\mathrm{F}}_{\mathrm{p}\xi},\ \widetilde{\mathrm{F}}_{\mathrm{ey}} = -\widetilde{\mathrm{F}}_{\mathrm{py}}. \tag{3.33}$$

The forces (3.31)-(3.33) should be introduced in the system of the hydrodynamic equations (3.10)-(3.15).

Suppose that the external field intensity **E** is equal to zero. The effective hydrodynamic velocity is directed along x axis. This fact can be used by averaging over $\widetilde{y}$ of the obtained system of quantum hydrodynamic equations. The averaging will be realized in the limit of one hexagonal crystal cell. Carry out the integration of the left and right hand sides of the hydrodynamic equations calculating the integral $\frac{1}{\sqrt{3}\widetilde{a}}\int\limits_{-\frac{\sqrt{3}}{2}\widetilde{a}}^{\frac{\sqrt{3}}{2}\widetilde{a}} d\widetilde{y}$ (see figure 1) and taking into account that $\frac{1}{\sqrt{3}\widetilde{a}}\int\limits_{-\frac{\sqrt{3}}{2}\widetilde{a}}^{\frac{\sqrt{3}}{2}\widetilde{a}} \frac{\partial \psi}{\partial \widetilde{y}} d\widetilde{y} = 0$ because of system symmetry for arbitrary function Ψ, characterizing the state of the physical system. We suppose also that by averaging all physical values (characterizing the state of the physical system) do not depend on $\widetilde{y}$ .As result we have the following system of equations:

Dimensionless Poisson equation for the self-consistent potential $\widetilde{\varphi}$ of the electric field:

$$\frac{\partial^2 \widetilde{\varphi}}{\partial \widetilde{\xi}^2} = -4\pi R\left\{\frac{m_e}{m_p}\left[\widetilde{\rho}_p - \frac{m_e H}{m_p \widetilde{u}^2}\frac{\partial}{\partial \widetilde{\xi}}\left(\widetilde{\rho}_p(\widetilde{u}-1)\right)\right] - \left[\widetilde{\rho}_e - \frac{H}{\widetilde{u}^2}\frac{\partial}{\partial \widetilde{\xi}}\left(\widetilde{\rho}_e(\widetilde{u}-1)\right)\right]\right\}. \tag{3.34}$$

Continuity equation for the positive particles:

$$\frac{\partial}{\partial \widetilde{\xi}}\left[\widetilde{\rho}_p(1-\widetilde{u})\right] + \frac{m_e}{m_p}\frac{\partial}{\partial \widetilde{\xi}}\left\{\frac{H}{\widetilde{u}^2}\frac{\partial}{\partial \widetilde{\xi}}\left[\widetilde{\rho}_p(\widetilde{u}-1)^2\right]\right\} + \frac{m_e}{m_p}\frac{\partial}{\partial \widetilde{\xi}}\left\{\frac{H}{\widetilde{u}^2}\left[\frac{V_{0p}^2}{u_0^2}\frac{\partial}{\partial \widetilde{\xi}}\widetilde{p}_p - \right.\right.$$
$$\left.\left.\frac{m_e}{m_p}\widetilde{\rho}_p E\left(-\frac{\partial \widetilde{\varphi}}{\partial \widetilde{\xi}} + \widetilde{U}'_{11}\sin\left(\frac{4\pi}{3\widetilde{a}}\widetilde{\xi} - \frac{\pi}{3}\right) - \widetilde{U}'_{22}\sin\left(\frac{8\pi}{3\widetilde{a}}\widetilde{\xi} - \frac{2\pi}{3}\right)\right)\right]\right\} = 0 \tag{3.35}$$

Continuity equation for electrons:

$$\frac{\partial}{\partial \widetilde{\xi}}\left[\widetilde{\rho}_e(1-\widetilde{u})\right] + \frac{\partial}{\partial \widetilde{\xi}}\left\{\frac{H}{\widetilde{u}^2}\frac{\partial}{\partial \widetilde{\xi}}\left[\widetilde{\rho}_e(\widetilde{u}-1)^2\right]\right\} + \frac{\partial}{\partial \widetilde{\xi}}\left\{\frac{H}{\widetilde{u}^2}\left[\frac{V_{0e}^2}{u_0^2}\frac{\partial}{\partial \widetilde{\xi}}\widetilde{p}_e - \right.\right.$$
$$\left.\left.\widetilde{\rho}_e E\left(\frac{\partial \widetilde{\varphi}}{\partial \widetilde{\xi}} - \widetilde{U}'_{11}\sin\left(\frac{4\pi}{3\widetilde{a}}\widetilde{\xi} - \frac{\pi}{3}\right) + \widetilde{U}'_{22}\sin\left(\frac{8\pi}{3\widetilde{a}}\widetilde{\xi} - \frac{2\pi}{3}\right)\right)\right]\right\} = 0 \tag{3.36}$$

Momentum equation for the movement along the *x* direction:

$$\frac{\partial}{\partial\tilde{\xi}}\left\{\left(\tilde{\rho}_p+\tilde{\rho}_e\right)\tilde{u}\left(\tilde{u}-1\right)+\frac{V_{0p}^2}{u_0^2}\tilde{p}_p+\frac{V_{0e}^2}{u_0^2}\tilde{p}_e\right\}-$$
$$\frac{m_e}{m_p}\tilde{\rho}_p E\left(-\frac{\partial\tilde{\varphi}}{\partial\tilde{\xi}}+\tilde{U}'_{11}\sin\left(\frac{4\pi}{3\tilde{a}}\tilde{\xi}-\frac{\pi}{3}\right)-\tilde{U}'_{22}\sin\left(\frac{8\pi}{3\tilde{a}}\tilde{\xi}-\frac{2\pi}{3}\right)\right)-$$
$$\tilde{\rho}_e E\left(\frac{\partial\tilde{\varphi}}{\partial\tilde{\xi}}-\tilde{U}'_{11}\sin\left(\frac{4\pi}{3\tilde{a}}\tilde{\xi}-\frac{\pi}{3}\right)+\tilde{U}'_{22}\sin\left(\frac{8\pi}{3\tilde{a}}\tilde{\xi}-\frac{2\pi}{3}\right)\right)+$$
$$\frac{m_e}{m_p}\frac{\partial}{\partial\tilde{\xi}}\left\{\frac{H}{\tilde{u}^2}\left[\frac{\partial}{\partial\tilde{\xi}}\left(2\frac{V_{0p}^2}{u_0^2}\tilde{p}_p\left(1-\tilde{u}\right)-\tilde{\rho}_p\tilde{u}\left(1-\tilde{u}\right)^2\right)-\right.\right.$$
$$\left.\left.\frac{m_e}{m_p}\tilde{\rho}_p\left(1-\tilde{u}\right)E\left(-\frac{\partial\tilde{\varphi}}{\partial\tilde{\xi}}+\tilde{U}'_{11}\sin\left(\frac{4\pi}{3\tilde{a}}\tilde{\xi}-\frac{\pi}{3}\right)-\tilde{U}'_{22}\sin\left(\frac{8\pi}{3\tilde{a}}\tilde{\xi}-\frac{2\pi}{3}\right)\right)\right]\right\}+$$
$$\frac{\partial}{\partial\tilde{\xi}}\left\{\frac{H}{\tilde{u}^2}\left[\frac{\partial}{\partial\tilde{\xi}}\left(2\frac{V_{0e}^2}{u_0^2}\tilde{p}_e\left(1-\tilde{u}\right)-\tilde{\rho}_e\tilde{u}\left(1-\tilde{u}\right)^2\right)-\right.\right.$$
$$\left.\left.\tilde{\rho}_e\left(1-\tilde{u}\right)E\left(\frac{\partial\tilde{\varphi}}{\partial\tilde{\xi}}-\tilde{U}'_{11}\sin\left(\frac{4\pi}{3\tilde{a}}\tilde{\xi}-\frac{\pi}{3}\right)+\tilde{U}'_{22}\sin\left(\frac{8\pi}{3\tilde{a}}\tilde{\xi}-\frac{2\pi}{3}\right)\right)\right]\right\}+$$
$$\frac{H}{\tilde{u}^2}E\left(\frac{m_e}{m_p}\right)^2\left(-\frac{\partial\tilde{\varphi}}{\partial\tilde{\xi}}+\tilde{U}'_{11}\sin\left(\frac{4\pi}{3\tilde{a}}\tilde{\xi}-\frac{\pi}{3}\right)-\tilde{U}'_{22}\sin\left(\frac{8\pi}{3\tilde{a}}\tilde{\xi}-\frac{2\pi}{3}\right)\right)\left(\frac{\partial}{\partial\tilde{\xi}}\left(\tilde{\rho}_p\left(\tilde{u}-1\right)\right)\right)+$$
$$\frac{H}{\tilde{u}^2}E\left(\frac{\partial\tilde{\varphi}}{\partial\tilde{\xi}}-\tilde{U}'_{11}\sin\left(\frac{4\pi}{3\tilde{a}}\tilde{\xi}-\frac{\pi}{3}\right)+\tilde{U}'_{22}\sin\left(\frac{8\pi}{3\tilde{a}}\tilde{\xi}-\frac{2\pi}{3}\right)\right)\left(\frac{\partial}{\partial\tilde{\xi}}\left(\tilde{\rho}_e\left(\tilde{u}-1\right)\right)\right)-$$
$$\frac{m_e}{m_p}\frac{\partial}{\partial\tilde{\xi}}\left\{\frac{H}{\tilde{u}^2}\frac{V_{0p}^2}{u_0^2}\frac{\partial}{\partial\tilde{\xi}}\left(\tilde{p}_p\tilde{u}\right)\right\}-\frac{\partial}{\partial\tilde{\xi}}\left\{\frac{H}{\tilde{u}^2}\frac{V_{0e}^2}{u_0^2}\frac{\partial}{\partial\tilde{\xi}}\left(\tilde{p}_e\tilde{u}\right)\right\}+$$
$$\left(\frac{m_e}{m_p}\right)^2 E\frac{\partial}{\partial\tilde{\xi}}\left\{\frac{H}{\tilde{u}^2}\left[\left(-\frac{\partial\tilde{\varphi}}{\partial\tilde{\xi}}+\tilde{U}'_{11}\sin\left(\frac{4\pi}{3\tilde{a}}\tilde{\xi}-\frac{\pi}{3}\right)-\tilde{U}'_{22}\sin\left(\frac{8\pi}{3\tilde{a}}\tilde{\xi}-\frac{2\pi}{3}\right)\right)\tilde{\rho}_p\tilde{u}\right]\right\}+ \quad (3.37)$$
$$E\frac{\partial}{\partial\tilde{\xi}}\left\{\frac{H}{\tilde{u}^2}\left[\left(\frac{\partial\tilde{\varphi}}{\partial\tilde{\xi}}-\tilde{U}'_{11}\sin\left(\frac{4\pi}{3\tilde{a}}\tilde{\xi}-\frac{\pi}{3}\right)+\tilde{U}'_{22}\sin\left(\frac{8\pi}{3\tilde{a}}\tilde{\xi}-\frac{2\pi}{3}\right)\right)\tilde{\rho}_e\tilde{u}\right]\right\}=0$$

Energy equation for the positive particles:

$$\frac{\partial}{\partial\tilde{\xi}}\left[\tilde{\rho}_p\tilde{u}^2\left(\tilde{u}-1\right)+5\frac{V_{0p}^2}{u_0^2}\tilde{p}_p\tilde{u}-3\frac{V_{0p}^2}{u_0^2}\tilde{p}_p\right]-$$
$$2\frac{m_e}{m_p}\tilde{\rho}_p E\left(-\frac{\partial\tilde{\varphi}}{\partial\tilde{\xi}}+\tilde{U}'_{11}\sin\left(\frac{4\pi}{3\tilde{a}}\tilde{\xi}-\frac{\pi}{3}\right)-\tilde{U}'_{22}\sin\left(\frac{8\pi}{3\tilde{a}}\tilde{\xi}-\frac{2\pi}{3}\right)\right)\tilde{u}+$$

$$\frac{\partial}{\partial\widetilde{\xi}}\left\{\frac{H}{\widetilde{u}^2}\frac{m_e}{m_p}\left[\frac{\partial}{\partial\widetilde{\xi}}\left(-\widetilde{\rho}_p\widetilde{u}^2(1-\widetilde{u})^2+7\frac{V_{0p}^2}{u_0^2}\widetilde{p}_p\widetilde{u}(1-\widetilde{u})+3\frac{V_{0p}^2}{u_0^2}\widetilde{p}_p(\widetilde{u}-1)-\frac{V_{0p}^2}{u_0^2}\widetilde{p}_p\widetilde{u}^2-\right.\right.\right.$$

$$\left.5\frac{V_{0p}^4}{u_0^4}\frac{\widetilde{p}_p^2}{\widetilde{\rho}_p}\right)+E\left(-2\frac{m_e}{m_p}\widetilde{\rho}_p\widetilde{u}(1-\widetilde{u})+\frac{m_e}{m_p}\widetilde{\rho}_p\widetilde{u}^2+5\frac{m_e}{m_p}\frac{V_{0p}^2}{u_0^2}\widetilde{p}_p\right)\left(-\frac{\partial\widetilde{\varphi}}{\partial\widetilde{\xi}}+\right.$$

$$\left.\left.\left.\widetilde{U}'_{11}\sin\left(\frac{4\pi}{3\widetilde{a}}\widetilde{\xi}-\frac{\pi}{3}\right)-\widetilde{U}'_{22}\sin\left(\frac{8\pi}{3\widetilde{a}}\widetilde{\xi}-\frac{2\pi}{3}\right)\right)\right]\right\}+2\frac{H}{\widetilde{u}^2}E\left(\frac{m_e}{m_p}\right)^2\left[-\frac{\partial}{\partial\widetilde{\xi}}\left(\widetilde{\rho}_p\widetilde{u}(1-\widetilde{u})\right)+\right.$$

$$\left.\frac{V_{0p}^2}{u_0^2}\frac{\partial}{\partial\widetilde{\xi}}\widetilde{p}_p\right]\left(-\frac{\partial\widetilde{\varphi}}{\partial\widetilde{\xi}}+\widetilde{U}'_{11}\sin\left(\frac{4\pi}{3\widetilde{a}}\widetilde{\xi}-\frac{\pi}{3}\right)-\widetilde{U}'_{22}\sin\left(\frac{8\pi}{3\widetilde{a}}\widetilde{\xi}-\frac{2\pi}{3}\right)\right)-$$

$$2\frac{H}{\widetilde{u}^2}E^2\left(\frac{m_e}{m_p}\right)^3\widetilde{\rho}_p\left[\left(-\frac{\partial\widetilde{\varphi}}{\partial\widetilde{\xi}}+\widetilde{U}'_{11}\sin\left(\frac{4\pi}{3\widetilde{a}}\widetilde{\xi}-\frac{\pi}{3}\right)-\widetilde{U}'_{22}\sin\left(\frac{8\pi}{3\widetilde{a}}\widetilde{\xi}-\frac{2\pi}{3}\right)\right)^2+\right.$$

$$\frac{1}{2}\left(\widetilde{U}'_{10}\sin\left(\frac{2\pi}{3\widetilde{a}}\widetilde{\xi}+\frac{\pi}{3}\right)+6\widetilde{U}'_{12}\sin\left(\frac{2\pi}{\widetilde{a}}\widetilde{\xi}\right)\right)^2+\frac{1}{2}\left(\widetilde{U}'_{12}\right)^2\cos^2\left(\frac{2\pi}{3\widetilde{a}}\widetilde{\xi}-\frac{\pi}{6}\right)+$$

$$\frac{1}{2}\left(\widetilde{U}'_{02}\right)^2\sin^2\left(\frac{4\pi}{3\widetilde{a}}\widetilde{\xi}+\frac{2\pi}{3}\right)-\frac{4}{3\pi}\widetilde{U}'_{02}\sin\left(\frac{4\pi}{3\widetilde{a}}\widetilde{\xi}+\frac{2\pi}{3}\right)\left(\widetilde{U}'_{10}\sin\left(\frac{2\pi}{3\widetilde{a}}\widetilde{\xi}+\frac{\pi}{3}\right)-\right.$$

$$\left.6\widetilde{U}'_{12}\sin\left(\frac{2\pi}{\widetilde{a}}\widetilde{\xi}\right)\right)-\frac{12}{5\pi}\widetilde{U}'_{02}\widetilde{U}'_{12}\sin\left(\frac{4\pi}{3\widetilde{a}}\widetilde{\xi}+\frac{2\pi}{3}\right)\cos\left(\frac{2\pi}{3\widetilde{a}}\widetilde{\xi}-\frac{\pi}{6}\right)+$$

$$\frac{3}{2}\left(\widetilde{U}'_{10}\cos\left(\frac{2\pi}{3\widetilde{a}}\widetilde{\xi}+\frac{\pi}{3}\right)+2\widetilde{U}'_{12}\cos\left(\frac{2\pi}{\widetilde{a}}\widetilde{\xi}\right)\right)^2+$$

$$\frac{3}{2}\left(2\widetilde{U}'_{11}-\widetilde{U}'_{02}\cos\left(\frac{4\pi}{3\widetilde{a}}\widetilde{\xi}+\frac{2\pi}{3}\right)\right)^2+\frac{27}{2}\left(\widetilde{U}'_{12}\right)^2\sin^2\left(\frac{2\pi}{3\widetilde{a}}\widetilde{\xi}-\frac{\pi}{6}\right)+6\left(\widetilde{U}'_{22}\right)^2+$$

$$\frac{8}{\pi}\left(\widetilde{U}'_{10}\cos\left(\frac{2\pi}{3\widetilde{a}}\widetilde{\xi}+\frac{\pi}{3}\right)+2\widetilde{U}'_{12}\cos\left(\frac{2\pi}{\widetilde{a}}\widetilde{\xi}\right)\right)\left(2\widetilde{U}'_{11}-\widetilde{U}'_{02}\cos\left(\frac{4\pi}{3\widetilde{a}}\widetilde{\xi}+\frac{2\pi}{3}\right)\right)-$$

$$\frac{96}{15\pi}\left(\widetilde{U}'_{10}\cos\left(\frac{2\pi}{3\widetilde{a}}\widetilde{\xi}+\frac{\pi}{3}\right)+2\widetilde{U}'_{12}\cos\left(\frac{2\pi}{\widetilde{a}}\widetilde{\xi}\right)\right)\widetilde{U}'_{22}-$$

$$\left.\frac{72}{5\pi}\widetilde{U}'_{12}\left(2\widetilde{U}'_{11}-\widetilde{U}'_{02}\cos\left(\frac{4\pi}{3\widetilde{a}}\widetilde{\xi}+\frac{2\pi}{3}\right)\right)\sin\left(\frac{2\pi}{3\widetilde{a}}\widetilde{\xi}-\frac{\pi}{6}\right)-\frac{288}{7\pi}\widetilde{U}'_{12}\widetilde{U}'_{22}\sin\left(\frac{2\pi}{3\widetilde{a}}\widetilde{\xi}-\frac{\pi}{6}\right)\right]=$$

$$-\frac{\widetilde{u}^2}{Hu_0^2}\left(V_{0p}^2\widetilde{p}_p-\widetilde{p}_eV_{0e}^2\right)\left(1+\frac{m_p}{m_e}\right) \qquad (3.38)$$

Energy equation for electrons:

$$\frac{\partial}{\partial\widetilde{\xi}}\left[\widetilde{\rho}_e\widetilde{u}^2(\widetilde{u}-1)+5\frac{V_{0e}^2}{u_0^2}\widetilde{p}_e\widetilde{u}-3\frac{V_{0e}^2}{u_0^2}\widetilde{p}_e\right]-$$

$$2\widetilde{\rho}_e\widetilde{u}E\left(\frac{\partial\widetilde{\varphi}}{\partial\widetilde{\xi}}-\widetilde{U}'_{11}\sin\left(\frac{4\pi}{3\widetilde{a}}\widetilde{\xi}-\frac{\pi}{3}\right)+\widetilde{U}'_{22}\sin\left(\frac{8\pi}{3\widetilde{a}}\widetilde{\xi}-\frac{2\pi}{3}\right)\right)+$$

$$\frac{\partial}{\partial\widetilde{\xi}}\left\{\frac{H}{\widetilde{u}^2}\left[\frac{\partial}{\partial\widetilde{\xi}}\left(-\widetilde{\rho}_e\widetilde{u}^2\left(1-\widetilde{u}\right)^2+7\frac{V_{0e}^2}{u_0^2}\widetilde{p}_e\widetilde{u}\left(1-\widetilde{u}\right)+3\frac{V_{0e}^2}{u_0^2}\widetilde{p}_e\left(\widetilde{u}-1\right)-\frac{V_{0e}^2}{u_0^2}\widetilde{p}_e\widetilde{u}^2-\right.\right.\right.$$

$$\left.\left.\left.5\frac{V_{0e}^4}{u_0^4}\frac{\widetilde{p}_e^2}{\widetilde{\rho}_e}\right)+E\left(-2\widetilde{\rho}_e\widetilde{u}\left(1-\widetilde{u}\right)+\widetilde{\rho}_e\widetilde{u}^2+5\frac{V_{0e}^2}{u_0^2}\widetilde{p}_e\right)\left(\frac{\partial\widetilde{\varphi}}{\partial\widetilde{\xi}}-\right.\right.\right.$$

$$\left.\left.\left.\widetilde{U}'_{11}\sin\left(\frac{4\pi}{3\widetilde{a}}\widetilde{\xi}-\frac{\pi}{3}\right)+\widetilde{U}'_{22}\sin\left(\frac{8\pi}{3\widetilde{a}}\widetilde{\xi}-\frac{2\pi}{3}\right)\right)\right]\right\}+$$

$$E\left(-2\frac{H}{\widetilde{u}^2}\frac{\partial}{\partial\widetilde{\xi}}\left(\widetilde{\rho}_e\widetilde{u}\left(1-\widetilde{u}\right)\right)+2\frac{H}{\widetilde{u}^2}\frac{V_{0e}^2}{u_0^2}\frac{\partial}{\partial\widetilde{\xi}}\widetilde{p}_e\right)\left(\frac{\partial\widetilde{\varphi}}{\partial\widetilde{\xi}}-\right.$$

$$\left.\widetilde{U}'_{11}\sin\left(\frac{4\pi}{3\widetilde{a}}\widetilde{\xi}-\frac{\pi}{3}\right)+\widetilde{U}'_{22}\sin\left(\frac{8\pi}{3\widetilde{a}}\widetilde{\xi}-\frac{2\pi}{3}\right)\right)-$$

$$2E^2\frac{H}{\widetilde{u}^2}\widetilde{\rho}_e\left[\left(-\frac{\partial\widetilde{\varphi}}{\partial\widetilde{\xi}}+\widetilde{U}'_{11}\sin\left(\frac{4\pi}{3\widetilde{a}}\widetilde{\xi}-\frac{\pi}{3}\right)-\widetilde{U}'_{22}\sin\left(\frac{8\pi}{3\widetilde{a}}\widetilde{\xi}-\frac{2\pi}{3}\right)\right)^2+\right.$$

$$\frac{1}{2}\left(\widetilde{U}'_{10}\sin\left(\frac{2\pi}{3\widetilde{a}}\widetilde{\xi}+\frac{\pi}{3}\right)+6\widetilde{U}'_{12}\sin\left(\frac{2\pi}{\widetilde{a}}\widetilde{\xi}\right)\right)^2+\frac{1}{2}\left(\widetilde{U}'_{12}\right)^2\cos^2\left(\frac{2\pi}{3\widetilde{a}}\widetilde{\xi}-\frac{\pi}{6}\right)+$$

$$\frac{1}{2}\left(\widetilde{U}'_{02}\right)^2\sin^2\left(\frac{4\pi}{3\widetilde{a}}\widetilde{\xi}+\frac{2\pi}{3}\right)-\frac{4}{3\pi}\widetilde{U}'_{02}\sin\left(\frac{4\pi}{3\widetilde{a}}\widetilde{\xi}+\frac{2\pi}{3}\right)\left(\widetilde{U}'_{10}\sin\left(\frac{2\pi}{3\widetilde{a}}\widetilde{\xi}+\frac{\pi}{3}\right)+\right.$$

$$\left.6\widetilde{U}'_{12}\sin\left(\frac{2\pi}{\widetilde{a}}\widetilde{\xi}\right)\right)-\frac{12}{5\pi}\widetilde{U}'_{02}\widetilde{U}'_{12}\sin\left(\frac{4\pi}{3\widetilde{a}}\widetilde{\xi}+\frac{2\pi}{3}\right)\cos\left(\frac{2\pi}{3\widetilde{a}}\widetilde{\xi}-\frac{\pi}{6}\right)+$$

$$\frac{3}{2}\left(\widetilde{U}'_{10}\cos\left(\frac{2\pi}{3\widetilde{a}}\widetilde{\xi}+\frac{\pi}{3}\right)+2\widetilde{U}'_{12}\cos\left(\frac{2\pi}{\widetilde{a}}\widetilde{\xi}\right)\right)^2+$$

$$\frac{3}{2}\left(2\widetilde{U}'_{11}-\widetilde{U}'_{02}\cos\left(\frac{4\pi}{3\widetilde{a}}\widetilde{\xi}+\frac{2\pi}{3}\right)\right)^2+\frac{27}{2}\left(\widetilde{U}'_{12}\right)^2\sin^2\left(\frac{2\pi}{3\widetilde{a}}\widetilde{\xi}-\frac{\pi}{6}\right)+6\left(\widetilde{U}'_{22}\right)^2+$$

$$\frac{8}{\pi}\left(\widetilde{U}'_{10}\cos\left(\frac{2\pi}{3\widetilde{a}}\widetilde{\xi}+\frac{\pi}{3}\right)+2\widetilde{U}'_{12}\cos\left(\frac{2\pi}{\widetilde{a}}\widetilde{\xi}\right)\right)\left(2\widetilde{U}'_{11}-\widetilde{U}'_{02}\cos\left(\frac{4\pi}{3\widetilde{a}}\widetilde{\xi}+\frac{2\pi}{3}\right)\right)-$$

$$\frac{96}{15\pi}\left(\widetilde{U}'_{10}\cos\left(\frac{2\pi}{3\widetilde{a}}\widetilde{\xi}+\frac{\pi}{3}\right)+2\widetilde{U}'_{12}\cos\left(\frac{2\pi}{\widetilde{a}}\widetilde{\xi}\right)\right)\widetilde{U}'_{22}-$$

$$\left.\frac{72}{5\pi}\widetilde{U}'_{12}\left(2\widetilde{U}'_{11}-\widetilde{U}'_{02}\cos\left(\frac{4\pi}{3\widetilde{a}}\widetilde{\xi}+\frac{2\pi}{3}\right)\right)\sin\left(\frac{2\pi}{3\widetilde{a}}\widetilde{\xi}-\frac{\pi}{6}\right)-\frac{288}{7\pi}\widetilde{U}'_{12}\widetilde{U}'_{22}\sin\left(\frac{2\pi}{3\widetilde{a}}\widetilde{\xi}-\frac{\pi}{6}\right)\right]=$$

$$-\frac{\widetilde{u}^2}{Hu_0^2}\left(V_{0e}^2\widetilde{p}_e-V_{0p}^2\widetilde{p}_p\right)\left(1+\frac{m_p}{m_e}\right) \qquad (3.39)$$

4. ESTIMATIONS OF THE NUMERICAL PARAMETERS

We need estimations for the numerical values of dimensionless parameters for solutions of the hydrodynamic equations (3.34) - (3.39). In its turn these parameters depend on choosing of the independent scales of physical values. Analyze the independent scales for the physical problem under consideration. It should be stressed that we choose just scales but not real physical values which may differ significantly from scale values. Real physical values will be obtained as a result of numerical self-consistent calculations.

Assume that the surface electron density in graphene is about $\breve{n}_e \approx 10^{10}\, см^{-2}$ (such value is typical for many experiments (see [35-37]), the thickness of the graphene layer is equal to ~ 1 *nm*. Then the electron concentration consists $n_e \approx 10^{17}\, cm^{-3}$, and the density for the electron species $\rho_e = m_e n_e \approx 10^{-10}\, g/cm^3$ which leads to the scale $\rho_0 = 10^{-10}\, g/cm^3$. For numerical solutions of the hydrodynamic equations (3.34)-(3.39) we need Cauchy conditions, obviously in the typical for graphene conditions the estimation $\widetilde{\rho}_e$~1 is valid which can be used as the condition by $\widetilde{\xi} = 0$.

The process of the carbon atoms polarization leads to displacement of the atoms from the regular chain and to the creation of the "effective" positive particles which concentration $n_p \approx n_e$. Masses of these particles is about the mass of the carbon atom $m_p \approx 2 \cdot 10^{-23}\, г$. Then, $\frac{L}{T} = \frac{m_e}{m_p} \approx 5 \cdot 10^{-5}$; $\rho_p = m_p n_p \approx 2 \cdot 10^{-6}\, g/cm^3$ and by the choosed scale for the density ρ_0 we have $\widetilde{\rho}_p \sim 2 \cdot 10^4$.

Going to the scales for thermal velocities for electrons and the positive particles we have by *T*=300°K:

$V_{0e} \sim \sqrt{\frac{k_B T}{m_e}} \approx 6.4 \cdot 10^6\, см/с$, take the scale $V_{0e} = 5 \cdot 10^6\, cm/s$;

$V_{0p} \sim \sqrt{\frac{k_B T}{m_p}} \approx 4.5 \cdot 10^4\, см/с$, take the scale $V_{0p} = 5 \cdot 10^4\, cm/s$.

The theoretical mobility in graphene reaches up to $10^6\, cm^2/V \cdot s$ [38]. Let us use the scale

$u_0 = 5 \cdot 10^6\, cm/s$. Then $N = \frac{V_{0e}^2}{u_0^2} = 1$, $P = \frac{V_{0p}^2}{u_0^2} = 10^{-4}$.

Let us estimate the parameters *E* and *R*. For this estimation we need the scale φ_0. Admit $\varphi_0 \approx \delta \frac{e}{a}$, where δ is a "shielding coefficient". Naturally to take $x_0 = a = 0.142\ nm$ (see

Figure. 1) as the length scale, then $\widetilde{a}=1$. In the situation of a uncertainty in φ_0 choosing let us consider two limit cases:

1) δ~1.

Then $E=\dfrac{e\varphi_0}{m_e u_0^2}$~1000, $R=\dfrac{e\rho_0 x_0^2}{m_e\varphi_0}\sim 3\cdot 10^{-7}$.

2) δ=0.0001.

Then $E=\dfrac{e\varphi_0}{m_e u_0^2}$~0.1, $R=\dfrac{e\rho_0 x_0^2}{m_e\varphi_0}\sim 3\cdot 10^{-3}$.

Consider the terms describing the lattice influence. We should estimate the coefficients (3.30) using φ_0 as the scale for the potential *V*, $V=\varphi_0\widetilde{V}$. Three possible cases under consideration:

1) $V\sim\varphi_0$

We choose $U=\widetilde{U}'_{10}$~10, $F=\widetilde{U}'_{11}$~10, $J=\widetilde{U}'_{20}$~±5, $B=\widetilde{U}'_{12}$~±2,5, $G=\widetilde{U}'_{22}$~±5.

In this case the coefficients of "the second order" are less than the coefficients of "the first order."

2) $V\prec\prec\varphi_0$ (The small influence of the lattice),

We choose $U=\widetilde{U}'_{10}$~0.1, $F=\widetilde{U}'_{11}$~0.1, $J=\widetilde{U}'_{20}$~0.05, $B=\widetilde{U}'_{12}$~0.025, $G=\widetilde{U}'_{22}$~0.05.

3) $V\succ\succ\varphi_0$ (The great influence of the lattice),

We choose $U=\widetilde{U}'_{10}$~1000, $F=\widetilde{U}'_{11}$~1000, $J=\widetilde{U}'_{20}$~500, $B=\widetilde{U}'_{12}$~250, $G=\widetilde{U}'_{22}$~500.

Estimate parameter $H=\dfrac{N_R\hbar}{m_e x_0 u_0}$ for two limit cases:

1) $N_R=1$, then *H*~15.
2) $N_R=100$, then *H*~1500.

Initial conditions demand also the estimations for the quantum electron pressure and the pressure for the positive species. For the electron pressure we have $p_e=\rho_0 V_{0e}^2\widetilde{p}_e$ and using for the scale estimation $p_e=n_e k_B T\sim n_e m_e V_{oe}^2=\rho_e V_{oe}^2\sim\rho_0 V_{oe}^2$, one obtains $\widetilde{p}_e$~1. Analogically for the positive particles $p_p=\rho_0 V_{0p}^2\widetilde{p}_p$, and using $p_p=n_p k_B T\sim n_p m_p V_{op}^2=\rho_p V_{0p}^2$, we have $p_p\sim 2\cdot 10^4\rho_0 V_{0p}^2$, $\widetilde{p}_p\sim 2\cdot 10^4$.

Tables 1, 2 contain the initial conditions and parameters which were not varied by the numerical modeling.

Table 1. Initial conditions

$\widetilde{\rho}_e(0)$	$\widetilde{\rho}_p(0)$	$\widetilde{\varphi}(0)$	$\widetilde{p}_e(0)$	$\widetilde{p}_p(0)$	$\frac{\partial\widetilde{\rho}_e}{\partial\widetilde{\xi}}(0)$	$\frac{\partial\widetilde{\rho}_p}{\partial\widetilde{\xi}}(0)$	$\frac{\partial\widetilde{\varphi}}{\partial\widetilde{\xi}}(0)$	$\frac{\partial\widetilde{p}_e}{\partial\widetilde{\xi}}(0)$	$\frac{\partial\widetilde{p}_p}{\partial\widetilde{\xi}}(0)$
1	$2\cdot10^4$	1	1	$2\cdot10^4$	0	0	0	0	0

Table 2. Constant parameters

$\widetilde{a}$	***L***	***T***	***N***	***P***
1	1	$2\cdot10^4$	1	10^{-4}

Table 3 contains parameters (for the six different cases) which were varied by the numerical modeling.

Table 3. Varied parameters

Variant №	***E***	***R***	***H***	***U***	***F***	***J***	***B***	***G***
1	0.1	0.003	15	10	10	5	2.5	5
2	0.1	0.003	15	0.1	0.1	0.05	0.025	0.05
3	0.1	0.003	15	10	10	-5	-2.5	-5
4	1000	$3\cdot10^{-7}$	15	10	10	5	2.5	5
5	0.1	0.003	1500	10	10	5	2.5	5
6	0.1	0.003	15	1000	1000	500	250	500

In the present time there no the foolproof methods of the calculations of the potential lattice forces in graphene. In the following mathematical modeling the strategy is taken consisting in the vast variation of the parameters defining the evolution of the physical system.

5. RESULTS OF THE MATHEMATICAL MODELING WITHOUT THE EXTERNAL ELECTRIC FIELD

The calculations are realized on the basement of equations (3.34)-(3.39) by the initial conditions and parameters containing in the Tables 1 – 3. Now we are ready to display the results of the mathematical modeling realized with the help of Maple (the versions Maple 9 or more can be used). The system of generalized hydrodynamic equations (3.34) – (3.39) have the great possibilities of mathematical modeling as result of changing of Cauchy conditions and parameters describing the character features of initial perturbations which lead to the soliton formation.

The mathematical software Maple (beginning with the version 9) is applicable; the following Maple notations on figures are used: r- density $\widetilde{\rho}_p$, s - density $\widetilde{\rho}_e$, u- velocity $\widetilde{u}$, p - pressure $\widetilde{p}_p$, q – pressure $\widetilde{p}_e$ and v - self consistent potential $\widetilde{\varphi}$. Explanations placed under all following figures, Maple program contains Maple's notations – for example, the

expression $D(u)(0) = 0$ means in the usual notations $\frac{\partial \widetilde{u}}{\partial \widetilde{\xi}}(0) = 0$, independent variable t responds to $\widetilde{\xi}$.

Important to underline that no special boundary conditions were used for all following cases. The aim of the numerical investigation consists in the discovery of the soliton waves as a product of the self-organization of matter in graphene. It means that the solution should exist only in the restricted domain of the 1D space and the obtained object in the moving coordinate system ($\widetilde{\xi} = \widetilde{x} - \widetilde{t}$) has the constant velocity $\widetilde{u} = 1$ for all parts of the object. In this case the domain of the solution existence defines the character soliton size. The following numerical results demonstrate the realization of mentioned principles.

Figures. 2-9 reflect the result of calculations for Variant 1 (Table 3) in the first and the second approximations. In the first approximation the terms of series (3.25) with $|g_1| \le 1$, $|g_2| \le 1$ (then coefficients *U* and *F*) were taken into account. The second approximation contains all terms of the series (3.25) with $|g_1| \le 2$, $|g_2| \le 2$ (then coefficients *U*, *F*, *J*, *B* and *G*).

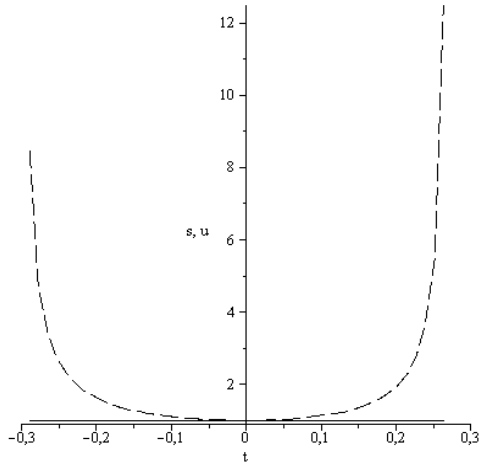

Figure. 2. s – the electron density $\widetilde{\rho}_e$, u – velocity $\widetilde{u}$ (solid line). (first approximation, Variant 1).

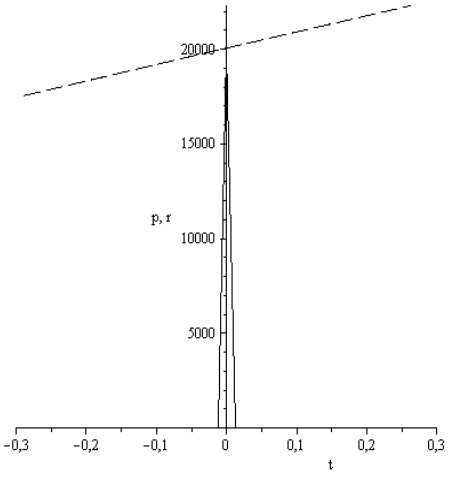

Figure 3. r – the positive particles density, (solid line); p – the positive particles pressure (first approximation, Variant 1)

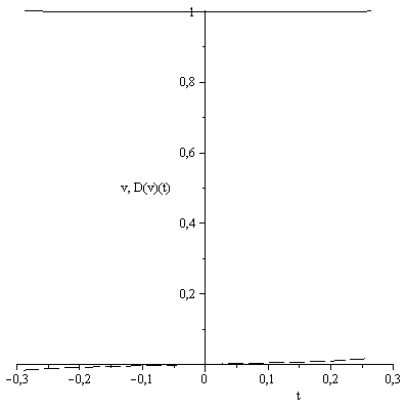

Figure 4. v – potential $\widetilde{\varphi}$ (solid line).
and derivative $\mathrm{D(v)(t)}$.
(first approximation, Variant 1).

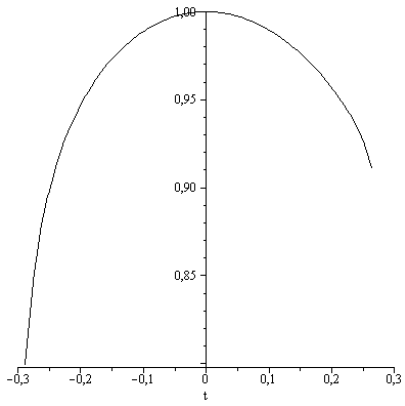

Figure 5. q – electron pressure.
(first approximation, Variant 1).

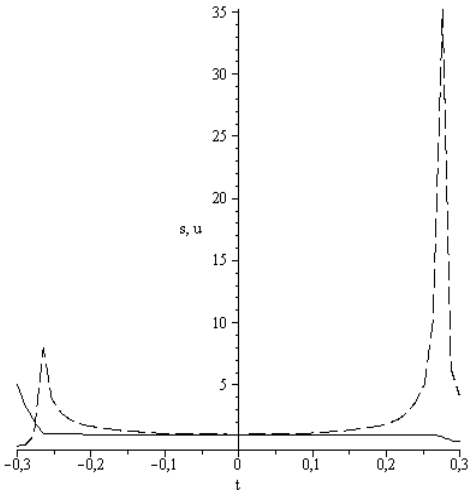

Figure 6. s – electron density $\widetilde{\rho}_e$,
u – velocity $\widetilde{u}$ (solid line),
(the second approximation, Variant 1).

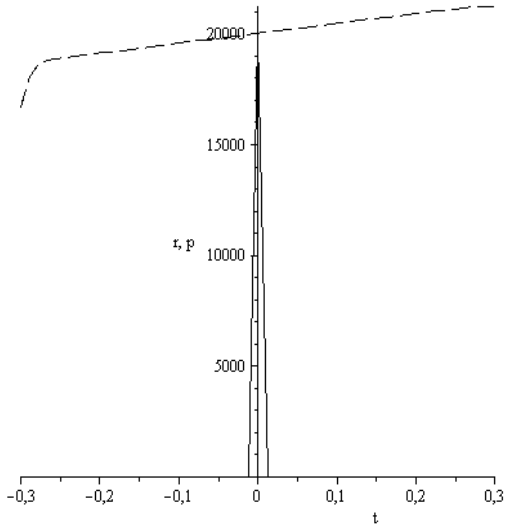

Figure 7. r – the positive particles density (solid line)
p – the positive particles pressure,
(the second approximation, Variant 1).

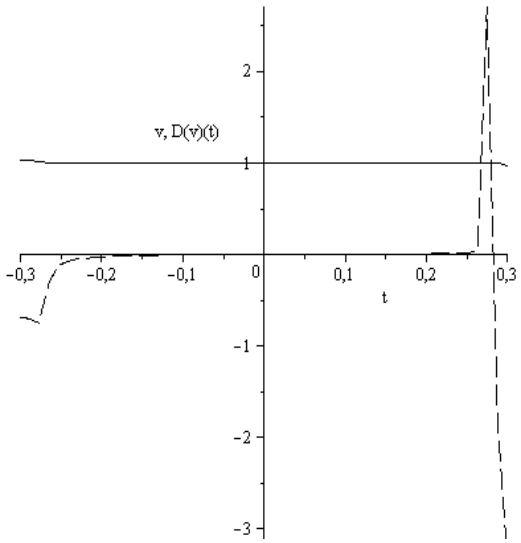

Figure 8. v – potential $\tilde{\varphi}$ (solid line), and derivative $\mathrm{D(v)(t)}$. (the second approximation, Variant 1).

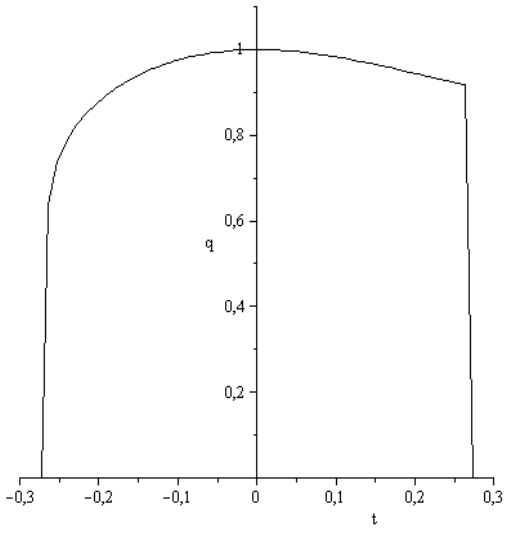

Figure 9. q – electron pressure. (the second approximation, Variant 1).

From Figures 2 - 9 follow that the size of the created soliton is about $0.5\,a$, where a =0.142 nm. The domain size occupied by the polarized positive charge is about $0.025\,a$ (see figures 3, 7). The negative charge distributes over the entire soliton domain (figures 2, 6), but the negative charge density increases to the edges of the soliton. Therefore the soliton structure reminds the 1D atom with the positive nuclei and the negative shell.

The self-consistent potential $\tilde{\varphi}$ is practically constant in the soliton boundaries, (Figures 4, 8). The small grows of the positive particles pressure exists in the x direction. This effect can be connected with the hydrodynamic movement along *x* and "the reconstruction" of the polarized particles in the soliton front.

Comparing the figures 2 – 5 and 6 – 9 we conclude that the calculation results in the first and the second approximation do not vary significantly. Seemingly significant difference of figures 2 and 6 on the edges of the domain has not the physical sense because corresponds to the regions where $u \neq const$. Then the restriction of two successive approximations is justified. Along with it the question about the convergence of the series leaves open because the first and the second approximations include only the restricted quantity of terms of the infinite series with the coefficients known with the small accuracy.

Figures 10 - 15 show the results of calculations responding to Variant 3 (Table 3). In the first approximation Variant 3 is identical to Variant 1 (coefficients $J = B = G = 0$) and only the results of the second approximation are delivered. These calculations are more complicated in the numerical realization and all curves are imaged separately, (Figures 10 – 15).

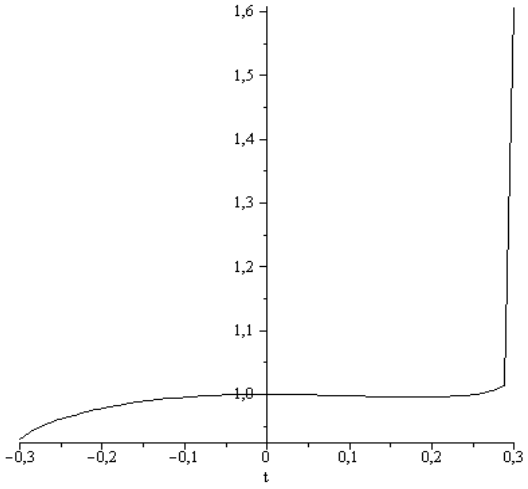

Figure 10. u – velocity $\widetilde{u}$.
(the second approximation, Variant 3).

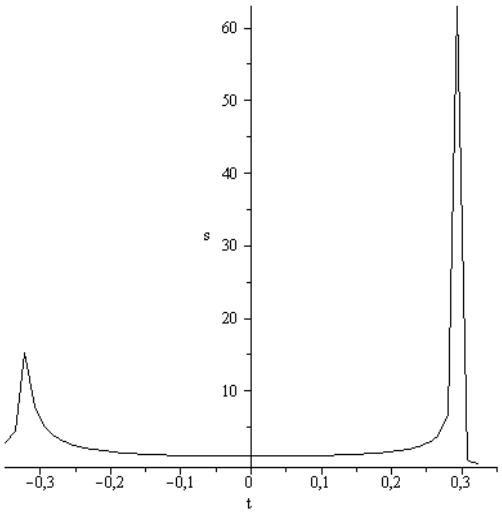

Figure 11. s – electron density $\widetilde{\rho}_e$,
(the second approximation, Variant 3).

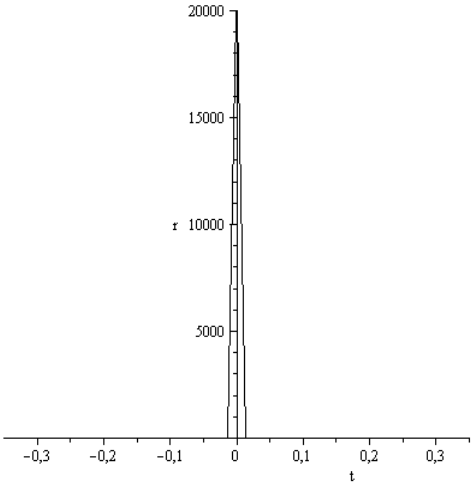

Figure 12. r – the positive particles density.
(the second approximation, Variant 3).

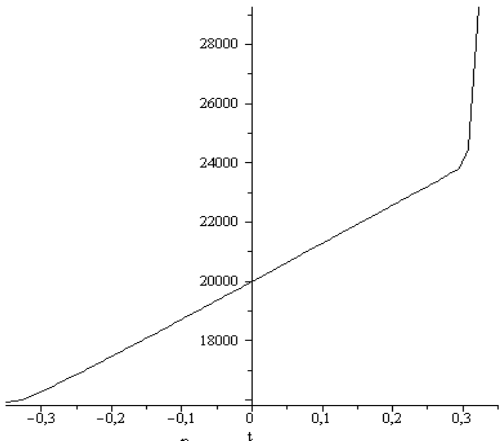

Figure 13. p – the positive particles pressure,
(the second approximation, Variant 3).

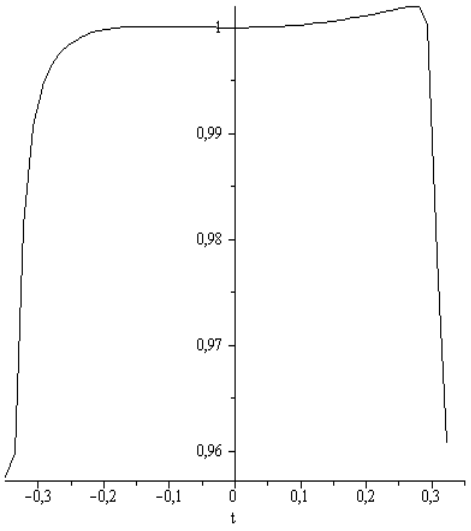

Figure 14. v – potential $\widetilde{\varphi}$.
(the second approximation, Variant 3).

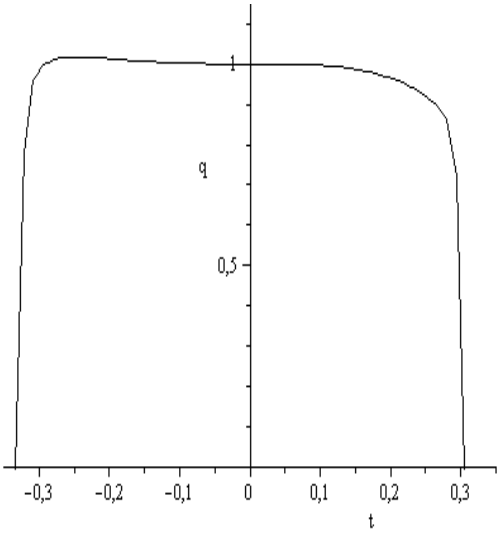

Figure 15. q – electron pressure.
(the second approximation, Variant 3).

In the comparison with Variant 1 the calculations in Variant 3 are realized for the case with opposite signs in front of the coefficients of second order. In this case the distortion of the left side of soliton is observed because by $\widetilde{\xi} < 0$ the velocity $\widetilde{u}$ is not constant. Then this kind of potential for lattice is not favorable for creation of the super-conducting structures.
Variant 2 (Table 3) correspond to diminishing of the lattice potential in 100 times by the same practically self-consistent potential, (Figures 16 – 23).

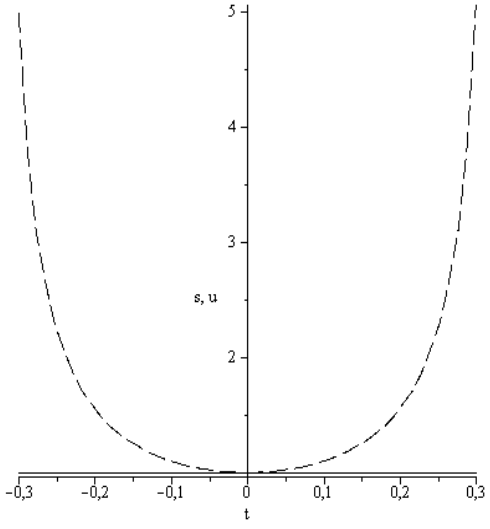

Figure 16. s – electron density $\widetilde{\rho}_e$,,
u – velocity $\widetilde{u}$ (solid line).
(the first approximation, Variant 2).

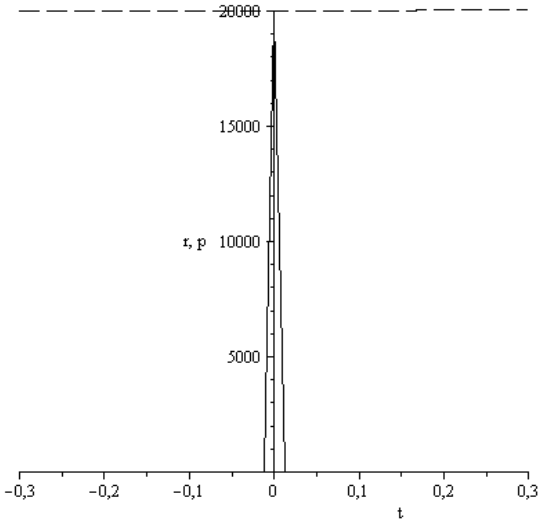

Figure 17. r – the positive particles density,
(solid line); p – the positive particles pressure
(the first approximation, Variant 2).

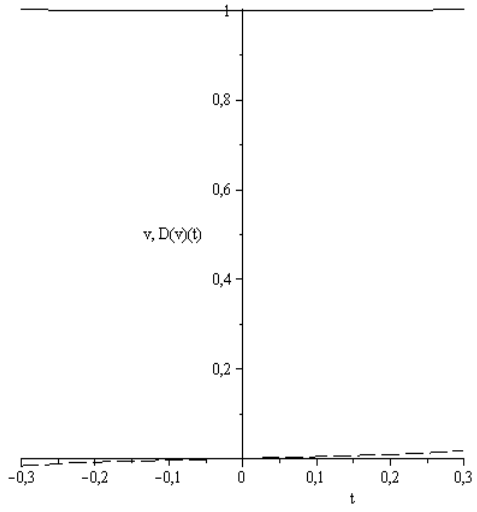

Figure 18. v – potential $\widetilde{\varphi}$ (solid line), $D(v)(t)$,(the first approximation, Variant 2).

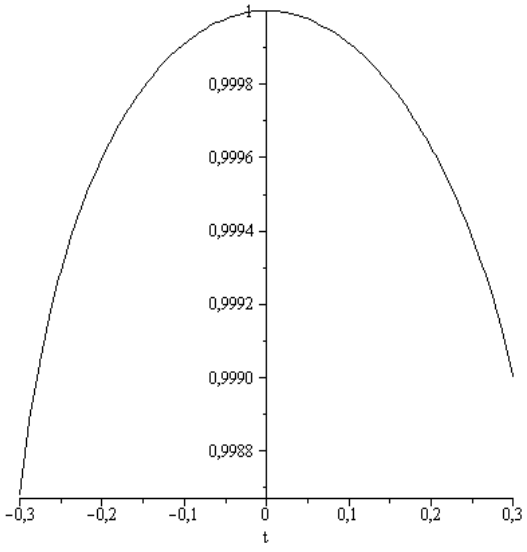

Figure 19. q – electron pressure. (the first approximation, Variant 2).

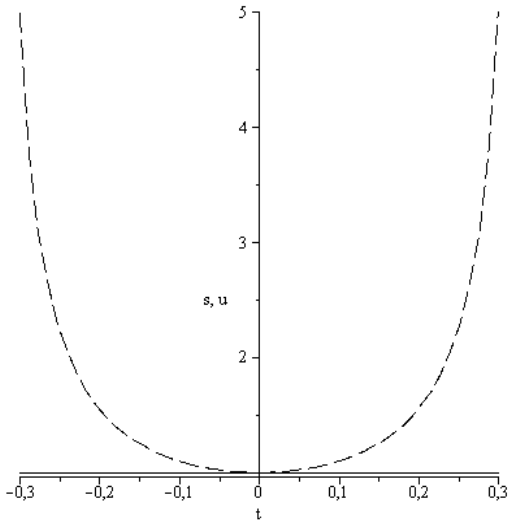

Figure 20. s – electron density $\widetilde{\rho}_e$, u – velocity $\widetilde{u}$ (solid line). (the second approximation, Variant 2).

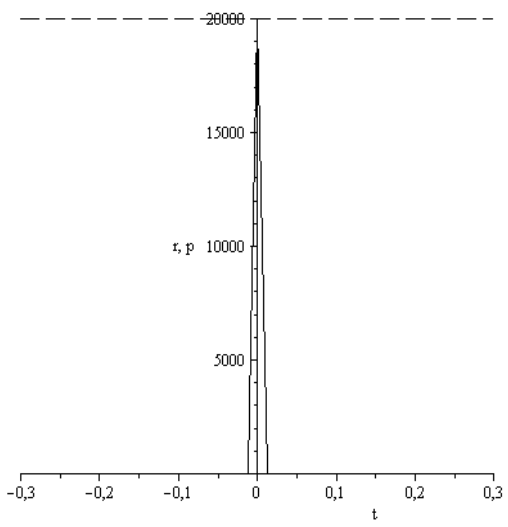

Figure 21. r – the positive particles density, (solid line); p – the positive particles pressure (the second approximation, Variant 2).

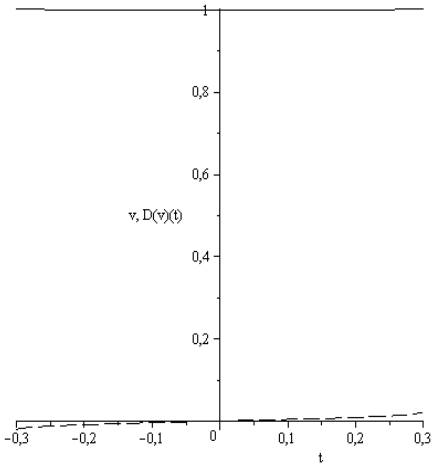

Figure 22. v – potential $\widetilde{\varphi}$ (solid line), $D(v)(t)$.
(the second approximation, Variant 2).

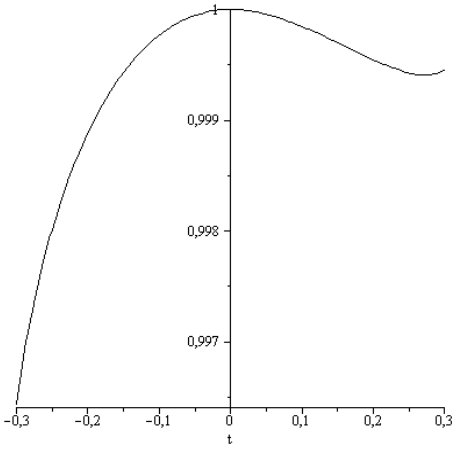

Figure 23. q – electron pressure.
(the second approximation, Variant 2).

From comparison of figures 2 - 9 and 16 - 23 follow that numerical diminishing of the lattice potential (by the practically the same value of the self-consistent potential) does not influence on soliton size. But at the same time the solitons gain the more symmetrical forms. Therefore namely the self-consistent potential plays the basic role in the soliton formation.
Let us analyze now the influence of *H* - parameter, practically the influence of the non-locality parameter. Figures 24 – 31 (Variant 5) correspond to increasing of the parameter H in 100 times in comparison with Variant 1.

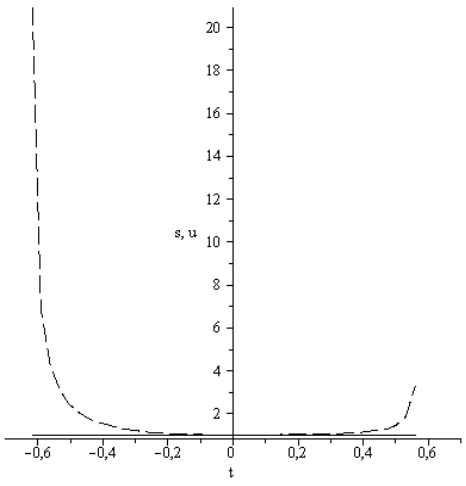

Figure 24. s – electron density $\widetilde{\rho}_e$,
u – velocity $\widetilde{u}$ (solid line).
(the first approximation, Variant 5).

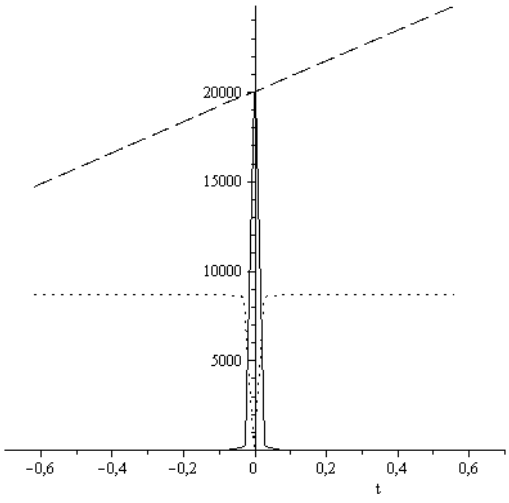

Figure 25. r – the positive particles density,
(solid line); p – the positive particles pressure (dashed line), $D(p)(t)$ - dotted line.
(the first approximation, Variant 5).

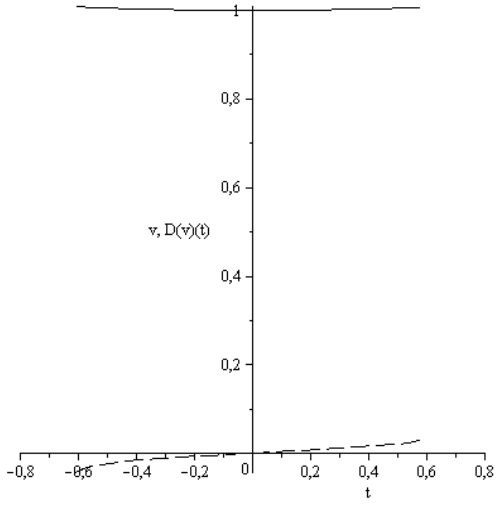

Figure 26. v – potential $\widetilde{\varphi}$ (solid line); $D(v)(t)$, (the first approximation, Variant 5).

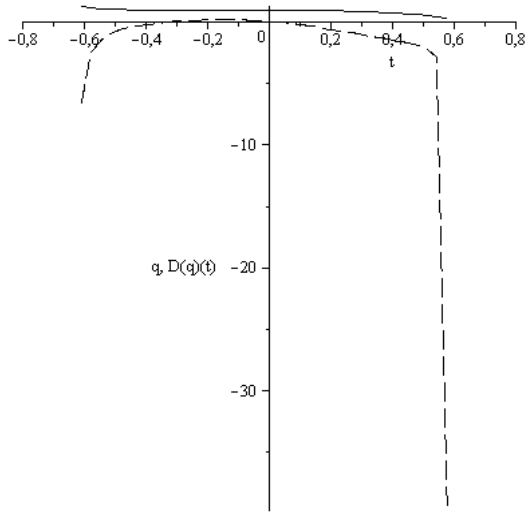

Figure 27. q – electron pressure. (solid line), $D(q)(t)$, (the first approximation, Variant 5)

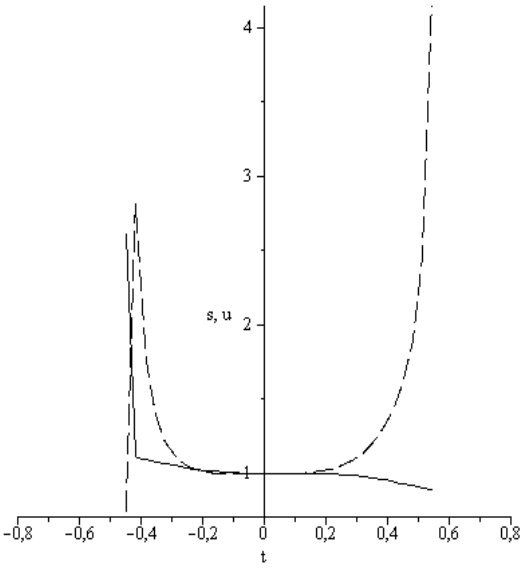

Figure 28. s – electron density $\widetilde{\rho}_e$, u – velocity $\widetilde{u}$ (solid line). (the second approximation, Variant 5).

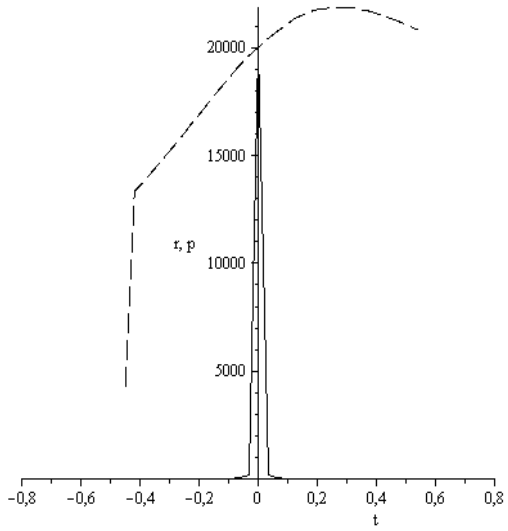

Figure 29. r – the positive particles density, (solid line); p – the positive particles pressure (the second approximation, Variant 5).

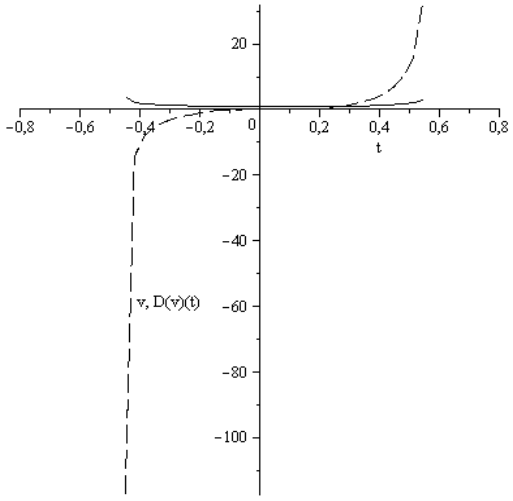

Figure 30. v – potential $\widetilde{\varphi}$ (solid line); $\mathrm{D(v)(t)}$, (the second approximation, Variant 5).

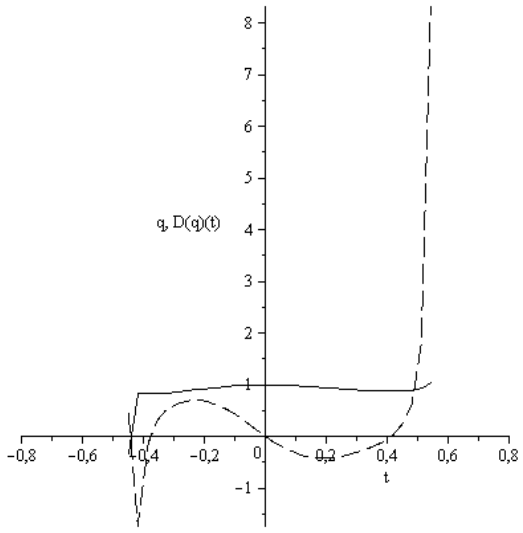

Figure 31. q – electron pressure (solid line), $\mathrm{D(q)(t)}$, (the second approximation, Variant 5).

The comparison of figures 2 - 5 and 24 - 27 indicates that in the first approximation the very significant increasing of the *H* value in 100 times leads to increasing of the soliton size only in two times without significant changing of the soliton structure. The comparison of calculations (see figures 6 and 28) in the second approximation leads to conclusion that the region (where the velocity $\widetilde{u}$ is constant) has practically the same size.

Consider now the calculations responding to Variant 4 (Table 3). Increasing in 10^4 times of the scale φ_0 denotes increasing the self consistent potential and the lattice potential introduced in the process of the mathematical modeling. This case leads to the drastic diminishing of the soliton size. Figures 32 - 35 demonstrate that in the calculations of the first approximation the soliton size is $\sim 10^{-4} a = 1.42 \cdot 10^{-12} cm$ and exceeds the nuclei size only in several times. The positive kernel of the soliton decreasing in the less degree and occupies now the half of the soliton size. It is no surprise because the low boundary of this kernel size is the character size of the nuclei. Application of the second approximation for the lattice potential function in the mathematical modeling leads to the significant soliton deformation but the same soliton size (Figures 36-39).

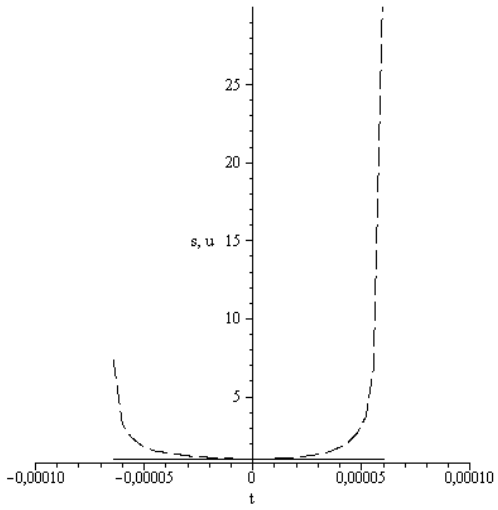

Figure 32. s – electron density $\widetilde{\rho}_e$, u – velocity $\widetilde{u}$ (solid line).
(the first approximation, Variant 4).

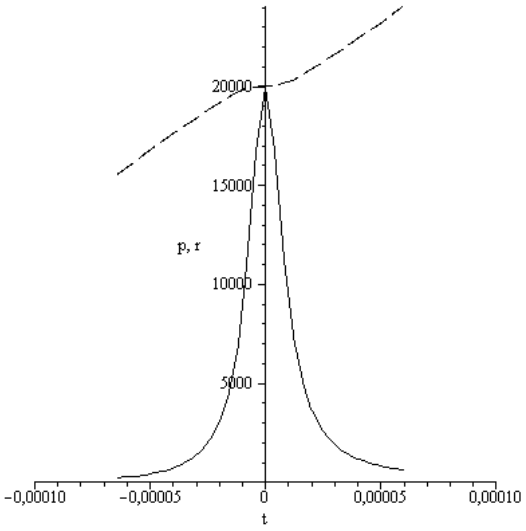

Figure 33. r – the positive particles density, (solid line); p – the positive particles pressure
(the first approximation, Variant 4).

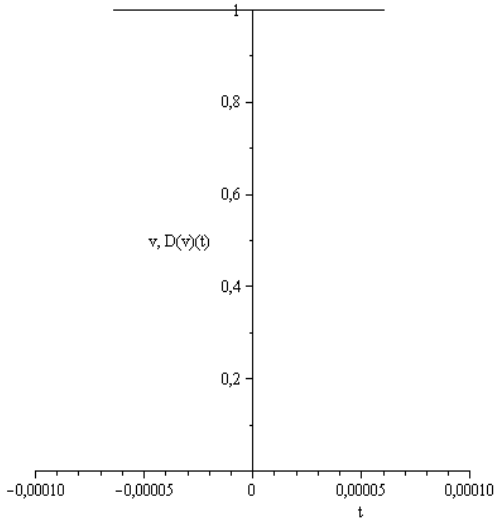

Figure 34. v – potential $\widetilde{\varphi}$ (solid line).
(the first approximation, Variant 4).

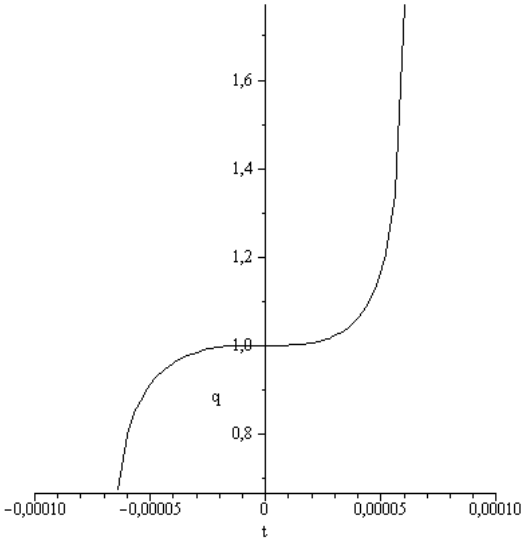

Figure 35. q – electron pressure.
(the first approximation, Variant 4).

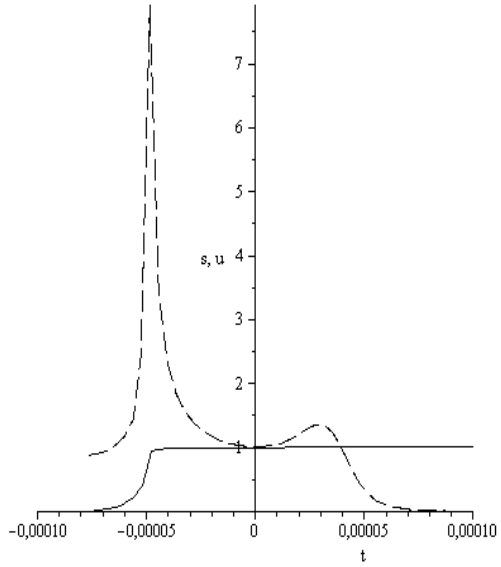

Figure 36. s – electron density $\widetilde{\rho}_e$, u – velocity $\widetilde{u}$ (solid line). (the second approximation, Variant 4).

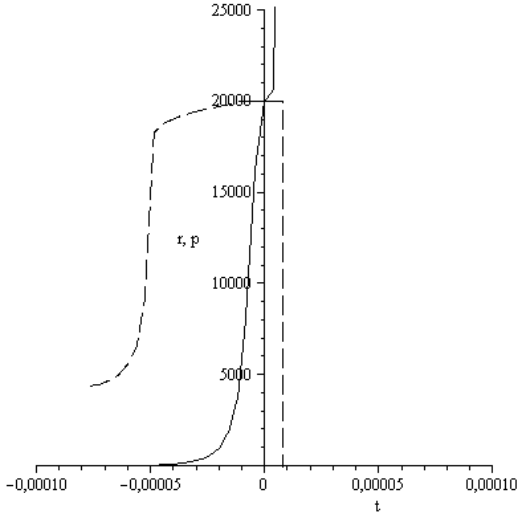

Figure 37. r – the positive particles density, (solid line); p – the positive particles pressure (the second approximation, Variant 4)

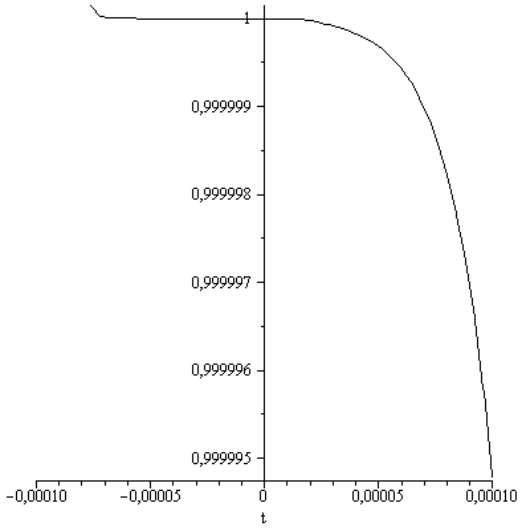

Figure 38. v – potential $\widetilde{\varphi}$ (solid line). (the second approximation, Variant 4)

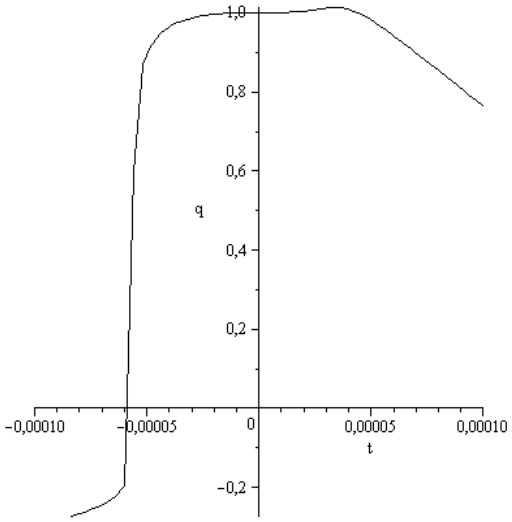

Figure 39. q – electron pressure. (the second approximation, Variant 4)

The drastic increasing of the periodic potential of the crystal lattice (in hundred times, see figures 40 – 48) in comparison with the self-consistent potential also leads to diminishing of the soliton size. For the case Variant 6, Table 3 this size consists only $\sim 10^{-2} a$. But this increasing does not lead to the relative increasing of the soliton kernel and to the mentioned above the soliton deformation in the second approximation (see figures 45 – 48). Figure 41

demonstrates the extremely high accuracy of the soliton stability, the velocity fluctuation inside the soliton is only $\sim 10^{-16}\widetilde{u}$.

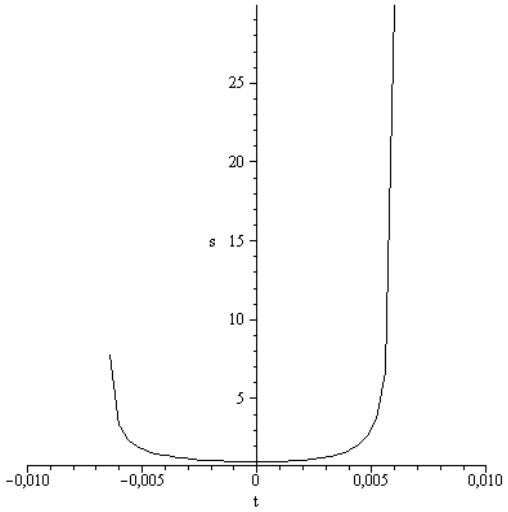

Figure 40. s – electron density $\widetilde{\rho}_e$, (the first approximation, Variant 6).

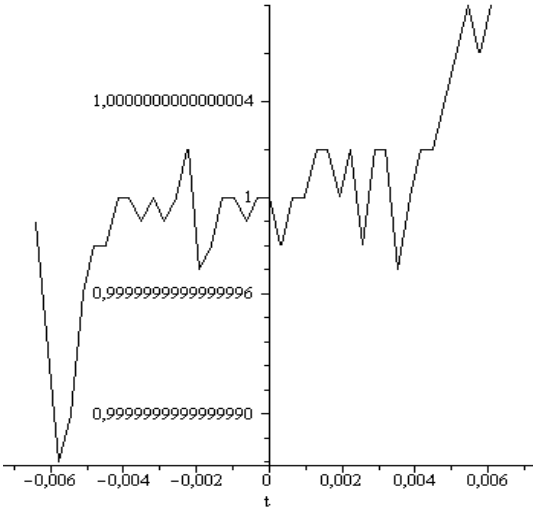

Figure 41. u – velocity $\widetilde{u}$. (the first approximation, Variant 6).

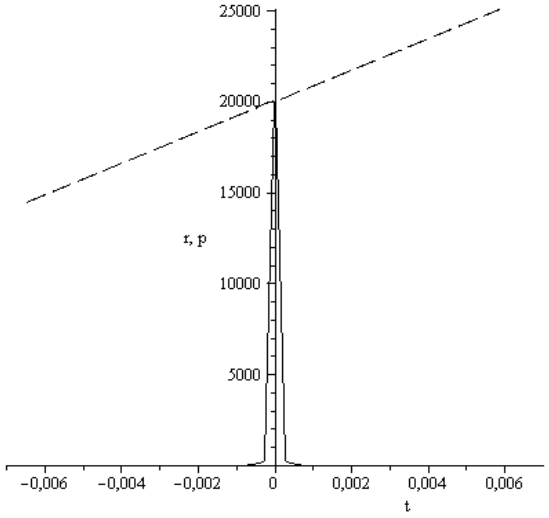

Figure 42. r – the positive particles density, (solid line); p – the positive particles pressure (the first approximation, Variant 6).

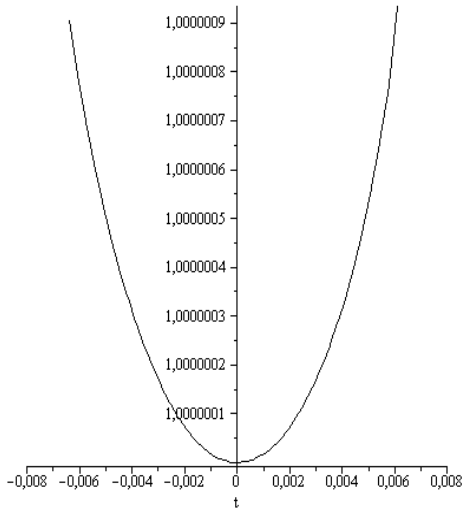

Figure 43. v – potential $\widetilde{\varphi}$. (the first approximation, Variant 6).

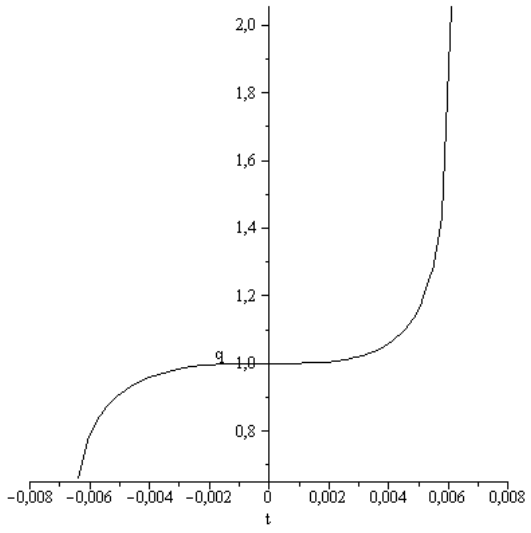

Figure 44. q – electron pressure.
(the first approximation, Variant 6).

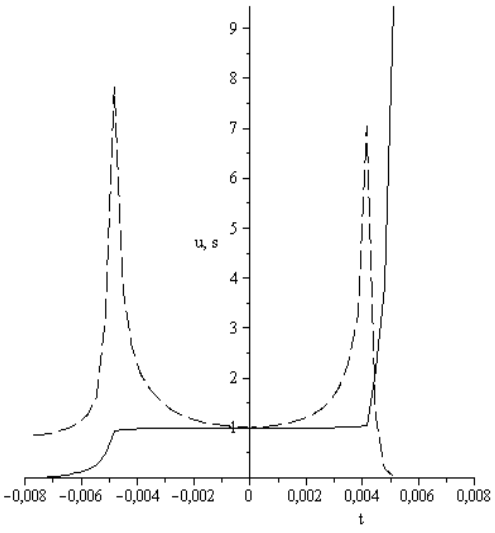

Figure 45. s – electron density $\widetilde{\rho}_e$,
u – velocity $\widetilde{u}$ (solid line).
(the second approximation, Variant 6).

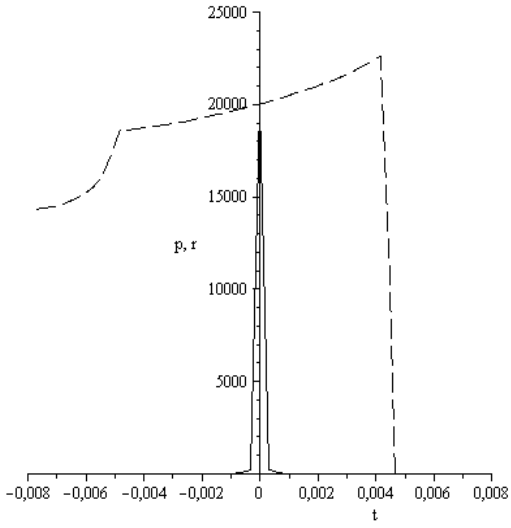

Figure 46. r – the positive particles density.
(solid line); p – the positive particles
pressure, (the second approximation, Variant 6).

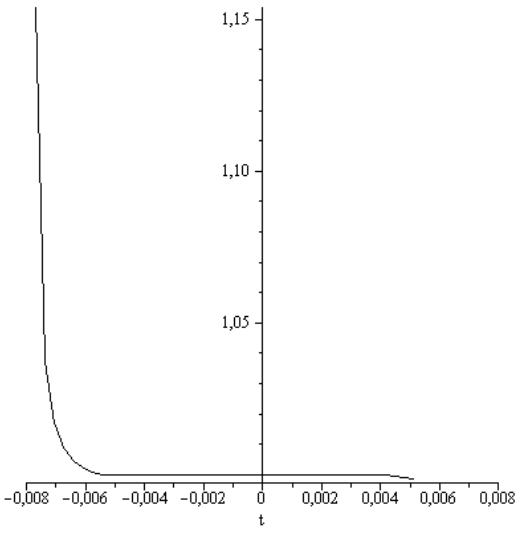

Figure 47. v – potential $\widetilde{\varphi}$.
(the second approximation, Variant 6).

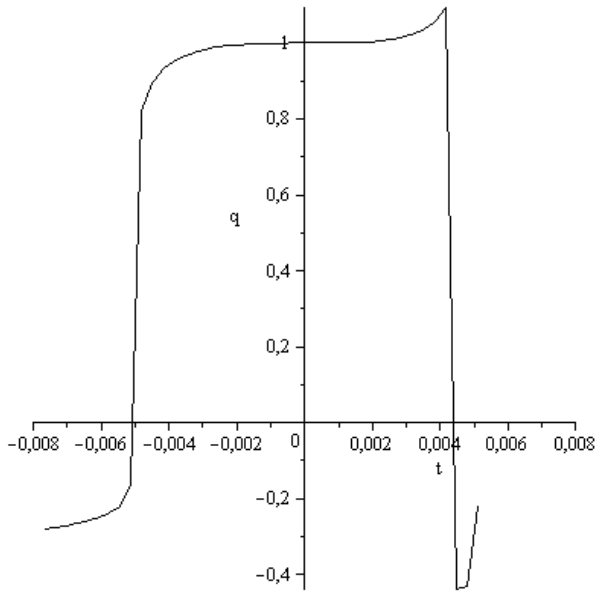

Figure 48. q – electron pressure.
(the second approximation, Variant 6).

6. RESULTS OF THE MATHEMATICAL MODELING WITH THE EXTERNAL ELECTRIC FIELD

Let us consider now the results of the mathematical modeling with taking into account the intensity of the external electric field which does not depend on y. In this case the solution of the hydrodynamic system (3.10) – (3.15) should be found. After averaging and in the moving coordinate system it leads to the following equations written in the first approximation (compare with the system (3.34) – (3.39)):

Poisson equation for the self-consistent electric field:

$$\frac{\partial^2 \widetilde{\varphi}}{\partial \widetilde{\xi}^{\,2}} = -4\pi R\left\{\frac{m_e}{m_p}\left[\widetilde{\rho}_p - \frac{m_e H}{m_p \widetilde{u}^{\,2}}\frac{\partial}{\partial \widetilde{\xi}}\left(\widetilde{\rho}_p\left(\widetilde{u}-1\right)\right)\right] - \left[\widetilde{\rho}_e - \frac{H}{\widetilde{u}^{\,2}}\frac{\partial}{\partial \widetilde{\xi}}\left(\widetilde{\rho}_e\left(\widetilde{u}-1\right)\right)\right]\right\}. \qquad (6.1)$$

Continuity equation for the positive particles:

$$\frac{\partial}{\partial \widetilde{\xi}}\left[\widetilde{\rho}_p\left(1-\widetilde{u}\right)\right] + \frac{m_e}{m_p}\frac{\partial}{\partial \widetilde{\xi}}\left\{\frac{H}{\widetilde{u}^{\,2}}\frac{\partial}{\partial \widetilde{\xi}}\left[\widetilde{\rho}_p\left(\widetilde{u}-1\right)^2\right]\right\} + \frac{m_e}{m_p}\frac{\partial}{\partial \widetilde{\xi}}\left\{\frac{H}{\widetilde{u}^{\,2}}\left[\frac{V_{0p}^2}{u_0^2}\frac{\partial}{\partial \widetilde{\xi}}\widetilde{p}_p - \right.\right.$$
$$\left.\left.\frac{m_e}{m_p}\widetilde{\rho}_p E\left(-\frac{\partial \widetilde{\varphi}}{\partial \widetilde{\xi}} + \widetilde{U}_{11}' \sin\left(\frac{4\pi}{3\widetilde{a}}\widetilde{\xi} - \frac{\pi}{3}\right) + \widetilde{E}_0\right)\right]\right\} = 0. \qquad (6.2)$$

Continuity equation for electrons:

$$\frac{\partial}{\partial\widetilde{\xi}}\left[\widetilde{\rho}_e\left(1-\widetilde{u}\right)\right]+\frac{\partial}{\partial\widetilde{\xi}}\left\{\frac{H}{\widetilde{u}^2}\frac{\partial}{\partial\widetilde{\xi}}\left[\widetilde{\rho}_e\left(\widetilde{u}-1\right)^2\right]\right\}+\frac{\partial}{\partial\widetilde{\xi}}\left\{\frac{H}{\widetilde{u}^2}\left[\frac{V_{0e}^2}{u_0^2}\frac{\partial}{\partial\widetilde{\xi}}\widetilde{p}_e-\right.\right.$$
$$\left.\left.\widetilde{\rho}_e E\left(\frac{\partial\widetilde{\varphi}}{\partial\widetilde{\xi}}-\widetilde{U}_{11}'\sin\left(\frac{4\pi}{3\widetilde{a}}\widetilde{\xi}-\frac{\pi}{3}\right)-\widetilde{E}_0\right)\right]\right\}=0. \tag{6.3}$$

Momentum equation for the *x* direction:

$$\frac{\partial}{\partial\widetilde{\xi}}\left\{\left(\widetilde{\rho}_p+\widetilde{\rho}_e\right)\widetilde{u}\left(\widetilde{u}-1\right)+\frac{V_{0p}^2}{u_0^2}\widetilde{p}_p+\frac{V_{0e}^2}{u_0^2}\widetilde{p}_e\right\}-$$
$$\frac{m_e}{m_p}\widetilde{\rho}_p E\left(-\frac{\partial\widetilde{\varphi}}{\partial\widetilde{\xi}}+\widetilde{U}_{11}'\sin\left(\frac{4\pi}{3\widetilde{a}}\widetilde{\xi}-\frac{\pi}{3}\right)+\widetilde{E}_0\right)-$$
$$\widetilde{\rho}_e E\left(\frac{\partial\widetilde{\varphi}}{\partial\widetilde{\xi}}-\widetilde{U}_{11}'\sin\left(\frac{4\pi}{3\widetilde{a}}\widetilde{\xi}-\frac{\pi}{3}\right)-\widetilde{E}_0\right)+$$
$$\frac{m_e}{m_p}\frac{\partial}{\partial\widetilde{\xi}}\left\{\frac{H}{\widetilde{u}^2}\left[\frac{\partial}{\partial\widetilde{\xi}}\left(2\frac{V_{0p}^2}{u_0^2}\widetilde{p}_p\left(1-\widetilde{u}\right)-\widetilde{\rho}_p\widetilde{u}\left(1-\widetilde{u}\right)^2\right)-\right.\right.$$
$$\left.\left.\frac{m_e}{m_p}\widetilde{\rho}_p\left(1-\widetilde{u}\right)E\left(-\frac{\partial\widetilde{\varphi}}{\partial\widetilde{\xi}}+\widetilde{U}_{11}'\sin\left(\frac{4\pi}{3\widetilde{a}}\widetilde{\xi}-\frac{\pi}{3}\right)+\widetilde{E}_0\right)\right]\right\}+$$
$$\frac{\partial}{\partial\widetilde{\xi}}\left\{\frac{H}{\widetilde{u}^2}\left[\frac{\partial}{\partial\widetilde{\xi}}\left(2\frac{V_{0e}^2}{u_0^2}\widetilde{p}_e\left(1-\widetilde{u}\right)-\widetilde{\rho}_e\widetilde{u}\left(1-\widetilde{u}\right)^2\right)-\right.\right.$$
$$\left.\left.\widetilde{\rho}_e\left(1-\widetilde{u}\right)E\left(\frac{\partial\widetilde{\varphi}}{\partial\widetilde{\xi}}-\widetilde{U}_{11}'\sin\left(\frac{4\pi}{3\widetilde{a}}\widetilde{\xi}-\frac{\pi}{3}\right)-\widetilde{E}_0\right)\right]\right\}+$$
$$\frac{H}{\widetilde{u}^2}E\left(\frac{m_e}{m_p}\right)^2\left(-\frac{\partial\widetilde{\varphi}}{\partial\widetilde{\xi}}+\widetilde{U}_{11}'\sin\left(\frac{4\pi}{3\widetilde{a}}\widetilde{\xi}-\frac{\pi}{3}\right)+\widetilde{E}_0\right)\left(\frac{\partial}{\partial\widetilde{\xi}}\left(\widetilde{\rho}_p\left(\widetilde{u}-1\right)\right)\right)+$$
$$\frac{H}{\widetilde{u}^2}E\left(\frac{\partial\widetilde{\varphi}}{\partial\widetilde{\xi}}-\widetilde{U}_{11}'\sin\left(\frac{4\pi}{3\widetilde{a}}\widetilde{\xi}-\frac{\pi}{3}\right)-\widetilde{E}_0\right)\left(\frac{\partial}{\partial\widetilde{\xi}}\left(\widetilde{\rho}_e\left(\widetilde{u}-1\right)\right)\right)-$$
$$\frac{m_e}{m_p}\frac{\partial}{\partial\widetilde{\xi}}\left\{\frac{H}{\widetilde{u}^2}\frac{V_{0p}^2}{u_0^2}\frac{\partial}{\partial\widetilde{\xi}}\left(\widetilde{p}_p\widetilde{u}\right)\right\}-\frac{\partial}{\partial\widetilde{\xi}}\left\{\frac{H}{\widetilde{u}^2}\frac{V_{0e}^2}{u_0^2}\frac{\partial}{\partial\widetilde{\xi}}\left(\widetilde{p}_e\widetilde{u}\right)\right\}+$$

$$\left(\frac{m_e}{m_p}\right)^2 E\frac{\partial}{\partial\widetilde{\xi}}\left\{\frac{H}{\widetilde{u}^2}\left[\left(-\frac{\partial\widetilde{\varphi}}{\partial\widetilde{\xi}}+\widetilde{U}'_{11}\sin\left(\frac{4\pi}{3\widetilde{a}}\widetilde{\xi}-\frac{\pi}{3}\right)+\widetilde{E}_0\right)\widetilde{\rho}_p\widetilde{u}\right]\right\}+$$
$$E\frac{\partial}{\partial\widetilde{\xi}}\left\{\frac{H}{\widetilde{u}^2}\left[\left(\frac{\partial\widetilde{\varphi}}{\partial\widetilde{\xi}}-\widetilde{U}'_{11}\sin\left(\frac{4\pi}{3\widetilde{a}}\widetilde{\xi}-\frac{\pi}{3}\right)-\widetilde{E}_0\right)\widetilde{\rho}_e\widetilde{u}\right]\right\}=0 \quad (6.4)$$

Energy equation for the positive particles:

$$\frac{\partial}{\partial\widetilde{\xi}}\left[\widetilde{\rho}_p\widetilde{u}^2(\widetilde{u}-1)+5\frac{V_{0p}^2}{u_0^2}\widetilde{p}_p\widetilde{u}-3\frac{V_{0p}^2}{u_0^2}\widetilde{p}_p\right]-$$
$$2\frac{m_e}{m_p}\widetilde{\rho}_pE\left(-\frac{\partial\widetilde{\varphi}}{\partial\widetilde{\xi}}+\widetilde{U}'_{11}\sin\left(\frac{4\pi}{3\widetilde{a}}\widetilde{\xi}-\frac{\pi}{3}\right)+\widetilde{E}_0\right)\widetilde{u}+$$
$$\frac{\partial}{\partial\widetilde{\xi}}\left\{\frac{H}{\widetilde{u}^2}\frac{m_e}{m_p}\left[\frac{\partial}{\partial\widetilde{\xi}}\left(-\widetilde{\rho}_p\widetilde{u}^2(1-\widetilde{u})^2+7\frac{V_{0p}^2}{u_0^2}\widetilde{p}_p\widetilde{u}(1-\widetilde{u})+3\frac{V_{0p}^2}{u_0^2}\widetilde{p}_p(\widetilde{u}-1)-\frac{V_{0p}^2}{u_0^2}\widetilde{p}_p\widetilde{u}^2-\right.\right.\right.$$
$$\left.\left.5\frac{V_{0p}^4}{u_0^4}\frac{\widetilde{p}_p^2}{\widetilde{\rho}_p}\right)+E\left(-2\frac{m_e}{m_p}\widetilde{\rho}_p\widetilde{u}(1-\widetilde{u})+\frac{m_e}{m_p}\widetilde{\rho}_p\widetilde{u}^2+5\frac{m_e}{m_p}\frac{V_{0p}^2}{u_0^2}\widetilde{p}_p\right)\left(-\frac{\partial\widetilde{\varphi}}{\partial\widetilde{\xi}}+\right.$$
$$\left.\left.\widetilde{U}'_{11}\sin\left(\frac{4\pi}{3\widetilde{a}}\widetilde{\xi}-\frac{\pi}{3}\right)+\widetilde{E}_0\right)\right]\right\}+2\frac{H}{\widetilde{u}^2}E\left(\frac{m_e}{m_p}\right)^2\left[-\frac{\partial}{\partial\widetilde{\xi}}\left(\widetilde{\rho}_p\widetilde{u}(1-\widetilde{u})\right)+\right.$$
$$\left.\frac{V_{0p}^2}{u_0^2}\frac{\partial}{\partial\widetilde{\xi}}\widetilde{p}_p\right]\left(-\frac{\partial\widetilde{\varphi}}{\partial\widetilde{\xi}}+\widetilde{U}'_{11}\sin\left(\frac{4\pi}{3\widetilde{a}}\widetilde{\xi}-\frac{\pi}{3}\right)+\widetilde{E}_0\right)-$$
$$2\frac{H}{\widetilde{u}^2}E^2\left(\frac{m_e}{m_p}\right)^3\widetilde{\rho}_p\left[\left(-\frac{\partial\widetilde{\varphi}}{\partial\widetilde{\xi}}+\widetilde{U}'_{11}\sin\left(\frac{4\pi}{3\widetilde{a}}\widetilde{\xi}-\frac{\pi}{3}\right)+\widetilde{E}_0\right)^2+\frac{1}{2}\left(\widetilde{U}'_{10}\sin\left(\frac{2\pi}{3\widetilde{a}}\widetilde{\xi}+\frac{\pi}{3}\right)\right)^2+\right.$$
$$\left.\frac{3}{2}\left(\widetilde{U}'_{10}\cos\left(\frac{2\pi}{3\widetilde{a}}\widetilde{\xi}+\frac{\pi}{3}\right)\right)^2+6\left(\widetilde{U}'_{11}\right)^2+\frac{16}{\pi}\left(\widetilde{U}'_{10}\widetilde{U}'_{11}\right)\cos\left(\frac{2\pi}{3\widetilde{a}}\widetilde{\xi}+\frac{\pi}{3}\right)\right]=$$
$$-\frac{\widetilde{u}^2}{Hu_0^2}\left(V_{0p}^2\widetilde{p}_p-\widetilde{p}_eV_{0e}^2\right)\left(1+\frac{m_p}{m_e}\right) \quad (6.5)$$

Energy equation for electrons:

$$\frac{\partial}{\partial\widetilde{\xi}}\left[\widetilde{\rho}_e\widetilde{u}^2(\widetilde{u}-1)+5\frac{V_{0e}^2}{u_0^2}\widetilde{p}_e\widetilde{u}-3\frac{V_{0e}^2}{u_0^2}\widetilde{p}_e\right]-2\widetilde{\rho}_e\widetilde{u}E\left(\frac{\partial\widetilde{\varphi}}{\partial\widetilde{\xi}}-\widetilde{U}'_{11}\sin\left(\frac{4\pi}{3\widetilde{a}}\widetilde{\xi}-\frac{\pi}{3}\right)-\widetilde{E}_0\right)+$$

$$\frac{\partial}{\partial\widetilde{\xi}}\left\{\frac{H}{\widetilde{u}^2}\left[\frac{\partial}{\partial\widetilde{\xi}}\left(-\widetilde{\rho}_e\widetilde{u}^2(1-\widetilde{u})^2+7\frac{V_{0e}^2}{u_0^2}\widetilde{p}_e\widetilde{u}(1-\widetilde{u})+3\frac{V_{0e}^2}{u_0^2}\widetilde{p}_e(\widetilde{u}-1)-\frac{V_{0e}^2}{u_0^2}\widetilde{p}_e\widetilde{u}^2-\right.\right.\right.$$

$$\left.\left.\left.5\frac{V_{0e}^4}{u_0^4}\frac{\widetilde{p}_e^2}{\widetilde{\rho}_e}\right)+E\left(-2\widetilde{\rho}_e\widetilde{u}(1-\widetilde{u})+\widetilde{\rho}_e\widetilde{u}^2+5\frac{V_{0e}^2}{u_0^2}\widetilde{p}_e\right)\left(\frac{\partial\widetilde{\varphi}}{\partial\widetilde{\xi}}-\widetilde{U}'_{11}\sin\left(\frac{4\pi}{3\widetilde{a}}\widetilde{\xi}-\frac{\pi}{3}\right)-\widetilde{E}_0\right)\right]\right\}+$$

$$E\left(-2\frac{H}{\widetilde{u}^2}\frac{\partial}{\partial\widetilde{\xi}}(\widetilde{\rho}_e\widetilde{u}(1-\widetilde{u}))+2\frac{H}{\widetilde{u}^2}\frac{V_{0e}^2}{u_0^2}\frac{\partial}{\partial\widetilde{\xi}}\widetilde{p}_e\right)\left(\frac{\partial\widetilde{\varphi}}{\partial\widetilde{\xi}}-\widetilde{U}'_{11}\sin\left(\frac{4\pi}{3\widetilde{a}}\widetilde{\xi}-\frac{\pi}{3}\right)-\widetilde{E}_0\right)-$$

$$2E^2\frac{H}{\widetilde{u}^2}\widetilde{\rho}_e\left[\left(-\frac{\partial\widetilde{\varphi}}{\partial\widetilde{\xi}}+\widetilde{U}'_{11}\sin\left(\frac{4\pi}{3\widetilde{a}}\widetilde{\xi}-\frac{\pi}{3}\right)+\widetilde{E}_0\right)^2+\right.$$

$$\frac{1}{2}\left(\widetilde{U}'_{10}\sin\left(\frac{2\pi}{3\widetilde{a}}\widetilde{\xi}+\frac{\pi}{3}\right)\right)^2+\frac{3}{2}\left(\widetilde{U}'_{10}\cos\left(\frac{2\pi}{3\widetilde{a}}\widetilde{\xi}+\frac{\pi}{3}\right)\right)^2+ \tag{6.6}$$

$$\left.6\left(\widetilde{U}'_{11}\right)^2+\frac{16}{\pi}\left(\widetilde{U}'_{10}\widetilde{U}'_{11}\right)\cos\left(\frac{2\pi}{3\widetilde{a}}\widetilde{\xi}+\frac{\pi}{3}\right)\right]=-\frac{\widetilde{u}^2}{Hu_0^2}\left(V_{0e}^2\widetilde{p}_e-V_{0p}^2\widetilde{p}_p\right)\left(1+\frac{m_p}{m_e}\right)$$

Two classes of parameters were used by the mathematical modeling – parameters and scales which were not changed during calculations and varied parameters indicated in Table 4.

Parameters, scales and Cauchy conditions which are common for modeling with the external field:

$\frac{m_e}{m_p}=5\cdot10^{-5}$, the scales $\rho_0=10^{-10}g/cm^3$, $u_0=5\cdot10^6 cm/s$, $V_{0e}=5\cdot10^6 cm/s$, $V_{0p}=5\cdot10^4 cm/s$, $x_0=a=0.142nm$, $\varphi_0=10^{-4}\frac{e}{a}=3.4\cdot10^{-6}CGSE_\varphi$.

Dimensionless parameters $R=3\cdot10^{-3}$, E=0.1, H =15 (by N_R=1). Admit that for the lattice $U\sim V_{1,(10)}\sim V_{1,(11)}\sim\varphi_0$ and choose $\widetilde{U}'_{10}=10$, $\widetilde{U}'_{11}=10$.

Cauchy conditions $\widetilde{\rho}_e(0)$=1, $\widetilde{\rho}_p(0)=2\cdot10^4$, $\widetilde{p}_e(0)=1$, $\widetilde{p}_p(0)=2\cdot10^4$, $\widetilde{\varphi}(0)=1$, $\frac{\partial\widetilde{\rho}_e}{\partial\widetilde{\xi}}(0)=0$, $\frac{\partial\widetilde{\rho}_p}{\partial\widetilde{\xi}}(0)=0$.

Table 4. Varied parameters in calculations with the external electric field

Variant №	$\widetilde{E}_0$	$\frac{\partial\widetilde{\varphi}}{\partial\widetilde{\xi}}(0)$	$\frac{\partial\widetilde{p}_p}{\partial\widetilde{\xi}}(0)$	$\frac{\partial\widetilde{p}_e}{\partial\widetilde{\xi}}(0)$
1	0	0	0	0
7.0	10	10	0	0
7.1	10	10	10	-1
8.0	100	100	0	0
8.1	100	100	10	0
9.0	10000	10000	0	0
9.1	10000	10000	10	-1

The external intensity of the electric field is written as $E_0 = \frac{\varphi_0}{x_0}\widetilde{E}_0 = 10^{-4}\frac{e}{a^2}\widetilde{E}_0 = 238CGSE_E\widetilde{E}_0 = 7.14\cdot 10^6\frac{V}{m}\widetilde{E}_0$. It means that even by $\widetilde{E}_0 = 1$ we are dealing with the rather strong fields. But namely strong external fields can exert the influence on the soliton structures compared with the Coulomb forces in the lattice. For example in [39] the influence of the external electric field in graphene up to $10^7 - 10^8 V/m$ is considered. The values $\widetilde{E}_0$ are indicated in Table 4, variants 9.0 and 9.1 respond to the extremely strong external field.

Table 4 contains in the first line the reminder about the first variant of calculations reflected on figures 2 – 5. These data (in the absence of the external field, $\widetilde{E}_0 = 0$) are convenient for the following result comparison. The variants of calculations in Table 4 are grouped on principle of the $\widetilde{E}_0$ increasing. In more details: figures 49 – 58 correspond to $\widetilde{E}_0 = 10$, figures 59 – 68 correspond to $\widetilde{E}_0 = 100$, figures 69 – 80 correspond to $\widetilde{E}_0 = 10000$.

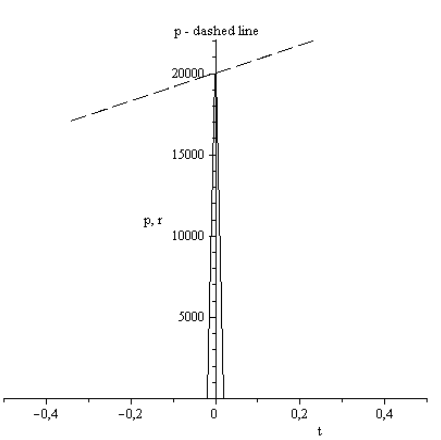

Figure 49. r – the positive particles density, (solid line); p – the positive particles pressure. (Variant 7.0).

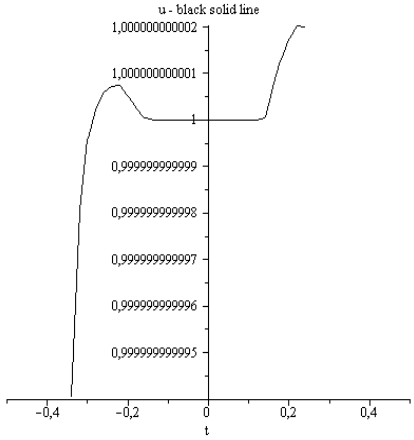

Figure 50. u – velocity $\widetilde{u}$. (Variant 7.0).

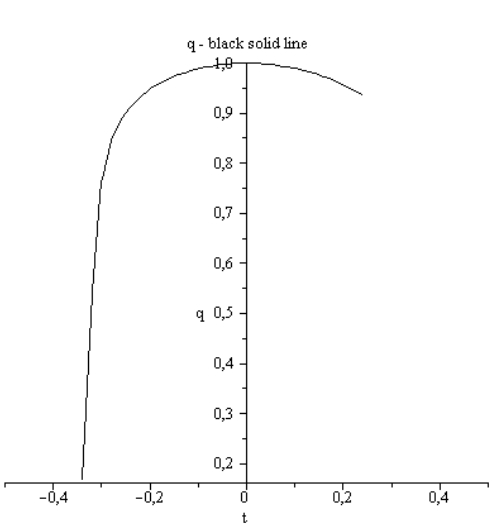

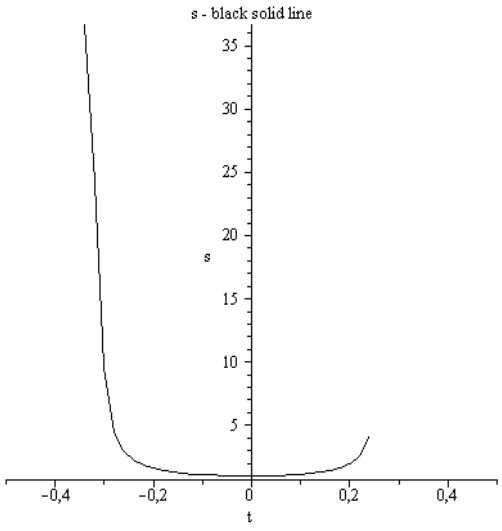

Figure 51. q–electron pressure (Variant 7.0). Figure 52. s–electron density $\widetilde{\rho}_e$ (Variant 7.0).

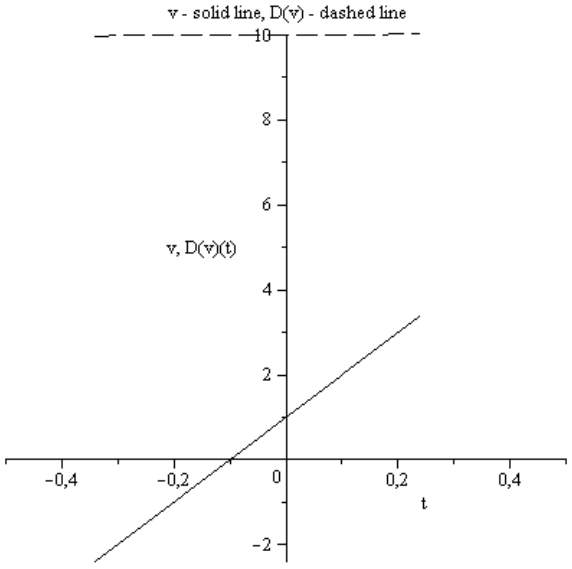

Figure 53. v – potential $\widetilde{\varphi}$ (solid line);
$\mathrm{D(v)(t)}$, (Variant 7.0).

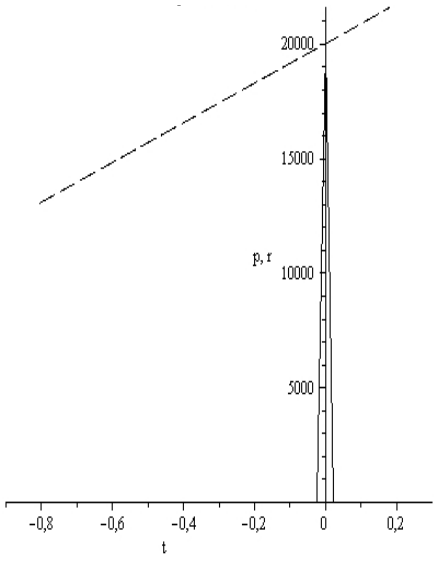

Figure 54. r – the positive particles density, (solid line); p – the positive particles pressure. (Variant 7.1).

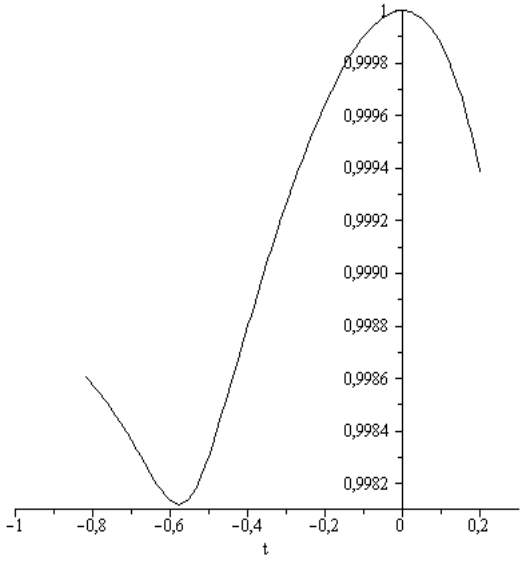

Figure 55. u – velocity $\widetilde{u}$. (Variant7.1).

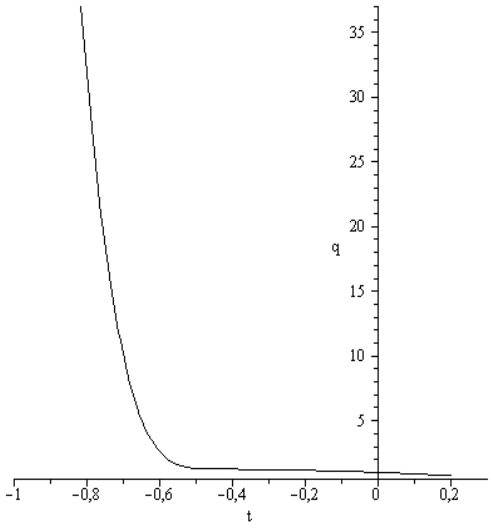

Figure 56. q – electron pressure. (Variant 7.1).

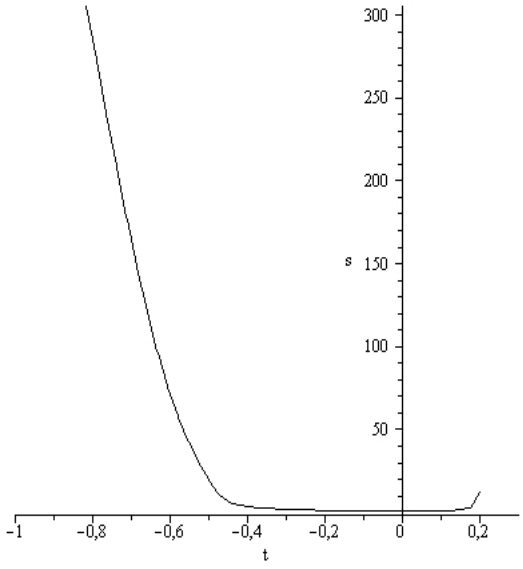

Figure 57. s – electron density $\widetilde{\rho}_e$, (Variant 7.1).

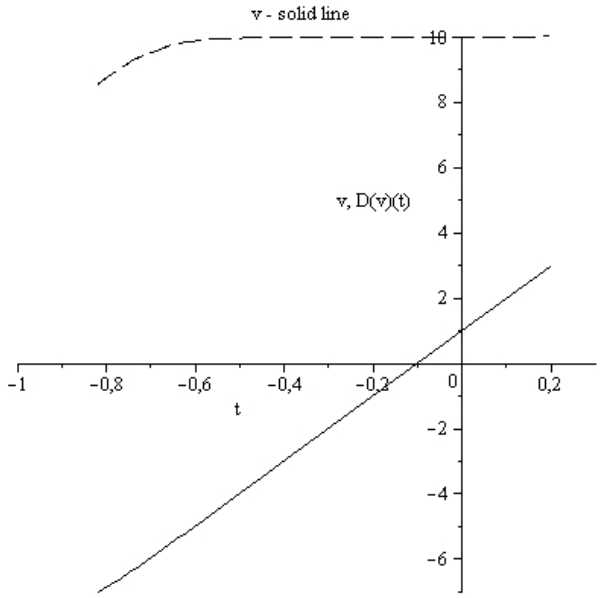

Figure 58. v – potential $\widetilde{\varphi}$ (solid line); $\mathrm{D(v)(t)}$, (Variant 7.1).

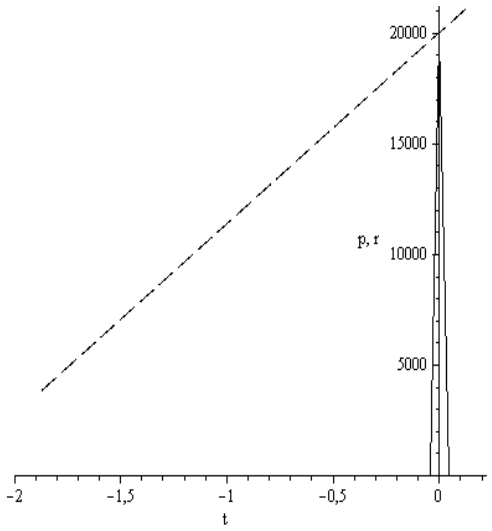

Figure 59. r – the positive particles density, (solid line); p – the positive particles pressure. (Variant 8.0).

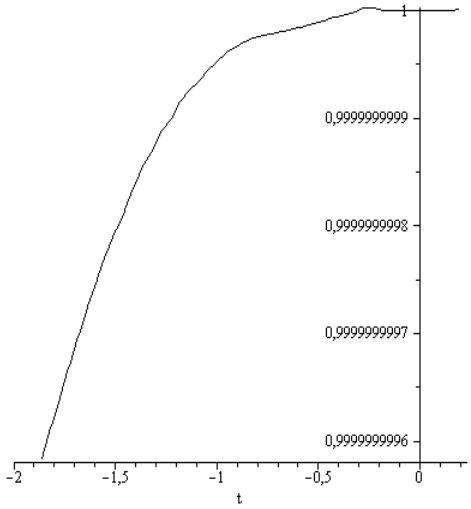

Figure 60. u – velocity $\widetilde{u}$. (Variant 8.0).

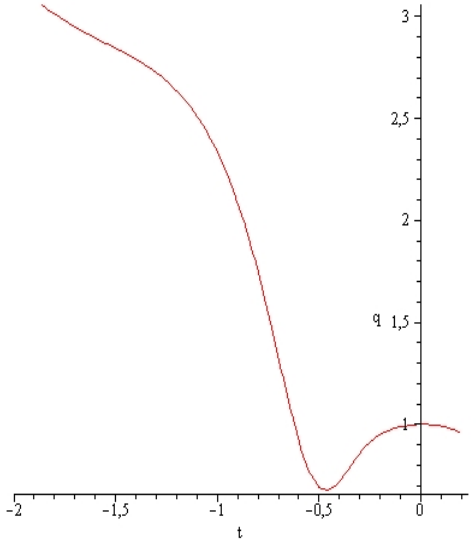

Figure 61. q – electron pressure. (Variant 8.0).

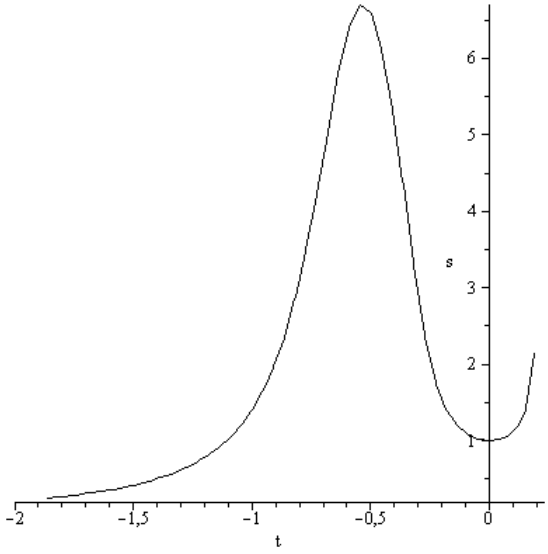

Figure 62. s – electron density $\widetilde{\rho}_e$, (Variant 8.0).

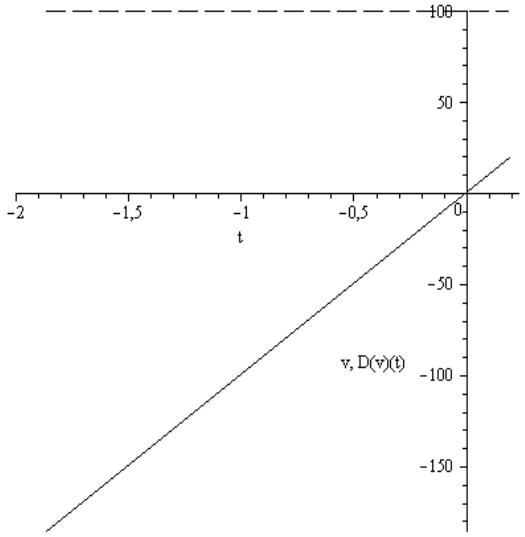

Figure 63. v – potential $\widetilde{\varphi}$ (solid line); $\mathrm{D(v)(t)}$, (Variant 8.0).

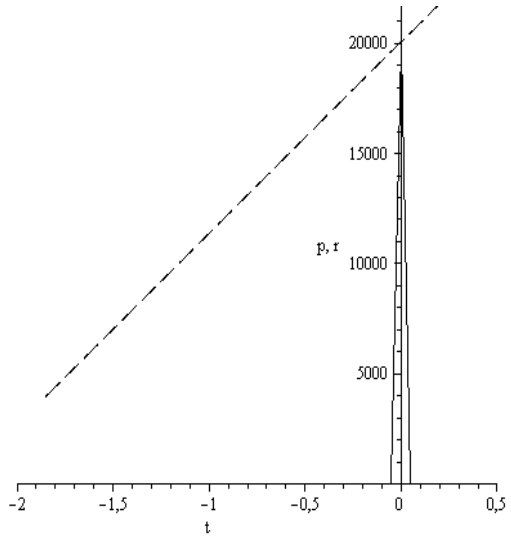

Figure 64. r – the positive particles density, (solid line); p – the positive particles pressure. (Variant 8.1).

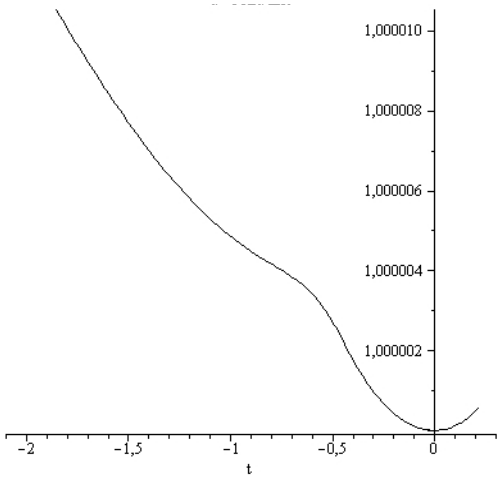

Figure 65. u – velocity $\widetilde{u}$. (Variant 8.1).

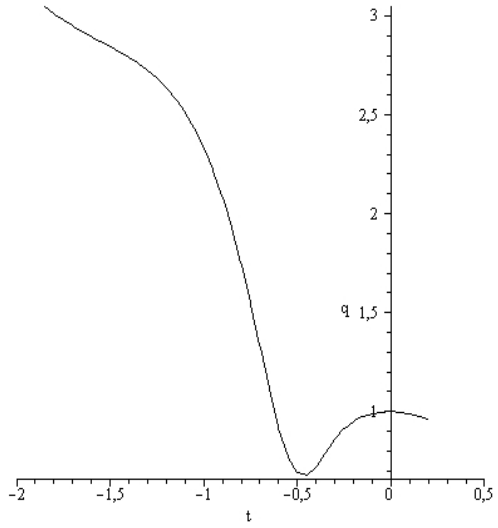

Figure 66. q – electron pressure. (Variant 8.1).

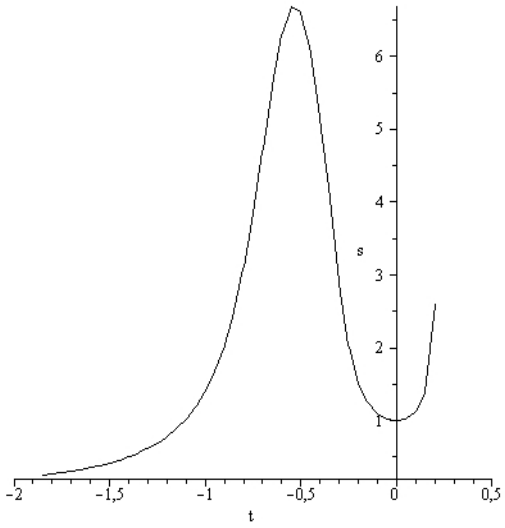

Figure 67. s – electron density $\widetilde{\rho}_e$, (Variant 8.1).

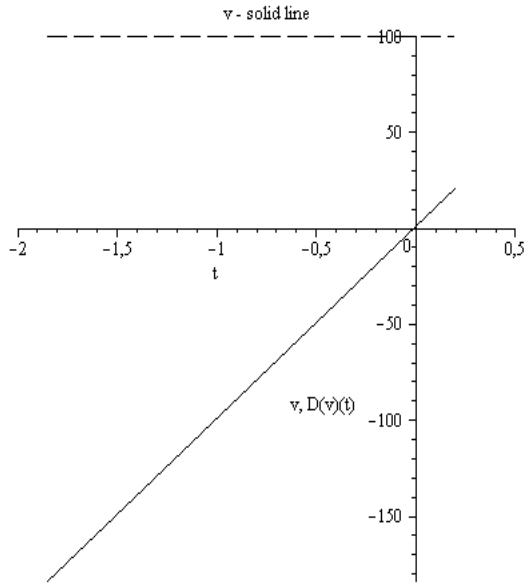

Figure 68. v – potential $\widetilde{\varphi}$ (solid line); $\mathrm{D(v)(t)}$, (Variant 8.1).

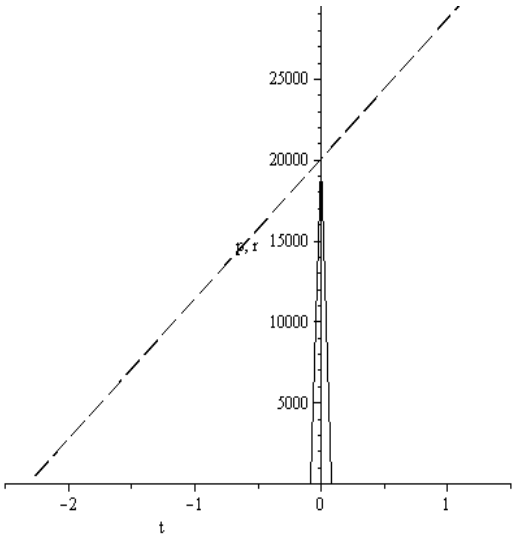

Figure 69. r – the positive particles density, (solid line); p – the positive particles pressure. (Variant 9.0).

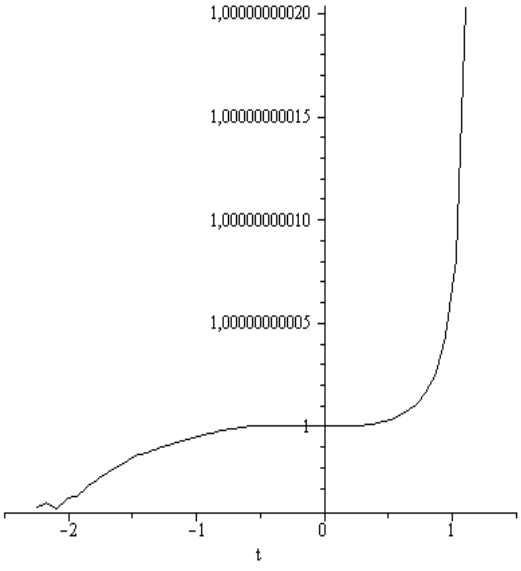

Figure 70. u – velocity $\widetilde{u}$. (Variant 9.0).

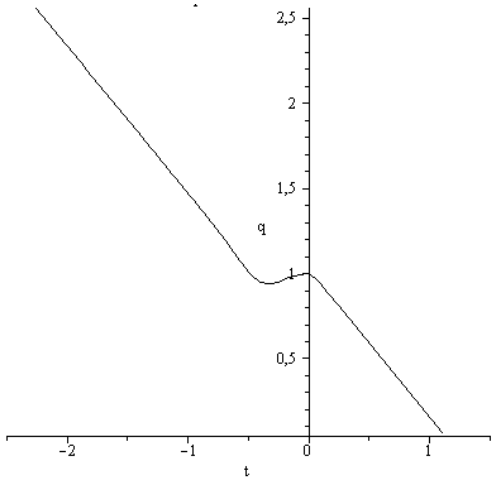

Figure 71. q – electron pressure. (Variant 9.0).

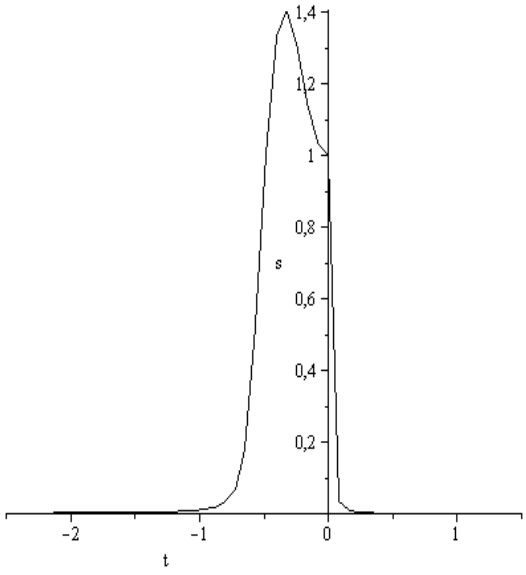

Figure 72. s – electron density $\widetilde{\rho}_e$, (Variant 9.0).

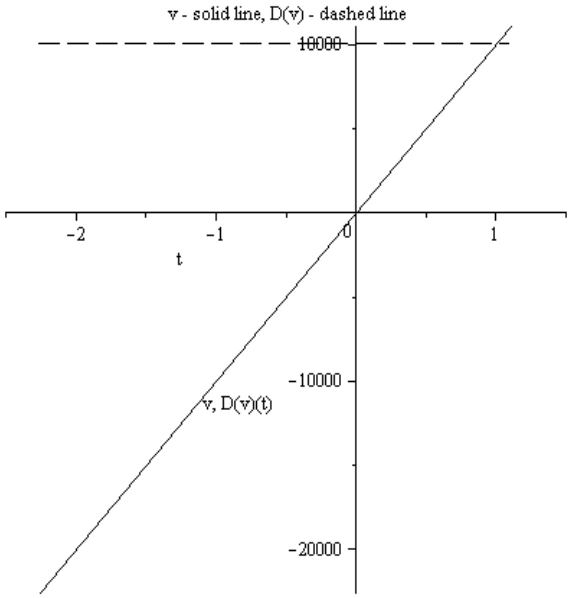

Figure 73. v – potential $\widetilde{\varphi}$ (solid line); $\mathrm{D(v)(t)}$, (Variant 9.0).

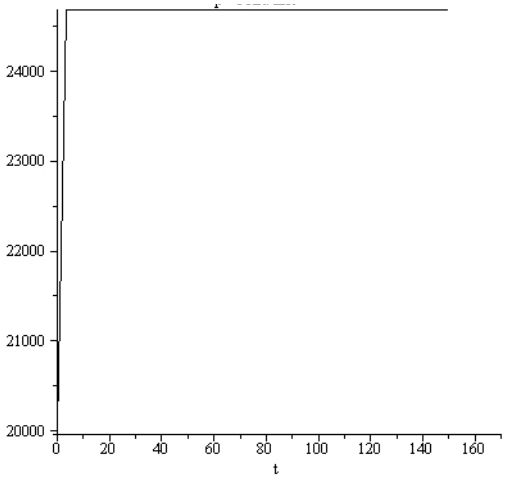

Figure 74. p – the positive particles pressure. (Variant 9.1).

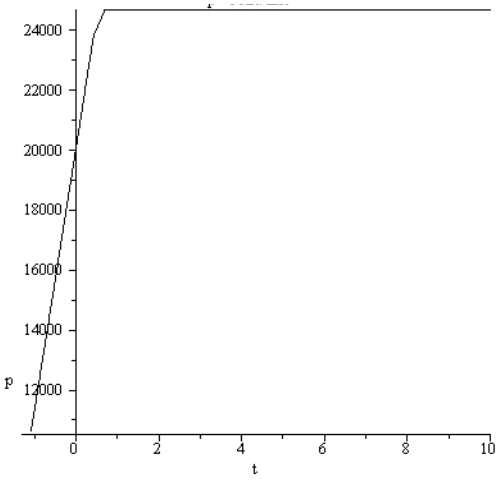

Figure 75. p – the positive particles pressure. (Variant 9.1).

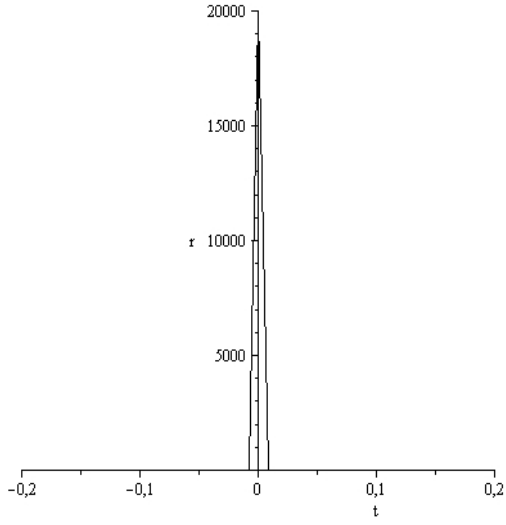

Figure 76. r – the positive particles density, (Variant 9.1).

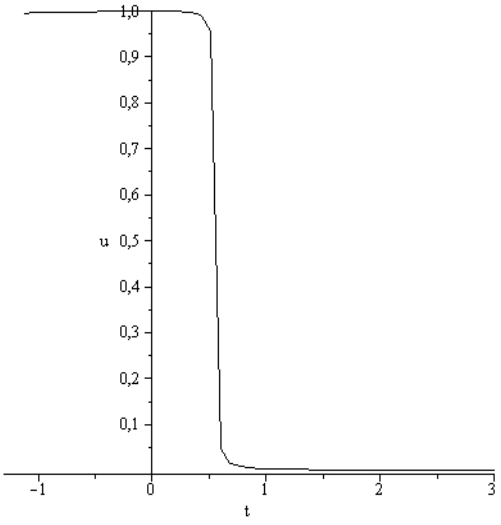

Figure 77. u – velocity $\widetilde{u}$. (Variant 9.1).

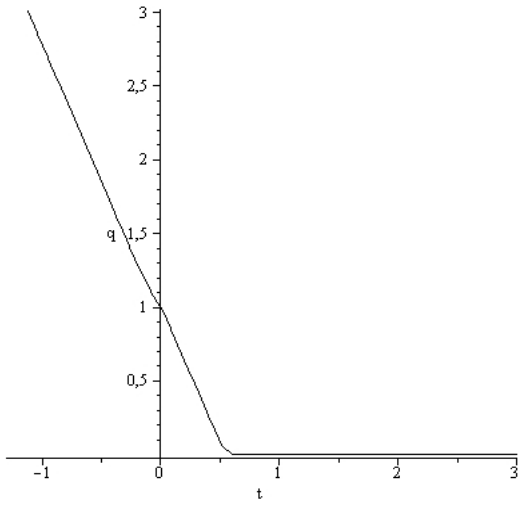

Figure 78. q – electron pressure. (Variant 9.1).

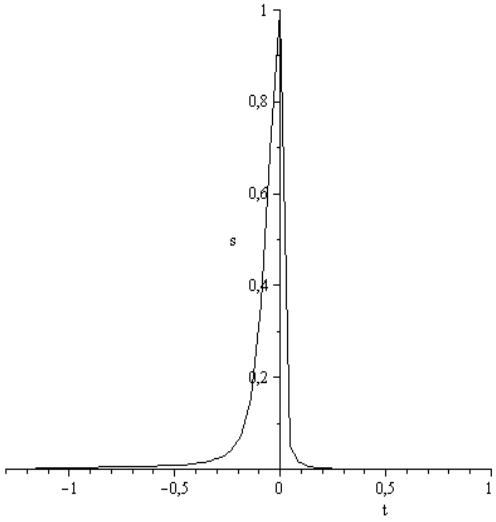

Figure 79. s – electron density $\widetilde{\rho}_e$, (Variant 9.1).

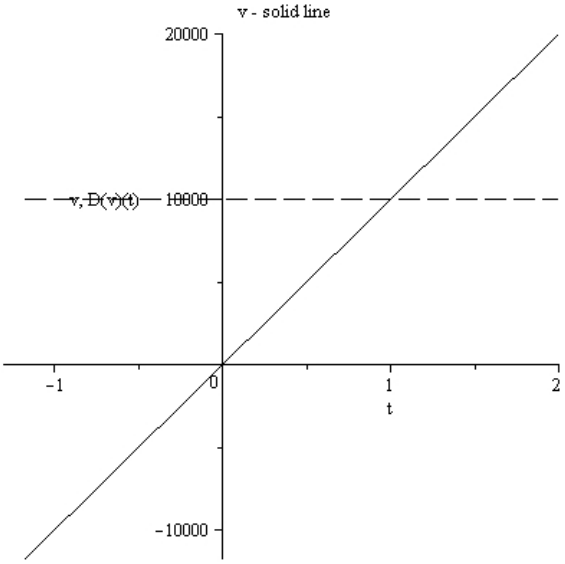

Figure 80. v – potential $\widetilde{\varphi}$ (solid line); $\mathrm{D(v)(t)}$, (Variant 9.1).

Consider now the character features of the soliton evolution and the change of the charge distribution in solitons with growing of the external field intensity:

1. The character soliton size is defined by the area where $\widetilde{u} = 1$. It means that all parts of the soliton wave are moving without destruction. The size of this area is practically independent on choosing of the numerical method of calculations.

2. Figures 75 – 77 demonstrate the typical situation when the area of possible numerical calculations for a physical variable does not coincide with area $\widetilde{u}=1$ where the soliton regime exists.
3. In the area of the soliton existence the condition $\widetilde{u}=1$ is fulfilled with the high accuracy defined practically by accuracy of the choosed numerical method (Figures 50, 55, 60, 65, 70, 77).
4. As a rule for the choosed topology of the electric field the size of the soliton existence is growing with increasing of the electric field intensity.
5. Under the influence of the external electric field the captured electron cloud is displacing in the opposite direction (of the negative variable $\widetilde{\xi}$). The soliton kernel is loosing its symmetry.
6. The redistribution of the self-consistent effective charge creates the self-consistence field with the opposite (to the external field) direction, (Figures 53, 58, 63, 68, 73, 80).
7. The quantum pressure of the positive particle is growing with the $\widetilde{\xi}$ increase. On the whole the specific features of the $\widetilde{p},\ \widetilde{q}$ pressures are defined by the process of the soliton formation.

7. CONCLUSION

The origin of the charge density waves (CDW) is a long-standing problem relevant to a number of important issues in condensed matter physics. Mathematical modeling of the CDW expansion as well as the problem of the high temperature superconduction can be solved only on the basement of the nonlocal quantum hydrodynamics in particular on the basement of the Alexeev non-local quantum hydrodynamics. It is known that the Schrödinger – Madelung quantum physics leads to the destruction of the wave packets and can not be used for the solution of this kind of problems. The appearance of the soliton solutions in mathematics is the rare and remarkable effect. As we see the soliton's appearance in the generalized hydrodynamics created by Alexeev is an "ordinary" oft-recurring fact. The realized here mathematical modeling CDW expansion support established in [22,24] mechanism of the relay ("estafette") motion of the soliton' system ("lattice ion – electron") which is realizing without creation of additional chemical bonds. Important to underline that the soliton mechanism of CDW expansion in graphene (and other substances like $NbSe_2$) takes place in the extremely large diapason of physical parameters. But CDW existence belongs to effects convoying the high temperature superconductivity. It means that the high temperature superconductivity can be explained in the frame of the non-local soliton quantum hydrodynamics.

Important to underline that the problem of existing and propagation of solitons in graphene and in the perspective high superconducting materials belong to the class of significantly non-local non-linear problems which can be solved only in the frame of vast numerical modeling.

COMPETING INTERESTS

Authors have declared that no competing interests exist.

REFERENCES

1. Alekseev BV. Mathematical theory of reacting gases. Moscow: Nauka; 1982. Russian.
2. Alexeev BV. The generalized Boltzmann equation, generalized hydrodynamic equations and their applications. Phil. Trans. Roy. Soc. Lond. 1994;349:417-43. doi:10.1098/rsta.1994.0140.
3. Alexeev BV. The generalized Boltzmann equation. Physica A. 1995;216:459-68. doi:10.1016/0378-4371(95)00044-8.
4. Alekseev BV. Physical basements of the generalized Boltzmann kinetic theory of gases. Physics-Uspekhi. 2000;43(6):601–29. doi:10.1070/PU2000v043n06ABEH000694.
5. Alekseev BV. Physical fundamentals of the generalized Boltzmann kinetic theory of ionized gases. Physics-Uspekhi. 2003;46(2):139–67. doi:10.1070/PU2003v046n02ABEH001221.
6. Alexeev BV. Generalized Boltzmann physical kinetics. Amsterdam: Elsevier; 2004.
7. Alexeev BV. Generalized quantum hydrodynamics and principles of non-local physics. J. Nanoelectron. Optoelectron. 2008;3:143 -58. doi:10.1166/jno.2008.207.
8. Alexeev BV. Application of generalized quantum hydrodynamics in the theory of quantum soliton evolution. J. Nanoelectron. Optoelectron. 2008;3:316-28. doi:10.1166/jno.2008.311.
9. Alexeev BV. Application of generalized non-local quantum hydrodynamics to the calculation of the charge inner structures for proton and electron. Journal of Modern Physics. 2012; 3: 1895-906. doi:10.4236/jmp.2012.312239. Available: http://www.SciRP.org/journal/jmp.
10. Alexeev BV**.** To the theory of galaxies rotation and the Hubble expansion in the frame of non-local physics**.** Journal of Modern Physics. 2012; 3: 1103-22.doi:10.4236/jmp.2012.329145. Available: http://www.SciRP.org/journal/jmp.
11. Boltzmann L. Weitere Studien über das Wärmegleichgewicht unter Gasmolekulen. Sitz. Ber. Kaiserl. Akad. Wiss. 1872;66(2):275. German.
12. Boltzmann L. Vorlesungen über Gastheorie. Leipzig: Verlag von Johann Barth; 1912. German.
13. Chapman S, Cowling TG. The mathematical theory of non-uniform gases. Cambridge: At the University Press; 1952.
14. Hirschfelder IO, Curtiss ChF, Bird RB. Molecular theory of gases and liquids. New York: John Wiley and sons, inc. London: Chapman and Hall, lim.; 1954. .
15. Bell JS. On the Einstein Podolsky Rosen paradox. Physics. 1964; 1: 195 - 200.
16. Madelung E. Quantum theory in hydrodynamical form. Zeit. f. Phys. 1927; 40: 322 - 25. doi:10.1007/BF01400372. German.
17. Landau L.D. Zur Theorie der Energieübertragung. Physics of the Soviet Union. 1932; II 2:46-51. German.
18. Zener C. Non-adiabatic crossing of energy levels. Proceedings of the Royal Society of London A. 1932;137(6):696–702. Bibcode 1932RSPSA.137.696Z. doi:10.1098/rspa.1932.0165. JSTOR 19320901
19. Gell-Mann M, Low F. Bound states in quantum field theory. Phys. Rev. 1951;84:350. doi:10.1103/PhysRev.84.350

20. Berry MV. Quantal phase factors accompanying adiabatic changes. Proc. Royal Soc. London A. 1984;392:45. doi:10.1098/rspa.1984.0023.
21. Simon B. Holonomy, the quantum adiabatic theorem and Berry's phase. Phys. Rev. Letters. 1983;51:2167-70. doi:10.1103/PhysRevLett.51.2167.
22. Alexeev BV. To the non-local theory of the high temperature superconductivity. ArXiv. 2012;0804.3489 [physics.gen-ph]. 30 Jan 2012.
23. Alexeev BV. Generalized quantum hydrodynamics. Vestnik MITHT. 2008;3(3):3-19. Russian.
24. Alexeev, BV. To the non-local theory of the high temperature superconductivity. Vestnik MITHT. 2012;7(3):3–21. Russian.
25. Dürkop T, Getty SA, Cobas Enrique, Fuhrer MS. Nano Letters. 2004;4:35.
26. Kohsaka Y, Hanaguri T, Azuma M, Takano M, Davis JC, Takagi H. Visualization of the emergence of the pseudogap state and the evolution to superconductivity in a lightly hole-doped Mott insulator. Nature Physics. 2012;8:534–8. doi:10.1038/nphys2321.
27. Chang J, Blackburn E, Holmes AT, Christensen NB, Larsen J, Mesot J, Ruixing Liang, Bonn DA, Hardy W.N, Watenphul A, v. Zimmermann M, Forgan EM, Hayden SM. Direct observation of competition between superconductivity and charge density wave order in $YBa_2Cu_3O_y$. ArXiv. 2012;1206.4333 [v2].Condensed Matter. Superconductivity. 3 Jul 2012.
28. Alexeev BV, Abakumov AI, Vinogradov VS. Mathematical modeling of elastic interactions of fast electrons with atoms and molecules. Moscow: Communications on the Applied Mathematics. Computer Centre of the USSR Academy of Sciences; 1986.
29. Alexeev BV. Non-local physics. Non-relativistic theory. Saarbrücken: Lambert Academic Press; 2011. Russian.
30. Lozovik YuE, Merkulova SP, Sokolik AA. Collective electron phenomenon in graphene. Physics – Uspekhi. 2008;178(7):757-76. Russian. Doi:10.3367/UFNr.0178.200807h.0757.
31. Barlas Y, Pereg-Barnea T, Polini M, Asgari R, MacDonald AH. Chirality and correlations in graphene. Phys. Rev. Letters. 2007;98:236601. doi:10.1103/PhysRevLett.98.236601.
32. Castro Neto AH, Guinea F, Peres NMR, Novoselov KS, Geim AK. The electronic properties of graphene. Reviews of Modern Physics. 2009; 81:109-62. doi:10.1103/RevModPhys.81109.
33. Vasko FT, Ryzhii V. Photoconductivity of an itrinsic graphene. ArXiv. 2008; 0801/3476v2 [cond-mat.mtrl-sci]. 27 May 2008.
34. Alexeev BV, Ovchinnikova IV. Non-local physics. Relativistic theory. Saarbrücken: Lambert Academic Press; 2011. Russian.
35. Pisana S, Lazzeri M, Casiraghi C, Novoselov KS, Geim AK, Ferrari AC. Mauri F. Breakdown of the adiabatic Born – Oppenheimer approximation in graphene. Nature Materials. 2007;6:198-201.
36. Zavyalov DV, Krychkov SV, Tyul'kina, TA. Numerical simulation of the current rectification effect induced by an electromagnetic wave in graphene. Fisika i Tehnika Poluprovodnikov. 2010;44(7):910-14. Russian.

37. Zavjalov DV, Kruchkov SV, Mestcheryakova NE. Influence of a nonlinear electromagnetic wave on the electric current density in a superficial superlattice in a strong electric field. Fisika i Tehnika Poluprovodnikov. 2005;39(2):214-17. Russian.
38. Hwang EH, Adam S, Sarma SD. Carrier transport in 2D graphene layers. ArXiv. 2007;0610157v2 [cond-mat.mes-hall]. 4 May 2007.
39. Belonenko MB, Lebedev NG, Pak AV, Yanushkina NN. Spontaneous transverse field in doped graphene. Journal of Technical Physics. 2011;81(8):64-69. Russian.

Peer-review history:
The peer review history for this paper can be accessed here:
http://www.sciencedomain.org/review-history.php?iid=201&id=4&aid=1049